CHESS AT THE MUD-FLAT

Using power-laws as indicator of salt-marsh ecosystem status and development

Jim van Belzen

Master of Science thesis – Environmental Sciences
School of Science
Open Universiteit Nederland
Heerlen

December 2010

NIOO

Open Universiteit
www.ou.nl

Colophon

Author: Jim van Belzen

Private address:

Firensstraat 21

4551 GZ, Sas van Gent

00 31 (0)115 850835 (home)

00 31 (0)113 577491 (work)

E-mail: J.vanBelzen@nioo.knaw.nl

Master's Thesis Master of Science Environmental Sciences (N94310)

Afstudeeropdracht WO-opleiding milieu-natuurwetenschappen (N94310)

Education institute:

Environmental Sciences

School of Science

Open Universiteit, the Netherlands

P.O. Box 2960

6401 DL, Heerlen

Research institute:

Department of Spatial Ecology

Centre for Estuarine and Marine Ecology

Netherlands Institute of Ecology

Cover photo: Patchy salt-marsh pioneer vegetation in winter at Ritthem (near Vlissingen, NL).

Chess at the mudflat:
Using power-laws as indicator of salt-marsh status and development

Schaken op het slik:
Het gebruik van wiskundige machtswetten als indicator voor gesteldheid en ontwikkeling van schorren

Master's graduation commission

Mentors at institute

Dr. Johan van de Koppel (external examiner)

Telephone: 0113-577455

j.vandekoppel@nioo.knaw.nl

Dr. Daphne van der Wal

Telephone: 0113-577468

d.vanderwal@nioo.knaw.nl

Tutors at university

Dr. Ansje Löhr (prime examiner and head of commission)

Telephone: 045-5762835

Ansje.lohr@ou.nl

Ir. Angelique Lansu (second examiner)

Telephone: 045-5762808

Angelique.lansu@ou.nl

Drs. Pieter Geluk (secretary)

Telephone: 045-5762757

Pieter.geluk@ou.nl

"The chess board is the world,
the pieces are the phenomena of the universe,
the rules of the game are what we call the laws of Nature."

Thomas Henry Huxley

Preface

I always thought that I would do research on animals, like insects or so. However, it turned out that I lost myself, of all things to study, on swamp vegetation.

The first ideas on doing research on swampy salt-marsh vegetation was during the Masters class 'Cutting Edge Ecology'. Organized by Louise Vet from NIOO and Wageningen University, we had to write a research proposal to get money for a four-year PhD-position. The proposal I wrote for this coarse was the beginning for the development of my MSc-research proposal. However, most of the research proposed in the original proposal written for the course was been conducted and reported in this thesis.

The preface is a good opportunity to thank and acknowledge some people that made it possible to develop and write this thesis. Because I worked for a long time on this thesis, and talked and discussed a lot with various people, the list of people who to acknowledge is becoming pretty long. Therefore, I'm only going to mention people on the 'short list'. All other that I don't mention here, thank you all for sharing ideas and give valuable input.

Foremost, I want to thank the people at the NIOO-CEME in Yerseke for their support throughout the years. Especially, Johan van de Koppel, who was my first external supervisor and helped me to develop the ideas for this thesis and all research from the Master class until now. I learned a lot from him on how to approach scientific questions, but I even learned more from him on how to communicate science. More than once he said to me something like, "And you expect people to understand that?…." Which helped me a lot on clarifying and improving my presentations and writing. Although I still can learn a lot here. Furthermore I want to thank Daphne van der Wal, my second supervisor at the NIOO. She gave me a lot of support and feedback on the data analysis and the final discussion, which helped me enormously to reflect critically on the used methodology. Moreover, I can't forget to acknowledge Tjeerd Bouma and Peter Herman that give me great feedbacks on technical issues and presentations from time to time during my MSc.

Second, I want to fully acknowledge the support from the Open University. Although I sometimes get a bit nervous of all the comments on the draft of this thesis I wanted to thank Ansje Löhr and Angelique Lansu a lot. You both had to struggle time after time through first drafts of my proposal, and later on my thesis. Ansje you have helped me a lot supporting and encouraging me where needed. I'm grateful for this. I also want to thank everybody else at the Open Universiteit that helped me during my study.

Additionally I want to thank Ellen Weerman, Sonia Kéfi, Maarten Eppinga and Quan-xing Liu for their input and inspiring discussions. I hope we can finish the papers for publication, that are, in some cases, more or less spin-off of the work on this thesis, in the coming year(s).

Last, but not least, I want to thank my family. Without their support, it was not possible to finish my study at all. So, Valarie, Lucas and Justin, thank you for being patient with me,

Jim van Belzen

December 2010

Content

Abstract

Salt-marshes across the world are still in decline, despite the acknowledgment of the importance of these coastal habitats. Lateral erosion is an important cause of this decline. Naturally lateral erosion is counterbalanced by growth resulting in cycles of salt-marsh rejuvenation. The growth phase is critical to the development of the salt-marsh and can be limited by natural or anthropogenic stresses and disturbances. Therefore, it is of importance to get a better insight into the processes controlling growth of vegetation in salt-marsh pioneer zones.

Recently a number of studies suggested that the spatial structure of vegetation reflects stress and disturbances exerted on the ecosystem. Those studies showed that, if disturbance and recovery act on similar temporal scales, vegetation is characterized by an irregular spatial structure and patch-size distributions exhibit power-law distributions. In other words, the number of patches decreases as a power of the patch-size. Possibly, salt-marsh pioneer zone vegetation exhibits a similar spatial structure, and, therefore, can be used as an indicator of the stress and disturbance experienced by the ecosystem.

To test if salt-marsh pioneer vegetation is structured in such a way empirical data and an spatially explicit model are compared. Multi-spectral aerial photographs from six salt-marshes along the Scheldt estuary (NL) are analyzed for: 1) erosion and growth, by comparing consecutive photographs from over a period of 30 years, 2) the spatial structure, by the spectral composition and spatial autocorrelation, and 3) the patch-size distribution of the vegetation. Moreover, the correlation between power-law scaling exponent and hydrodynamic forcing, like exposure to currents and waves, and duration of inundation, is tested. Furthermore, it was investigated if the patch-size distributions found in the aerial photographs could be explained by localized spatial erosion and growth processes.

The analysis of the aerial photographs reveals that: 1) erosion and growth occurs at a similar temporal scale, 2) that the spatial structure of the pioneering vegetation is irregular, and 3) that the patch-size distributions approximate power-law distributions. Furthermore, the analysis shows that there is a strong positive correlation between the power-law scaling exponent and exposure to currents. So, this suggests that it is more difficult to develop towards large patches when currents are strong. In addition, the model analysis revealed that growth and erosion processes occurring at the edges of the vegetation patches explained the patch-size distributions on the aerial pictures very well.

In conclusion, because localized spatial erosion and growth processes can explain the spatial structure of vegetation found at the salt-marsh pioneer zone, power-laws can be used as an indicator of stress and disturbance. Furthermore, the data seems to support that growth is more critical than erosion, because patch-size distributions of growth show more variability between sites. Therefore, it is recommended that processes limiting growth, like seedling recruitment and patch development, will be investigated further.

Samenvatting

Ondanks de onderkenning van de waarde van schorren gaat het areaal van schorren (kwelders) wereldwijd nog steeds achteruit. Een belangrijke oorzaak van deze afname is laterale erosie van het schor. Deze vorm van erosie kan een natuurlijke oorzaak hebben, maar zal onder normale omstandigheden weer worden gecompenseerd door hergroei van het schor. Dit resulteert in een natuurlijke cyclus van erosie en hergroei. De ontwikkeling van het schor in de hergroei fase is kritisch en kan belemmerd worden door stress en verstoring van natuurlijke en antropogene aard. Het is daarom van belang om een beter inzicht te krijgen in de processen die een rol spelen in de hergroei van vegetatie in de pionierzone van schorren.

Recente studies suggereren dat de ruimtelijke organisatie van vegetatie de mate van stress en verstoring op het ecosysteem kunnen weerspiegelen. Op basis van deze studies kan men een wiskundige machtverdeling van de polgrote verwachten in vegetaties waar verstoring en hergroei op eenzelfde tijdschaal plaatsvinden en waar de ruimtelijke organisatie onregelmatige is. Dit wil zeggen dat het aantal pollen dat gevonden wordt afneemt met de mach van de polgrootte. Mogelijk heeft ook de grootte verdeling van de pollen in de pionierzone in schorren deze eigenschappen, en kan daarmee de ruimtelijke structuur van de pioniervegetatie gebruikt worden als een indicatie voor de mate van stress en verstoring.

Om te testen of de pioniervegetatie van schorren voldoet aan deze veronderstelling, is gekozen voor een geïntegreerde onderzoeksopzet waarbij empirische data en een ruimtelijk model worden vergeleken. Hiervoor zijn luchtfoto's met multispectrale data van zes schorren langs de Westerschelde (NL) geanalyseerd op: 1) erosie en hergroei, door foto's van meerdere jaren over een periode van 30 jaar te vergelijken, 2) de ruimtelijke structuur, door te kijken naar spectrale samenstelling en autocorrelatie, en 3) de polgrootte verdelingen. Verder is er gekeken of de machtverdeling in de polgrootte verdeling is te correleren met de lokale hydrodynamische stress in de pionierzone, zoals blootstelling aan stroming, golfslag en overstromingsduur. Tevens is met een ruimtelijk expliciet model nagegaan of specifieke locale ruimtelijke groei en erosie processen de vorming van de gevonden polgrote verdelingen kan verklaren.

De analyse van de luchtfoto's van de verschillende schorren laat zien dat: 1) erosie en hergroei processen in de pionierzone op dezelfde tijdschaal plaatsvinden, 2) dat de vegetatie in de pionierzone een onregelmatige ruimtelijke structuur heeft, en dat 3) de grootteverdeling van de pollen een machtverdeling benadert. Daarnaast blijkt dat de exponent van de machtverdeling sterk positief gecorreleerd is met de stroming bij het schor, waarbij er in pionierzones dus minder grote pollen voorkomen naarmate de stroomsterkte toeneemt. Verder blijkt uit de analyse van het model dat erosie- en groeiprocessen, die aan de randen van de pollen plaatsvinden, de gevonden polgrote verdelingen goed kunnen verklaren.

Omdat de ruimtelijke erosie- en groeiprocessen van de vegetatie zich lokaal afspelen kunnen ze voor een belangrijk deel de structuur van de pionierzone verklaren. Daarom zijn de machtverdelingen een reflectie van de mate van hydrodynamische stress in de pionierzone en kunnen als een indicator gebruikt worden. Verder lijkt de data te ondersteunen dat de hergroei een kritische fase in de cyclus is, omdat verschillen tussen locaties voornamelijk in de polgrootte verdelingen van de hergroei te vinden zijn. Verder onderzoek naar de processen die groei belemmeren, zoals zaailing vestiging en uitgroei van pollen, is dan ook aan te raden.

1. Introduction

The last century, human dominance over global ecosystems has increased with ever increasing pace (MEA, 2005a). All kinds of human activities induce changes that globally affect ecosystems and human well-being. The complexity of ecological systems makes it extremely difficult to predict responses to environmental change. In some cases, ecosystem responses to changing environmental conditions may be gradually and continuous. In other cases, ecosystems also can respond in a discontinuous way. Due to specific internal dynamics, changing external conditions can be buffered or attenuated to some extent by ecosystems. However, when a critical point is surpassed this buffering breaks down and a sudden shift in ecosystems state is possible (Scheffer, et al., 2001; Scheffer, 2009). Where these abrupt transitions occur, the consequences can be devastating. In the worst case, these catastrophic shifts are irreversible and can have considerable impact on ecosystem services, economics and human well-being (MEA, 2005b). Consequently, it would be particularly valuable to develop ecosystem-level indicators to assess current status and predict future development of ecosystems under changing environmental conditions, which in most cases are lacking (Halloy & Barratt, 2007; Scheffer, et al., 2009). One of the frontiers of ecology, and of vital importance to society, is to address the unresolved question (Thompson, et al., 2001): How do ecosystems respond to changes in human pressure and climate?

In particular wetlands are globally important to human well-being, as recognized by the international community, and evidenced by the Ramsar Convention (MEA, 2005c). Coastal wetlands (e.g. mangroves, coral reefs and estuaries containing salt-marshes) are among the most productive ecosystems and they provide numerous services to riparian societies (MEA, 2005b). Regardless of this recognition, most coastal wetlands are highly threatened because of anthropogenic pressures. Reducing stress on these precious ecosystems is challenging because nearly 40% of the world's population live within 100 kilometres of the shoreline and demographic trends suggest their numbers are still rising rapidly (MEA, 2005b).

1.1. Tidal salt-marsh ecosystems

Salt-marshes can be found at the interface between land and sea in low-energy environments within estuaries (see Box I on geomorphology of tide dominated estuaries; Allen, 2000; OzCoasts, 2010). These wetland ecosystems provide a number of essential services for maintaining biodiversity and human well-being (Adam, 2002; Boorman, 1999). They provide habitat for a variety of species, for example, migratory and wintering birds use these habitats to rest and forage. They also provide spawning and nursery locations for commercially important fish and crustaceans. Next to their natural capital, salt-marshes can provide other services. For instance, they play an important role in coastal defence by dissipating wave and tidal forces. Moreover, salt-marshes have the capacity to filter suspended solids and to fixate surplus nitrogen improving water quality. Despite these clear advantages, a decline in salt-marsh area has been the general trend last century (Adam, 2002; Boorman, 1999). Historically, wetlands in general, were perceived as 'wastelands'. By converting salt-marshes into fertile agricultural land, by urbanization and industrialization, or exploitation by mining for salt and fuel, these

'wastelands' could be turned into economically valuable use. Consequently, considerable salt-marsh area is lost by changing land-use, and compared to their original extent only marginally present in North-West Europe nowadays (Adam, 2002; Allen, 2000).

Box I – Geomorphology of tide dominated estuaries in North-West Europe (Allen, 2000; OzCoasts, 2010)

In general, an estuary is a semi enclosed water body connected to the sea, where fresh water runoff (e.g. river) mixes with salt water. The geomorphology of these systems, at the interface between land and sea, largely depend on the relative influence of waves and tidal energy. These hydrodynamic conditions determine to a great extent how sediment transport is influenced. Different habitats will develop if waves, instead of tide, are the dominant hydrodynamic force in the estuary. So, which habitat types will develop largely depends on the sedimentary environment. In this information box geomorphologic explanation is restricted to tide dominated estuaries, as can predominantly be found in the North-West of Europe due to large tidal differences. This kind of system is most relevant for the tidal marshes aimed for in this study.

From the land seaward, roughly three zones can be distinguished (see fig. I.1). Each has their own distinct habitats. (1) In the first zone riverine sediment input is predominant, and flood- and alluvial plains can be found. (2) Wide tidal channel networks, flanked by large areas of inter- and sub-tidal areas are found in the middle. Due to strong tidal influence the water is generally well mixed in this part of the estuary. Although resuspension of fine sediments, like clay and silt, occurs in all parts of the estuary, here they play a dominant role in shaping the inter- and sub-tidal habitat. (3) Finally the estuary pours in a funnel-shaped entrance, containing tidal sand bars. Here, large tidal exchange takes place.

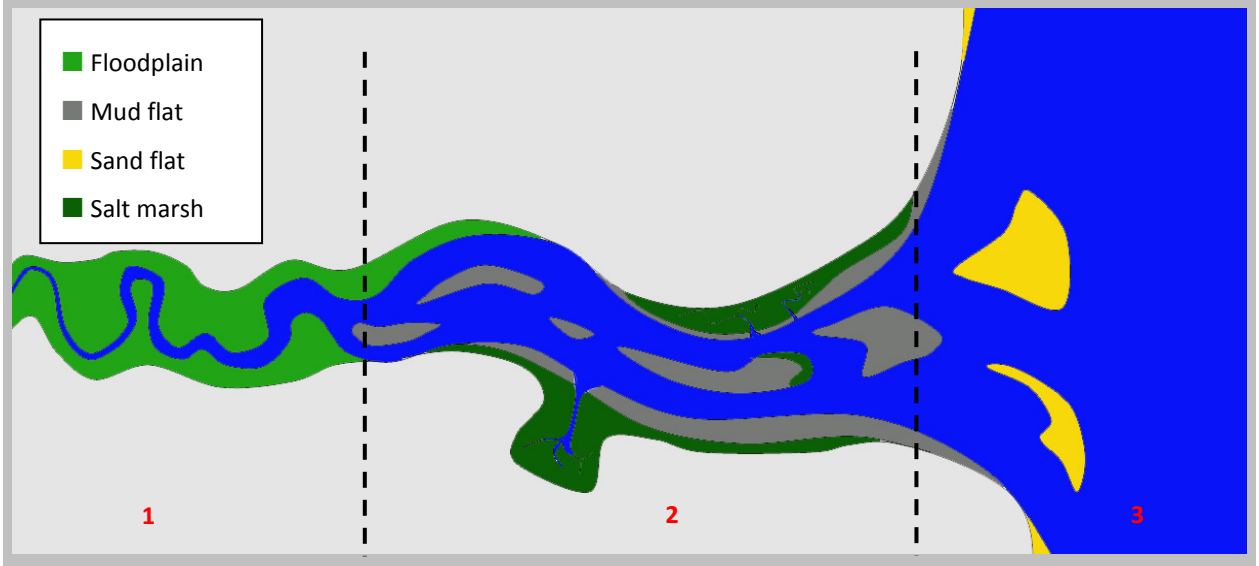

Figure I.1. Conceptual overview of geomorphology of tide dominated estuary (see text for explanation).

Sand-flat – Unvegetated tidal-flat, which develops toward elongated bodies of sand oriented perpendicular to the tidal current direction. Usually associated with strong tidal currents. Where, sand flats become dry at low tide, these habitats can be important foraging grounds for wading birds.

Mud-flat – Unvegetated tidal-flat, low-gradient flats comprised of mud and sand. Generally inundated during high tide, and contains a variety of burrowing organisms. Like sand-flats, these can be very important foraging grounds for different species of wading birds.

Salt-marsh – High inter- to supra-tidal area which is vegetated with grasses, sedges, reeds, and small shrubs. Also these swamps can be important as foraging grounds for grazing birds like geese, are used by numerous bird species to settle breeding colonies, and are important nursery and spawning grounds for fish and crustaceans.

Although the importance of sustaining salt-marshes is now generally acknowledged, loss of salt-marsh habitat due to erosion is still a major problem across the world. For example the marshes in the Venice lagoon (Italy) laterally erode with 1.2-2.2 m yr^{-1} at their seaward edges (Day, et al., 1998) and the estuaries of South-East England lose about 4,000 m^2 yr^{-1} of tidal marsh area due to erosion at the seaward edges and channel widening of creeks dissection the marsh (Hughes & Paramor, 2004). However, what the main drivers of salt-marsh erosion are, is still subject of debate (Wolters, et al., 2005). Generally it is believed that human activities are responsible for increasing erosion rates (Adam, 2002; Allen, 2000; Wolters, et al., 2005). Pollution, shipping traffic, and dredging are some of the proposed anthropogenic causes. In addition, climate change and sea level rise are receiving much attention as a cause of salt-marsh disappearance. However, in contrast to these extrinsic forcing factors, intrinsic biological processes are also proposed (Allen, 2000; Wolters, et al., 2005). For example, vegetation-sediment feedbacks (Allen, 2000) and sediment destabilization by bioturbation and herbivory by worms (Hughes & Paramor, 2004; van der Wal & Pye, 2004) and geese (Dionne, 1985) can both result in erosion of salt-marsh area. These seeming opposite views in which erosion is caused either by extrinsic or intrinsic processes point out that there is a need for fundamental understanding of the highly dynamic functioning of salt-marsh ecosystems in order to support protective measures.

1.2. Accretion and erosion of tidal salt-marshes

Coastal areas, like estuaries, are very energetic systems because of the interplay between hydrodynamic forces, like waves and tidal currents. Ecosystem engineering species (Jones, et al., 1997) play an important role in shaping the tidal and intertidal landscape (Temmerman, et al., 2007; Weerman, et al., 2010). For instance, the presence of salt-marsh plants is an important determinant of the effects of local hydrodynamics (Bouma, et al., 2007), as tidal current and waves are dampened by salt-marsh vegetation. This has a positive effect on sedimentation rates, and hence results in increased sediment elevation. In turn, increased sediment elevation stimulates plant growth because inundation duration of the vegetation is shortened. This results in a positive feedback between plant growth and sediment accretion. Implications of this feedback can be observed in the field in the form of dome shaped hummocks of cord-grass (*Spartina* spp.) that can be found at the mud-flat seaward of the salt-marsh edge (see fig.1.1.B).

Large scale lateral erosion of salt-marshes can set in when the marsh edge becomes disturbed, a phenomenon often referred to as cliff erosion (see fig.1.1.A; Adam, 2002; Allen, 2000). A disturbance, for example a storm surge, can initialize this erosion process by forming a steep slope. At the disturbed edge, sediment is more vulnerable to wave action and currents, and once a cliff takes shape erosion is not easily halted. The steep slope remains particularly vulnerable for waves and currents until it is stabilized, or lost completely. Likely, human activities, contribute significantly to the severity of the cliff erosion (Adam, 2002; Allen, 2000). Shipping traffic and dredging activities can increase exposure to currents and waves, speeding

up the pace at which lateral erosion proceeds. Nevertheless, the initiation of cliff erosion, which decimates salt-marsh area, might be natural and intrinsic to salt-marsh dynamics (Allen, 2000; van de Koppel, et al., 2005a).

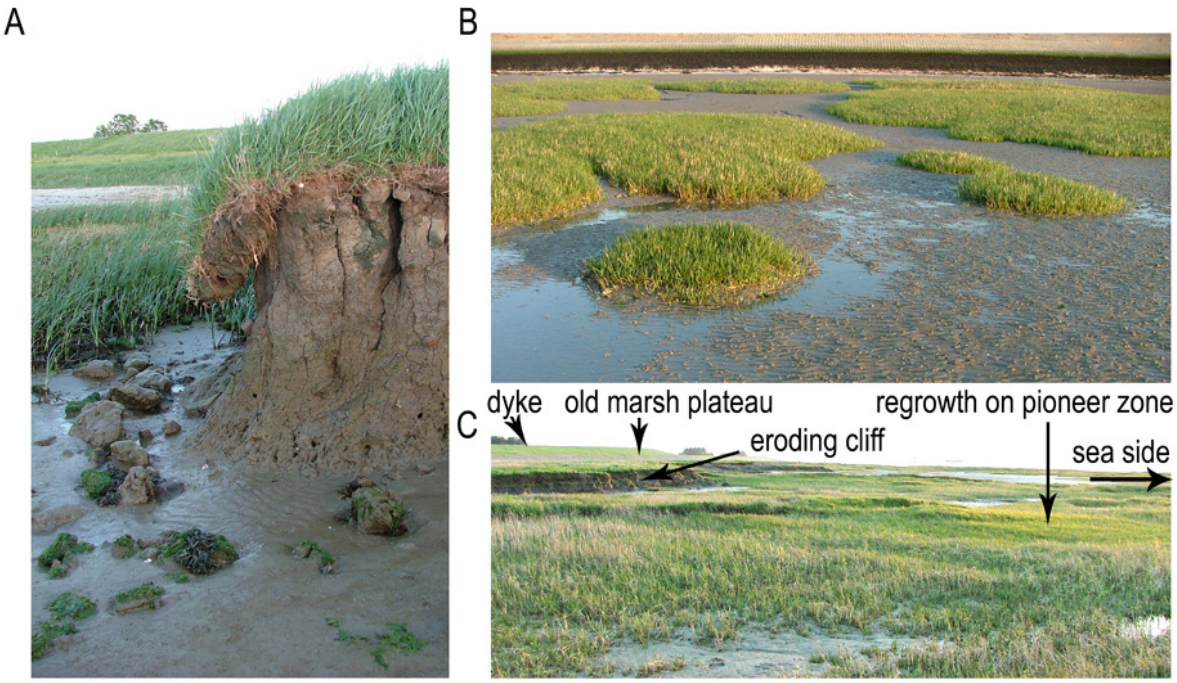

Figure 1.1. (A) Eroding cliff approximately 1 meter in height. (B) Patchy vegetation at pioneer zone of mud-flat and salt-marsh interface. A dome-shaped patch is seen in front. (C) Side view at the ground of a typical situation at salt marshes. At the sea side in front of the eroding cliff pioneer vegetation (Spartina) is growing (see also fig.2.A).

Recently, it was suggested that the same processes that are shaping salt-marshes can, on the long run, lead to large scale lateral erosion and collapse of salt-marsh ecosystems (Allen, 2000; van de Koppel, et al., 2005a). Conceptual modelling and empirical evidence supported this line of reasoning (van de Koppel, et al., 2005a). Due to the vegetation-sediment feedback the seaward edge of the marsh becomes steeper in time. As a consequence, salt-marsh edges become more vulnerable to disturbance as they mature (see fig.1.2.B). Eventually, the onset of cliff erosion at the marsh edge is likely to occur due to even small disturbances, like minor storm events. So, cliff erosion is hypothesized to be an inevitable and intrinsic consequence of the ecomorphological dynamics of (some) salt-marshes (van de Koppel, et al., 2005a). So, in a wide range of circumstances, lateral retreat due to cliff erosion will happen sooner or later. Data on sedimentation in salt-marshes, obtained from sediment core transects and spatiotemporal analysis of aerial photographs, support these results from the conceptual model (van de Koppel, et al., 2005a; van der Wal, et al., 2008).

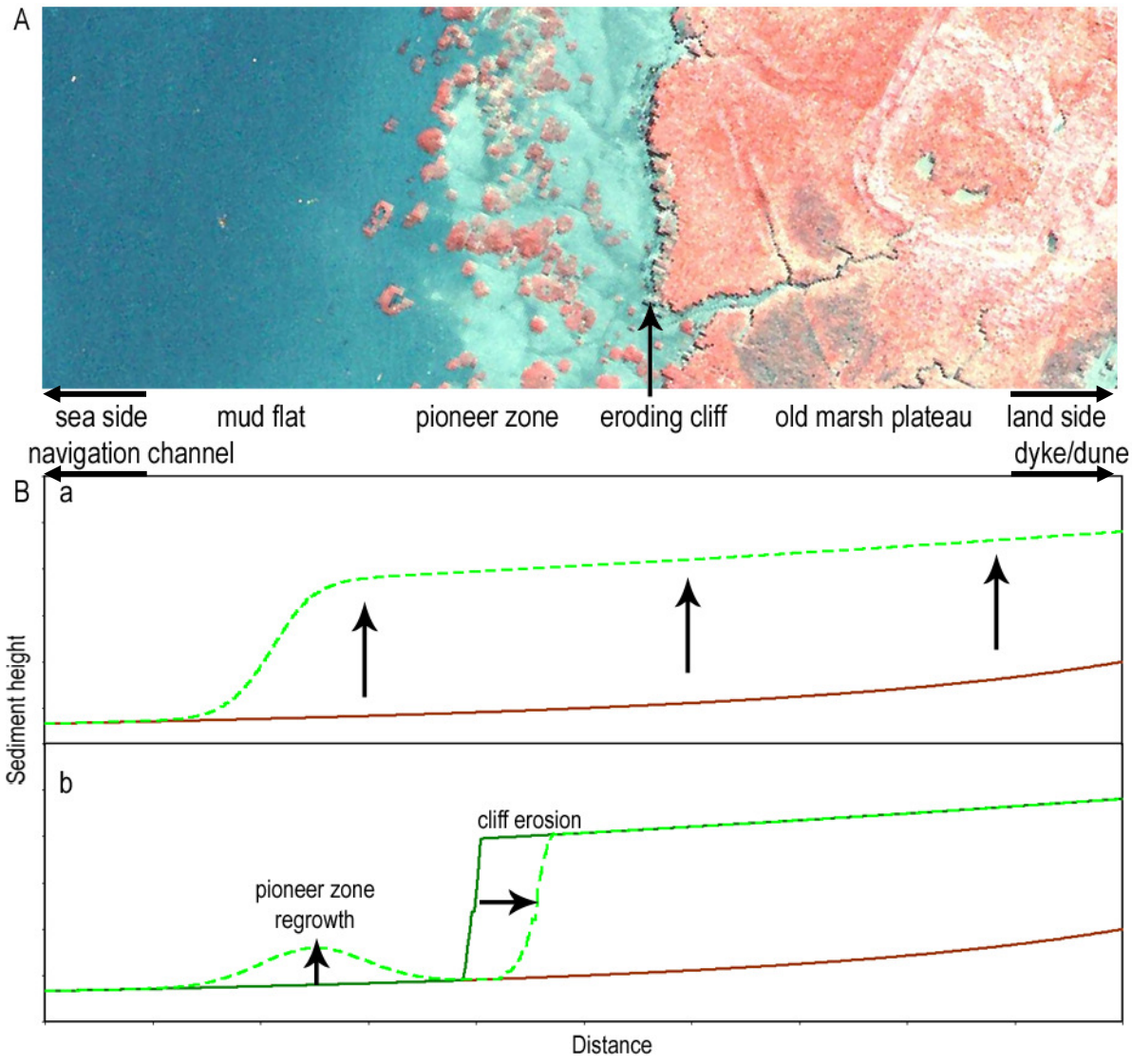

Figure 1.2. (A) Overview of salt-marsh by aerial photograph (RWS), comparable to situation (B.b) and see view from the ground in fig.1.1.C. (B) Cross-shore profile of salt-marsh dynamics of conceptual ecomorphological model, which mimics the development of the marsh in (A). Here, (—) is the initial bare mud-flat profile, (—) is vegetated marsh profile at beginning, and (- - -) is the final profile. First, (a) salt-marsh generation due to the positive feedback between vegetation and sedimentation. Second, (b) cliff erosion of old marsh and subsequent growth at the pioneer zone (after van de Koppel, et al., 2005a).

Even though erosion appears inevitable, the same conceptual modelling highlights another interesting feature of salt-marsh dynamics. Alongside cliff erosion, regrowth of pioneer vegetation on the cleared mud-flat in front of the salt-marsh cliff can take place at the same time. Thereby, resulting in rejuvenation of the mature marsh (see fig.1.2.B; van de Koppel, et al., 2005a; van der Wal, et al., 2008). Thus, erosion and sediment accretion of salt-marshes can be controlled by these same plant-sediment feedbacks. In addition, regrowth results in a buffer

against hydrodynamic forces in front of the old marsh plateau. So, this pioneer vegetation determines the conditions for lateral retreat and gradually slows down erosion of the salt-marsh edge. Therefore, of vital importance to the development and recovery of salt-marshes is establishment of this pioneer vegetation. These findings emphasize the importance of initial conditions for establishment and growth of vegetation, and the physical conditions that may constrain these intrinsic processes for salt-marsh development (van der Wal, et al., 2008).

1.3. Vegetation patchiness as indicator of ecosystem dynamics

Understanding vegetation dynamics at recovering pioneer zones may hold the key for effective and sustainable management decisions on measures for salt-marsh restoration and conservation. Pioneer vegetation at the interface of tidal flat and salt-marsh, often displays a striking mosaic of vegetated patches and bare mudflat as a result of the interplay between sediment-vegetation feedbacks and hydrodynamic forces (fig.1.2.A). However, little is known about driving processes behind this spatial patchiness of salt-marsh pioneer vegetation. Unravelling the processes determining establishment and development of plant growth might deliver valuable insight into biophysical constraints to initial salt-marshes development and recovery after cliff erosion. Recent advancements in research and theory on vegetation patchiness (Guichard, et al., 2003; Kéfi, et al., 2007a; Pascual & Guichard, 2005; Rietkerk, et al., 2004; Rietkerk & van de Koppel, 2008) are promising, because the conceptual ideas emerging from it, might give a good starting point providing important insight into patch dynamics at the salt-marsh pioneer zone.

It is suggested that spatial feedback processes can result in the formation of self-organized spatial patterns (Rietkerk & van de Koppel, 2008). Key to self-organization is that there is no external forcing that can on its own explain the observed order in ecosystems (or any other dynamic system). Instead, internal processes are responsible for the organized state (Camazine, et al., 2001). Self-organization implies that large-scale spatial patterns emerge from random initial conditions and local interactions between the components of the system. Mechanisms explaining spatial self-organization include consumer-resource interactions inducing wave-like dynamics (Hassell, et al., 1991; Rohani, et al., 1997), scale-dependent feedback causing regular patterning (see fig.1.3.A&B; Rietkerk & van de Koppel, 2008), and localized disturbance-recovery processes inducing scale-invariant cluster-size distributions (Pascual, et al., 2002b; Pascual & Guichard, 2005). Striking self-organized large-scale regular patterns (see for some examples fig.3.A) are found in, for instance, arid ecosystems (Klausmeier, 1999), savannas, mussel-beds (van de Koppel, et al., 2005b) and peatlands (Eppinga, et al., 2009). Nevertheless, regardless of the growing body of theoretical literature (Solé & Bascompte, 2006), the mechanism involved are in many cases still speculative. There are only a few studies describing spatial self-organization in real ecosystems (Rohani, et al., 1997, but see Rietkerk & van de Koppel, 2008).

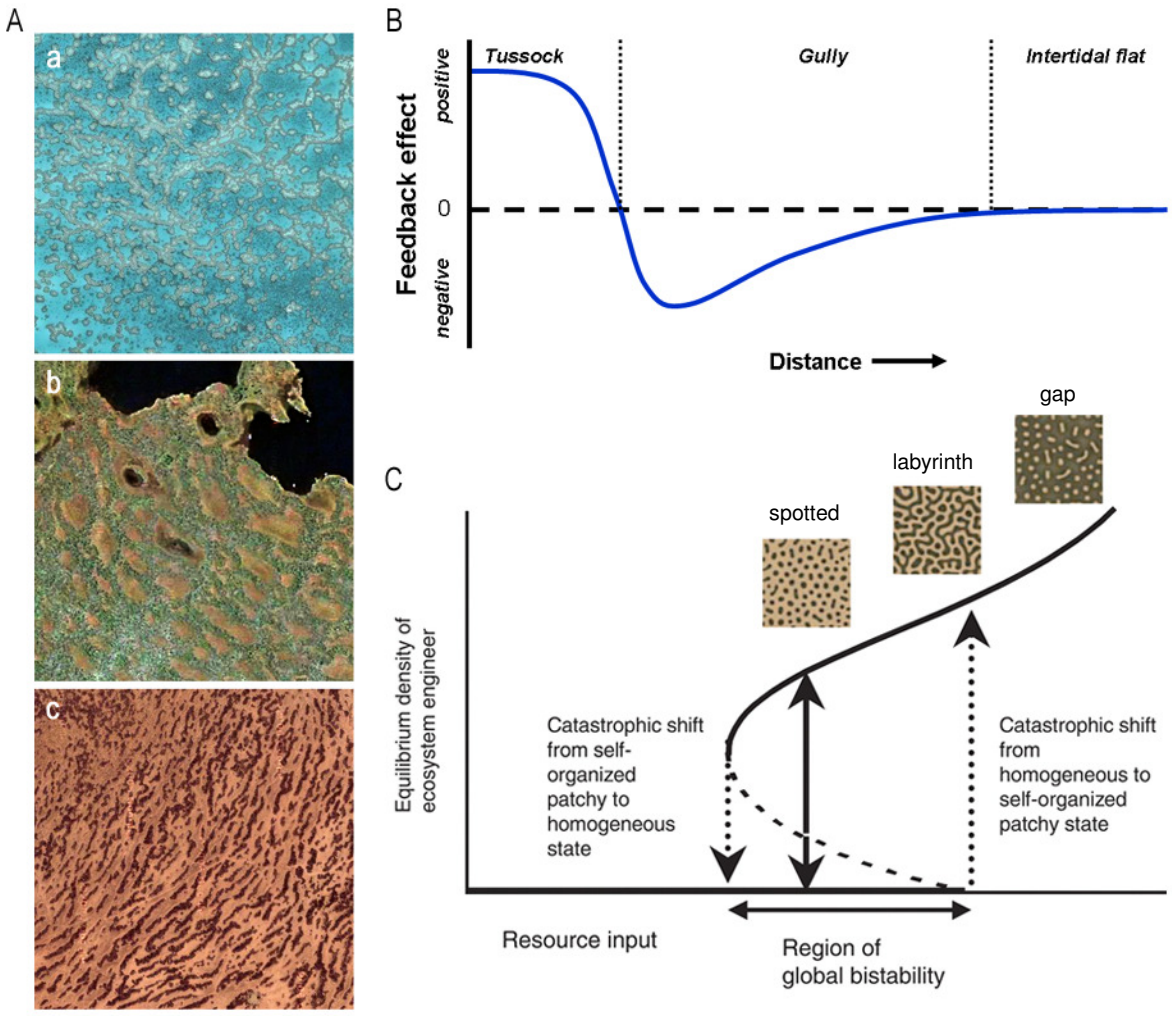

Figure 1.3. (A) Examples of regular spatial patterns in (a) coral reef near Australia, (b) peatlands in Siberia, and (c) tiger bush in Nigeria (from Google maps). (B) Scale-dependent feedback from Spartina sp. at the mudflat result in dome shaped tussocks and gullies (after van Wesenbeeck, et al., 2008). (C) Changes in regular spatial patterns could point to changes in environmental conditions like resource input (e.g. average annual rainfall) and potentially indicate proximity to a catastrophic shift (from Rietkerk, et al., 2004).

Theoretical models show that disturbance-recovery processes can result in predictable patterns over a range of spatial scales. These patterns are not regular but consist of patches of all sizes, which, despite their irregularity, are characterized by predictable patch-size distributions. Typically, the frequency of patches, *f(S)*, of a particular patch size, *S*, decreases as a power of the patch-size (Pascual, et al., 2002b; Pascual & Guichard, 2005):

$$f(S) = CS^{-\alpha} \qquad (1.1)$$

Herein is *C* the normalization constant, and *α* the scaling exponent. This relation, the power-law, is characterized by a straight line when plotted on logarithmic scales (see for example fig.1.4.a). This inverse power relation is called scale-invariant or self-similar, because the same pattern is found for any scale of observation. Models that have been used to uncover the causes of the

emergence of these power laws reveal a common mechanism: the large-scale spatial vegetation dynamics (or spatial dynamics of e.g. mussels, oysters, and diatoms in other ecosystems) are determined by spatial extension or contraction of patches. This implies that spatial processes occurring at the boundaries of existing patches, like growth and mortality, are important for the dynamics of these ecosystems as a whole. Examples that have been put forward of such processes are disturbance-recovery cycles of forests by fires (Bak, 1997; Malamud, et al., 1998) or storms (Pascual & Guichard, 2005) and wave disturbed mussel-beds (Guichard, et al., 2003). So, local disturbance and recovery processes might be general applicable, explaining dynamics in a wide range of ecosystems.

Not only can power-law patch-size distributions be used to characterize the spatial structure of an ecosystem, but these patterns may also be used as indicator to assess ecosystem status and predict potential catastrophic shifts. In general, the idea has been put forward that the way in which spatial patterns manifests themselves reflects the level of stress exerted on an ecosystem (Rietkerk, et al., 2004). In regular spatial patterns increasing stress might be characterized by a sequential change from gap, to labyrinth, to spotted pattern (see fig 1.3.C). If this assumption (Kéfi, et al., 2007a; Rietkerk, et al., 2004) is correct, self-organized patchiness can be used as an indication of ecosystems health. Recent studies on semi arid ecosystems suggest that the spatial configuration of vegetation patches indeed reflects annual rainfall patterns (Barbier, et al., 2006; Kéfi, et al., 2007a; Rietkerk, et al., 2004; Scanlon, et al., 2007). More specific, also irregular spatial patterns in semi arid ecosystems have shown that power-laws in vegetation patches change along a gradient of annual precipitation (Scanlon, et al., 2007). Furthermore, these spatial patterns deviate from power-laws if the ecosystem is proximate to a sudden shift to imminent desertification which is driven by increased grazing pressure (see fig.1.4) or drought stress (Kéfi, et al., 2007a).

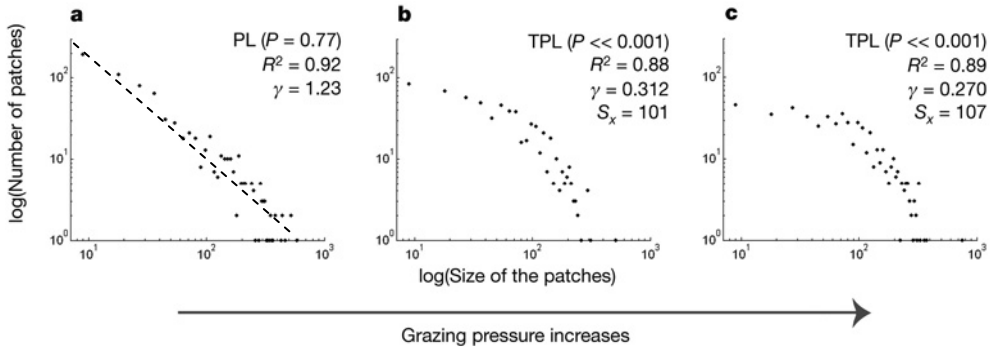

Figure 1.4. An example of vegetation patch-size distributions in a semi arid ecosystem at different levels of grazing pressure. The power distribution becomes truncated if grazing pressure increases (from Kéfi, et al., 2007a).

1.4. Vegetation patterns in pioneering *Spartina anglica*

Localized disturbance and recovery processes might also explain the spatial structure of salt-marsh pioneer zones. English cord-grass (*Spartina anglica*), the primary perennial pioneer species at many salt-marsh pioneer zones in north-west Europe, forms unevenly spaced hummocks of different sizes at the mud flat (see fig.1.1.B & fig.1.2.A, and box II). Disturbance can occur by currents and waves, which attack the edges of patches, inducing lateral erosion (fig.1.5), counterbalanced by lateral growth of the tussocks by means of rhizomes (van Hulzen, et al., 2007). In the field, contraction and extension of *S. anglica* patches by these local disturbance-recovery processes, determining the spatial structure of the pioneer zone of salt-marshes, can be observed. Some vegetation-patch edges seem disturbed, because the roots of the vegetation are partly dislodged from the mud (see arrow in fig.1.5.A&B). It is likely that, once this disturbed edge is formed, the vegetation becomes more susceptible to hydrodynamic forces like currents and waves, and will dislodge and erode even further. So, due to this disturbed edge, adjacent vegetation is likely to erode as well. This erosion process is spatially correlated and self-propelling. Like a fire, the disturbance spreads through the vegetation patch eroding it completely (see fig.1.5.C). However, vegetation patches can recover by lateral spread of roots, which allow *S. anglica* to colonize adjacent bare mud flat. Thus, these local spatial processes might explain the spatial vegetation structure at the pioneer zone, and, if so, power-law patch-size distributions can be expected. Consequently, pioneer zones, at the interface of mud-flat and salt-marsh ecosystems, may provide a unique opportunity to test whether the dynamics are governed by local disturbance-recovery processes, and if power-law patch-size distributions characterize the irregular vegetation patchiness.

Power-law patch-size distributions might reflect the level of stress exerted on the pioneer vegetation resembling semi arid ecosystems. Exposure to currents and waves, are likely to influence the relative importance of disturbance and recovery processes. If salt-marsh pioneer zone sites experience high exposure to currents or waves, erosion processes are likely to play a larger role in shaping the spatial configuration of the *S. anglica* tussocks compared to sheltered locations. This might result in differences in, or even deviations from, power-law behaviour at high levels of stress (see fig.1.4). For instance, due to high stress it will become more difficult for patches to grow and merge. Therefore, in stressed pioneer zones less large patches are to be expected compared to sheltered locations. In this example the scaling exponent of the power-law will be larger (or the slope of the line will be steeper) when a pioneer zone experiences high stress, compared to sites with low stress levels. Furthermore, deviations from the power-law could potentially point to changes in the environmental conditions that exist at the marsh edge. Increased influences of hydrodynamic forces might cause these deviations. Just like increased grazing pressure in semi-arid ecosystems resulted in truncation and pointed to proximity of a sudden shift to a desert state (see fig.1.4). So, truncation in salt-marsh pioneer vegetation might point to proximity of a shift to bare mud-flat, if the hydrodynamic conditions become too harsh. Consequently, power-law patch-size distributions might be good indicators of vegetation dynamics at the pioneer zone, and may be used to assess current status and potential for future recovery of tidal-salt marshes.

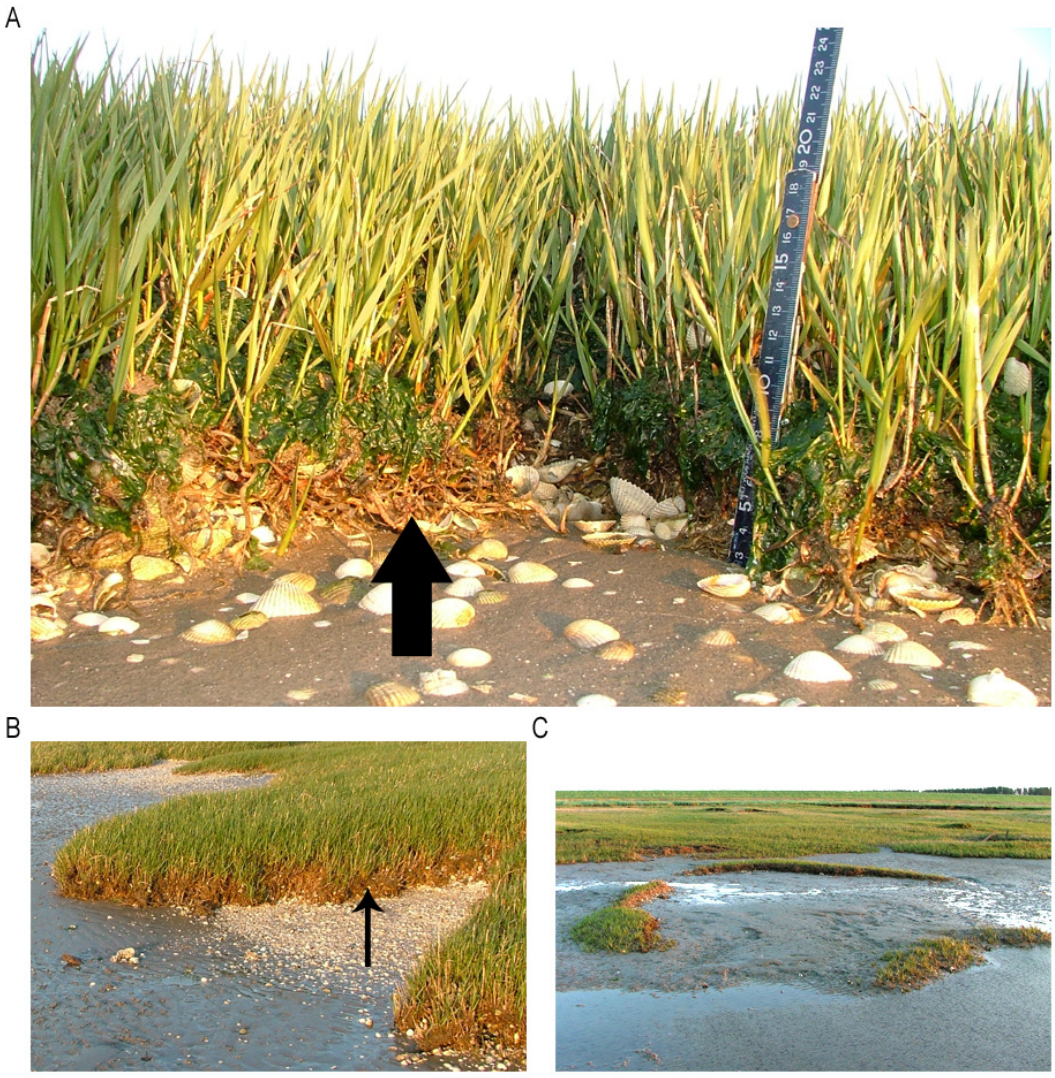

Figure 1.5. (A) Close-up of disturbed edge of vegetation patch (black arrow). Roots of S. anglica are partly dislodged from the mud-flat. (B) The same disturbed edge (black arrow) shows a typical V-shaped disturbance of the patch. (C) An example of a vegetation patch almost completely eroded by propagation of the disturbed edge through the patch.

Box II – English cordgrass (*Spartina anglica*): morphology and life-history traits of a pioneer species

English cordgrass (*Spartina anglinca, formerly known as Spartina townsendii*) belongs to the family of grasses (*Poaceae*), and is a salt tolerant perennial plant (Olofson, et al., 2009; van Hulzen, et al., 2007). This species is a hybrid of the alien species Smooth cordgrass (*S. alterniflora*), originating from North-America, and the in north-west Europe endemic Small cordgrass (*S. maritimae*), and probably originated in England around 1870, after the introduction of *S. alterniflora* due to shipping traffic to the New World (Hemminga, et al., 1998; Jacobusse & Hemminga, 2001). Now, in most of the North-West European marshes *Spartina anglica* has outcompeted the endemic *Spartina* species.

Although the morphology is highly variable, probably dependent on the level of stress by inundation and salinity, the stems reach a height of 30 to 130 cm, and the leafs are 20 to 60 cm long and about 2 to 17 cm wide. Its colour is yellowish green in spring and summer and becomes light brown in autumn and winter. In North-West Europe this species is flowering in July to November.

Figure II.1. English cordgrass (Spartina anglica). On the left a single stem is shown, and on the right a fragment of a S. anglica patch is shown, which clearly demonstrates the intertwined rhizomes.

S. anglica can persist under a wide range of tidal conditions and can be found in the low to high salt-marsh. However, this grass species is usually associated with the lower salt-marsh and pioneer zone because it often is the primary colonizer of the mud-flat. *S. anglica* is a wind pollinated species that spreads by seeds and vegetative means. Sending out underground rhizomes, resulting in dens interwoven roots (see fig. II.1), it initially spreads into circular tussocks (Olofson, et al., 2009). If conditions are good these patches may merge into large stands or meadows. *Spartina anglica* can increase sedimentation accretion of fine suspended material like silt and clay (Hemminga, et al., 1998).

1.5. The Scheldt-estuary (Westerschelde)

A typical estuary in which salt marshes are facing severe lateral erosion is the Scheldt-estuary. This estuary is part of the Scheldt basin and runs into the North Sea in the South-West of the Netherlands (see fig.1.6). Running through three countries the Scheldt catchment area is 22,116 km^2. The length of the river, from its origin in France to the mouth at Vlissingen (Flushing) is 355 km (Baeyens, et al., 1998). The last 160 km trajectory from Gent downstream is referred to as the Scheldt estuary. Tidal forces are strong along this part of the river, and fresh river water and

salty sea water are responsible for a salt gradient (see also info Box I on geomorphology of tide driven estuaries). Because of this gradient and the river's extent, the Scheldt is unique and the last real estuary in Western Europe (Baeyens, et al., 1998; Meire, et al., 2005). Downstream of the Dutch-Belgian border to the mouth the estuary is called Westerschelde. The Westerschelde estuary is more diverse compared to the river, as in this part of the estuary multiple deep and shallow gullies alternate with salt-marshes, mud- and sand-flats. The wetlands in this estuary are protected under the Ramsar convention and EU legislation, Natura-2000 (Baeyens, et al., 1998; Meire, et al., 2005).

Next to the ecological value, the Scheldt is economically important because it links the harbours of Gent, Antwerpen, Terneuzen and Vlissingen to the North Sea. Consequently, keeping the navigation channels open is very important for local business and employment (SIC, 2009). A treaty between Belgium and the Netherlands obliges the Dutch government to keep the Westerschelde open since 1839. Because of this agreement, maintenance dredging and dredge spoil deposition are executed continuously. In addition, capital dredging was carried out in the period 1970-1975 and 1997-1998 to deepen and widen the navigation channels to allow larger ships to reach Antwerp harbour, and to be less dependent on the tide. Further deepening is carried out at the moment (van der Wal, et al., 2008).

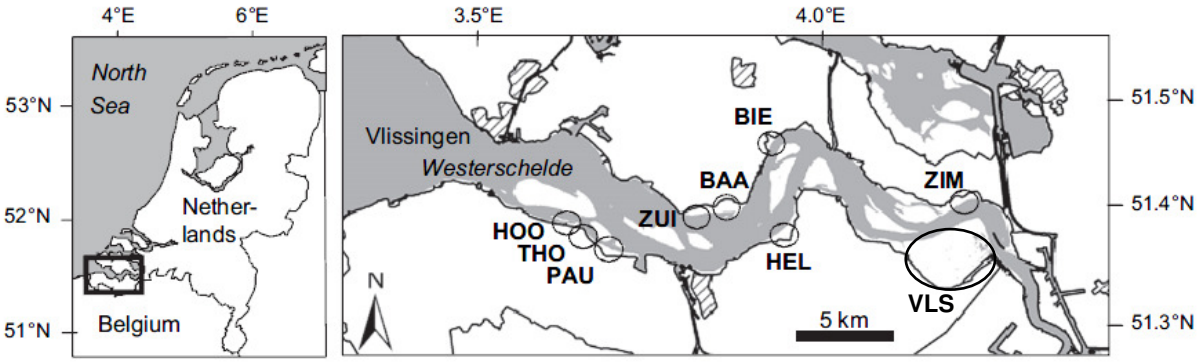

Figure 1.6. Location of nine salt-marshes along the Scheldt-estuary (Westerschelde), southwest Netherlands, of which six are used in this study. Baarland (BAA), Biezelingsche Ham (BIE), Hellegatpolder (HEL), Hoofdplaat (HOO), Paulinapolder (PAU), Thomaespolder (THO), Verdronken land van Saeftinghe (VLS), Zimmermanpolder (ZIM), and Zuidgors (ZUI) (figure from van der Wal, et al., 2008). Locations Biezelingsche Ham, Verdronken land van Saeftinghe, and Zimmermanpolder are not used in this study.

Through the centuries the estuarine landscape in the Scheldt basin is reshaped to comply to human needs (Meire, et al., 2005). The scale of economic activity in the Scheldt basin has increased even more profoundly in the last century due to increasing human population and wealth. This has resulted in a significant increase in anthropogenic pressure on the estuary (Baeyens, et al., 1998; Meire, et al., 2005). Pollution, alteration and fixation of the navigation channels, and changes in land use have changed the initial natural landscape elements and biodiversity. These have either been severely degraded or lost entirely. Especially, large parts of the salt-marsh, mud-flat and other wetland area have been claimed and transferred into agricultural land. For instance, about 6040 ha estuary is acclaimed since 1900 matching a decline of 56% between 1900 and 1990. With these changes the estuary lost much of its dynamic nature (Meire, et al., 2005).

Now, compared to their original extent, tidal salt-marshes are present as marginal fringes along the Scheldt-estuary (apart from the 'Verdronken land van Saeftinghe'), and further degradation of the wetlands (mud- and sand-flats, and salt-marshes) in the estuary is undesirable. Additional deepening of the navigation channel, shipping traffic and relative sea level rise might cause further degradation of these habitats in the estuary (Kirwan & Temmerman, 2009; Temmerman, et al., 2004). Monitoring the effects of these economical activities on the wetlands is important to aid conservation of the valued wetlands. So, developing indicators to assess the balance between disturbance and recovery (erosion and growth) is important to support decision-making. Thus, using power-laws as indicator of salt-marsh ecosystem status and development might be a valuable new tool which is suitable for this purpose.

1.6. Research questions

The aim of this thesis is to address the main research questions:

Research Question 1:

> ***Do disturbance and recovery processes at the pioneer zone of tidal salt-marshes determine spatial structure of salt-marsh pioneer vegetation in such a way that patch-size distributions exhibit power-laws?***

And if this is indeed a fact:

Research Question 2:

> ***Can these vegetation patch-size distributions be used as indicators of vegetation dynamics to assess current status and future development of salt-marsh ecosystems at the interface with the tidal flats?***

To follow the aim of this thesis four sub questions will be addressed:

Sub Question 1:

> *How should power-law frequency distributions be used in spatial ecological data?*

Sub Question 2:

> *Does spatial vegetation patch structure in salt-marsh pioneer zones exhibit power-law distributions and how are they related to external forcing factors?*

Sub Question 3:

> *Can generic and spatial explicit models explain pattern formation in salt-marsh pioneer vegetation at the mud-flat?*

Sub Question 4:

> *Are power-laws useful indicators to assess current status and future development of salt-marshes?*

1.7. Outline of thesis

In order to support protective measures of salt-marsh ecosystems, there is a need for fundamental understanding of the highly dynamic nature at the interface of mud-flat and salt-marsh ecosystems. Here, the balance between disturbance, by lateral erosion, and recovery, by growth of pioneering vegetation, determines the outcome and variation in space and time. In this study, I aim for an integrative approach, combining empirical and theoretical work to get more insight into the main drivers of this dynamics. Therefore this research will be conducted in three parts with three different approaches, each having their own objective:

First, power-law methodology will be reviewed (chapter 2). As discussed in the introduction power-laws are used to describe patchiness in a variety of ecosystems. However, there is a lack of consistency in the methods used to show power-laws in the size distribution. To show these patterns are present in spatial ecological data, it is crucial to use a reliable methodology, as other distributions, like lognormal and exponential, could be wrongly identified as power-laws. So, a literature survey on methodologies used to analyse ecological data for power-law patterns is the first step of this research to assure reliable methods. An overview of mathematical and statistical properties and procedures, on the use of patch-size distribution in spatial ecology, will be given and discussed.

Second, a spatiotemporal analysis of vegetation patches at the salt-marsh pioneer zone will be presented (chapter 3). The site-specific level of exposure to currents and waves is potentially a major determinant of salt-marsh development, determining the balance between erosion and growth at the pioneer zones. Six salt-marsh locations along the Scheldt-estuary are chosen for this correlative approach. All six marshes have a distinctly different hydrodynamic exposure. For these six salt-marsh locations, remotely sensed data is available. So, the main objective of this part of the research is to analyse the spatial vegetation structure at pioneer zones from different salt-marshes and relate this to the local hydrodynamic conditions. If there is a strong link between the spatial structure (patch-size distribution) and hydrodynamic conditions of salt-marsh locations, this is in favour of using power-law patch-size distributions as indicator of hydrodynamic stress.

Third, the salt-marsh pioneer zone is modelled to get insight into the vegetation dynamics (chapter 4). A spatial-explicit modelling technique, called cellular automata (CA), that integrates disturbance and recovery processes in the rules of the model, will be used to investigate the consequences of erosion and growth on the spatial structure of the salt-marsh pioneer zone. Because of the typical stochastic nature of disturbance, the use of continuous time models that are based on partial differential equations, is not appropriate, because these models are suboptimal for incorporation of random events. In contrast, CA do have the ability to incorporate random processes like wave disturbance (Guichard, et al., 2003; Pascual & Guichard, 2005). The qualitative agreements between model and data form the basis of the final discussion (chapter 5) on the use of power-law patterns as indicator in salt-mash monitoring. Here, the results are discussed, with emphasis on the applicability of power-laws as monitoring and assessment tool, followed by the conclusions point-wise summarizing answers to the main research questions.

2. Using power-law size-distributions to evaluate patchiness in spatially organized ecosystems

2.1. Introduction

Power-law relations, where the response variable is related to the power of the control variable, are widely known across sciences describing various natural phenomena. Examples range from the magnitude distribution of earthquakes (Gutenberg-Richter law) and solar flares, to the distribution of income or city-sizes (Zipf's law) (but see for extensive review e.g. Newman, 2006). Power-law scaling is also a familiar phenomenon in biological sciences with Kleiber's law applying too body size distributions (Enquist & Niklas, 2001), the species-area relationship (MacArthur & Wilson, 1967), or self-thinning in plant populations (Enquist, et al., 1998) as classical examples. Moreover, recent claims of power-laws in ecological data show their apparent ubiquity across this scientific discipline. For example, networks of trophic (Garlaschelli, et al., 2003) and mutualistic (Jordano, et al., 2003) interactions, animal foraging behavior (Sims, et al., 2008), and relative species abundance in ecological communities (Harte, et al., 1999) al seem to follow power-law distributions. More recent, power-laws are shown to appear in the patchy spatial aggregation of mussels (Guichard, et al., 2003), ant colonies (Vandermeer, et al., 2008) and semi-arid vegetation (Kéfi, et al., 2007a; Scanlon, et al., 2007). It has been suggested that these patch-size distributions, or deviations from them, are useful as leading indicators of stress and disturbance of those ecosystems.

Despite of the general use, there is a lot of controversy about scaling laws in general (Avnir, et al., 1998), and especially in ecology (Halley, et al., 2004). The variety of methods used and the debate about power-law claims indicates there is a lot of misunderstanding regarding power-law analysis. Furthermore, improper implementation of power-law analysis in ecology could results in incorrect claims or interpretations. For instance, other long-tailed (skewed) distributions (e.g. log-normal, or exponential) are easily mistaken to follow power-law distribution because lack of observed scales, limited number of observations, or flawed statistical techniques. That makes is possible that other distributions are wrongly identified to follow an inverse power distribution. It is clearly a complicated, but fundamental, question whether an apparent linear relation along logarithmic axis really suggests power-law behavior or not. How do we distinguish noise, most of the time inevitable in ecological-data sets, from systematic departure from power-law behavior? How strict do we have to be to avoid missing out on existing power-law relationships? Despite these questions and uncertainties, remarkably little literature is devoted on how to avoid pitfalls in analyzing spatial ecological data for power-law presence (but see Edwards, et al., 2007; Okuyama, 2008; Sims, et al., 2007).

2.2 Power-law patch-size distributions in spatial data

2.2.1 The power-law

Natural phenomena are described by a power-law if the dependent variable *y* varies as a power of the independent variable, *x*, like:

$$y = bx^a \qquad (2.1)$$

Were *a* is the scaling exponent and *b* a constant. Only the scaling exponent holds phenomena specific information, because the constant is only related to the number of observations and disappears when normalizing. When the logarithm of both dependent and independent variables are taken, power-laws follow a linear function:

$$\log(y) = a\log(x) + \log(b) \qquad (2.2)$$

The use of power-laws is appealing because of the mathematical simplicity. Describing complex (rough) natural phenomena by just one defining parameter (the scaling exponent) makes these laws very practical. Related to its simplicity is the scale-invariant property of power-laws. The distribution is the same at every scale of observation. So, power-laws are closely related to fractals (Solé, et al., 1999), and proving power-law presence implies the phenomenon is at least a statistical fractal (Li, 2000). Moreover, the idea of this scale-free behavior and self-similarity at all levels is very attractive because it suggests a common underlying mechanism for the dynamics and properties of different kinds of systems. Therefore, power-laws, scale invariance, and self-similarity across scales are considered a characteristic property of complex systems, where small-scale interactions scale up to determine the large-scale property of the system (Solé, et al., 1999).

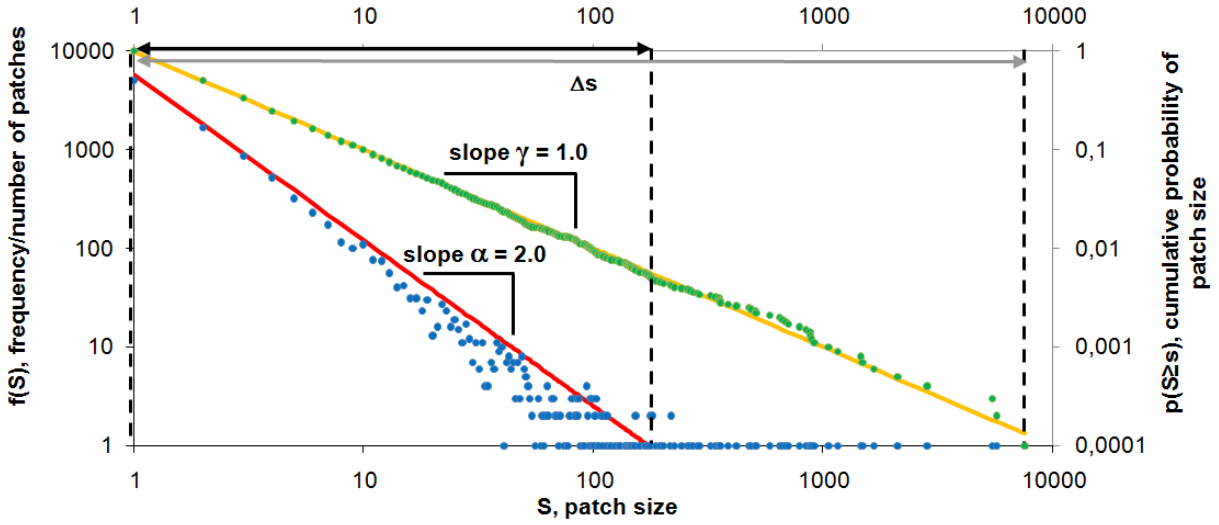

Figure 2.1. Power-law frequency (blue) and inverse cumulative (green) distributions of same data-set. The slope of the best fitted straight lines (red and orange) gives an estimate on the scaling exponents (α and γ, slope of the lines, where γ=α-1). The gray arrow indicates the range of data which usually is referred to as the order of magnitude difference, ΔS. However, a more robust, but conservative, estimate on ΔS is given by the black arrows.

Generally, power-laws can be divided into two classes when addressing ecological phenomena. On one hand there are 1) bivariate relations between two variables, for example allometric relationships like Kleiber's law. And the relation between deer antlers and body mass (Clutton-Brock, et al., 1980), or the species-area relation (MacArthur & Wilson, 1967) are examples of this kind of relationship. On the other hand there are 2) power-law frequency distributions, where the number of occurrences of an event declines with the size of the event as an inverse power distribution. Spatial patchiness can be described using power-laws in different ways, which all are related to fractal analysis (Li, 2000). Most common are relationships expressing patch area as function of its boundaries, observed area as function of observation scale using box-counting methods, or computing the patch-size frequency distribution. Although both kinds of relations can be used to describe landscapes and spatial patchiness, here we will focus on the latter one. Typically, the number of patches, *f(S)*, of a particular patch size, *S*, decrease as a power of the patch size (see equation 1.1). Were α is the scaling exponent, which, on logarithmic scales, determines the slope of the linear relation (fig.1.A), and *C* is a constant dependent on the number of observations.

A disadvantage of the way in which patch-size distributions are usually displayed (as non-cumulative distributions, see eq. 1.1 and fig.2.1 blue dots) is that it tends to make many non-power-law distribution power-law like. Especially, when data is derived empirically and contains a lot of noise. To resolve this, power-law distributions can be expressed as inverse cumulative distributions (see fig.2.1). This means the probability, *p*, to find patches equally or larger than a threshold value, *s*, falls of as:

$$p(S \geq s) = S^{-\gamma} \qquad (2.3)$$

Where γ is the scaling exponent. This inverse cumulative distribution is also referred to as 'survival curve' (Sims, et al., 2007). Inverse cumulative distributions show only a straight line on logarithmic axis in case phenomena exhibit real power-law behavior over all scales of observation. Any deviation from power-law behavior is accentuated with the inverse cumulative distribution because successive points along the distribution are correlated. These properties make inverse cumulative distributions a good visualization tool, and give a good first impression if patch-size data exhibits actual power-law behavior, or not. The slope of the strait line, when plotted on logarithmic axis, is less steep in this representation than the actual data. So, there has to be corrected for this bias when the slope is used for parameter estimation.

2.2.2. Defining patches

Obviously, recognizing patches, or clusters, of similar species composition or habitat type is crucial in analyzing spatial data for patch-size distributions. Unfortunately, defining patches is not always straightforward (Fagan, et al., 2003). Delineating areas needs firm definitions on what is considered patch and what is not. So, technical issues concerning cluster analysis deserve special attention, and are discussed in the next section (2.3.4 Acquisition and preparation of spatial data). Furthermore, how to approach spatial cluster analysis depends on the data type. Here, only grid-based data are considered because this is relevant to the data available in this study, but similar issues defining patches holds for continuous spatial data.

When defining patches on a grid, occupied cells are considered to be part of the same cluster if they are adjacent (connected) to cells with the same species, or state (e.g. grass, tree, or disturbed, undisturbed). Connectedness of the grid cell with nearby cells to form a cluster is

defined by the nearest neighbourhood. The most commonly used neighbourhood types are the four nearest adjacent grid cells (*z*=4), this is called the von Neumann neighbourhood (fig.2.2.A above), whereas the Moore neighbourhood (fig.2.2.A below) also includes the four nearest diagonal cells (z=8; Balzter, et al., 1998). But, a variety of other neighbourhoods can be used as well, depending on the local rules of interaction that are assumed or identified in the study. As a result of the neighbourhood type chosen, the connectivity, and thus, the clusters-size distribution differs, as demonstrated in figure 2.2.B, and 2.3. Using the von Neumann or Moore neighbourhood on the same grid data 'perceives' a different level of connectivity, because the first find eight separate clusters where the latter one finds just one cluster of connected cells. So, the neighbourhood used in the analysis, strongly influences the size and number of patches that is found in the grid based spatial data. Therefore, it is important to use the same neighbourhood type when comparing spatial data.

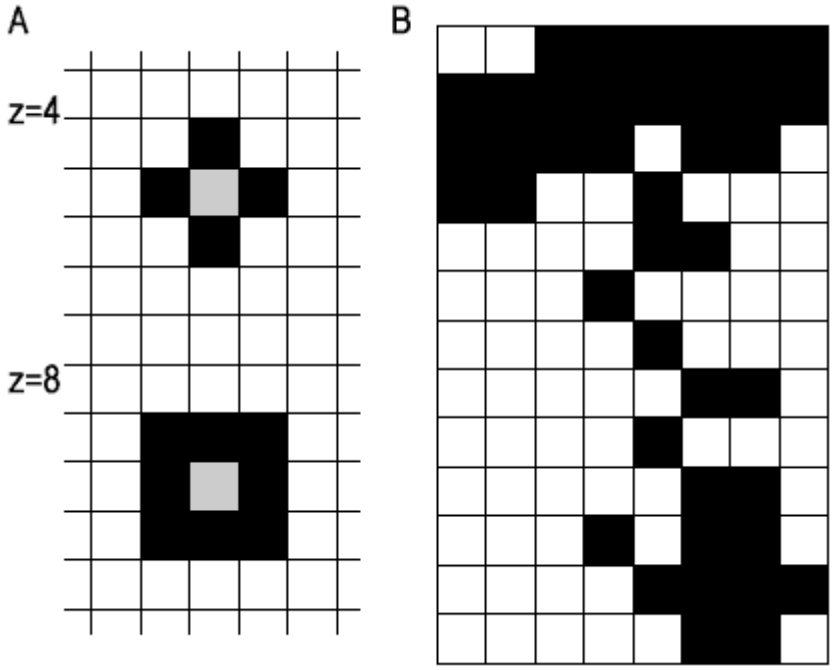

Figure 2.2. Nearest neighbourhood types used in cluster analysis. (A) two typical neighbourhoods mostly used in cluster analysis of grid based data: the von Neumann neighbourhood are the four adjacent cells (z=4), and the Moore neighbourhood with additional the four nearest diagonal sites (z=8). (B) An example patch where the von Neumann neighbourhood will find eight clusters, and one cluster is found using the Moore neighbourhood.

2.2.3 Processes from which power-laws arise: key concepts

In absence of an underlying topographic template, patchiness in ecosystems arises due to an environmental driver which prevents the system from reaching complete coverage of the area. This driver can be an edaphic factor, like a stress or disturbance. In case we consider disturbances, like fire or wind, a disturbance event will remove biomass from the ecosystem, leaving a gap behind. This event will induce a cycles of succession, where the ecosystem eventually will recovery from this disturbance. When considering a vegetated ecosystem under a specific disturbance regime, the relative importance between disturbance and recovery determines the functioning of the ecosystem. Its state can then be described by, for example,

the fraction of vegetation cover (see fig.2.4, where a hypothetical response of an ecosystem at different levels of disturbance is shown by the equilibrium vegetation cover). At low to moderate disturbance regimes, the ecosystem remains in a relative healthy state, maintaining a high level of vegetation coverage because recovery can keep up with the disturbances of the system. However, when the disturbance probability is gradually increased, vegetation cover will decline faster toward a significantly lower vegetation cover. Increasing the level of disturbance even further, the spatial pattern can become so much fragmented that it loses its large scale connectivity. This implies that there is no remaining vegetation patch that spans the area from one to the other side anymore. "Percolation" through the system (a term that originates from mathematics to describe, for instance, the flow through a porous medium), through this spanning vegetation patch, is no longer possible. At this critical point power-laws are found, which are also called 'percolation fractals' (see also patch-size distributions and corresponding critical points in fig 2.3). This critical or percolation point is often referred to as 'criticality', and systems exhibiting such kind of dynamics without clear localized spatial processes are referred to as 'classical critical' systems (Pascual & Guichard, 2005).

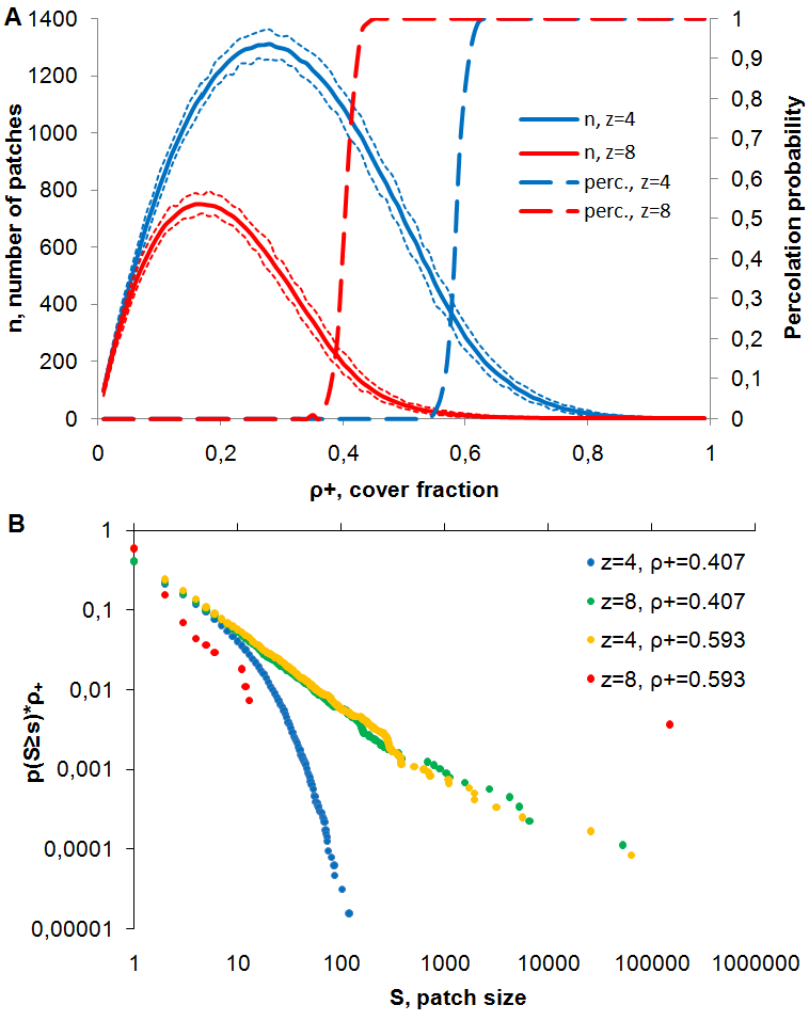

Figure 2.3. Computer simulations of the effect of neighbourhood type on probability to have percolation in the system, patch number and patch-size distribution in neutral model (lattice 100x100 pixels). (A) Depict number of patches (solid lines) and percolation probability (dashed

lines) with increasing cover fraction (dotted lines indicate 95% confidence interval), using two different neighbourhood types (blue lines for z=4 or von Neumann neighbourhood, and red lines for z=8, or Moore neighbourhood. In (B) the patch-size distributions belonging to the percolation points (ρ_{crit}) are shown. At z=4, we find $\rho_{crit.}$=0.593, and if z=8, then $\rho_{crit.}$=1-0.593=0.407 (Newman, 2006). But, also distributions at sub- (z=4, ρ_{+}=0.407) and supercritical (z=8, ρ_{+}=0.593) values are shown.

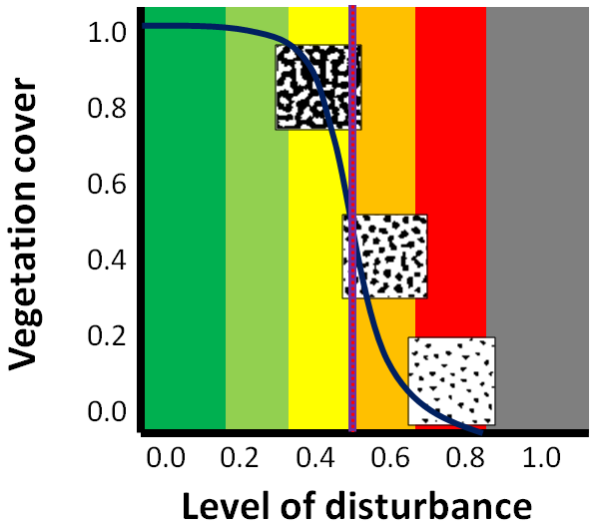

Figure 2.4. Phase transition of hypothetical spatially structured ecosystem under increasing disturbance. At the critical point (red dotted line) of the system the large scale connectivity is lost. Power-laws are found in the patch-size distribution at and near this point (purple area). In 'robust critical' systems the range over which power-laws can be found is wider (yellow and orange area). Explanation on the coloured bands: (dark green) closed canopy, (light green) gaps, (yellow) patchiness with large scale connectivity, (orange) patchiness where large scale connectivity is lost, (red) critically fragmented pattern, (gray) no vegetation at all, only bare sediment left.

Because of the apparent ubiquity of power-laws in nature it was thought that many systems are close to the critical threshold point. The concept of Self-Organized Criticality (SOC) was posed to explain why power-laws are so wide spread (Bak, 1997). SOC assumes that in most natural systems, intrinsic processes are at work that drive the system toward this critical point. A well-known example of SOC applied to ecology is the distribution of forest fires, which seem to exhibit power-laws in the distribution of gaps created by fire (Malamud, et al., 1998). After a fire, the forest slowly recovers and burned trees are replaced. The remaining fragmented landscape, however, hampers fire propagation, and new forest fires remain localized events. As the forest recovers and patches merge into homogeneous stands, the vulnerability of the forest to fires increases, and there is a higher likelihood of a large fire occurring that again fragments the landscape. Due to this enduring interplay between fire (disturbance) and succession (recovery), a fragmented landscape emerges that has power-laws in the distribution of gap-sizes (Malamud, et al., 1998).

A critical assumption for the models of self-organized criticality is that the spatial dynamics of the disturbance act on a much faster timescale than the recovery. This is the case in the forest fire example, where fire propagates in a time frame of hours, while recovery can last for years. A large number of systems, however, display power-laws but have recovery rates that are similar

to that of the disturbance. Recent studies show that a variety of spatially organized ecosystems can even exhibit power-law patchiness in systems that not meet the terms of classical or self-organized criticality (Guichard, et al., 2003; Kéfi, et al., 2007b; Pascual, et al., 2002b; Pascual & Guichard, 2005; Scanlon, et al., 2007). In these so called 'robust critical' ecosystems, power-laws can be found in a wider range of environmental conditions (disturbance regimes) than in classical critical systems. Consequently, this kind of dynamics can explain a wide variety of spatiotemporal patterns encountered in nature, which are not reflected well by classical or self-organized criticality concepts. Moreover, in these systems, deviation from power-laws were proposed to indicate the proximity of critical points where switches to degraded ecosystem states are expected, as was suggested to occur in fragmented arid ecosystems (Kéfi, et al., 2007a; Kéfi, et al., 2010 in press-b).

However, power-laws in spatial data not necessarily arise through spatial self-organization processes, as described above. It is possible that power-laws in spatial patters are forced by the underlying topology or heterogeneity in soil. For example, various geographical morphologies like mountain ridges or fjords are known to approximate self-similar (fractal) structures, and thus to exhibit power-laws (Halley, et al., 2004; Li, 2000). Nevertheless, this type of forced patterns seems not to be relevant to this study. On the intertidal mud flat where *Spartina anglica* is pioneering, soil or sediment type are reasonably homogenous. Even when little variations are important for the initial settlement of individual plants, it is expected that vegetation-sediment feedbacks will have an overriding effect on the structuring of the pioneer vegetation. There is, however, an inclining elevation gradient from the mud flat up the shore. Vegetation will develop along this gradient where the duration of inundation is not to large. Moreover, the height along this gradient determines the potential for vegetation to grow. So, this will influence the interplay of processes resulting in spatial self-organization of vegetation, but it will not force a spatial pattern upon the vegetation. Therefore, it is expected that patterns will emerge from the spatially explicit interactions of the biological components here.

In conclusion, patchiness in real spatially organized ecosystems can be generated by a variety of different dynamics, or even mixtures of them. Therefore, it is not possible to predict ecosystems behavior merely on the fact that an ecosystem exhibits power-laws. It is crucial to identify the spatial processes that structure power-law patchiness in ecosystems (Pascual & Guichard, 2005). Identifying how species locally influence their environment and their main mode of growth and reproduction (do the species recover dispersed or as aggregates) should provide valuable information to deduce systems behavior and predict its spatiotemporal dynamics. Different spatial signatures accompanying dissimilar local dynamics can be identified by modeling, and reciprocal validation of models with those spatiotemporal patterns, and vice versa. Therefore, such approaches can provide valuable insight into the dynamics of the ecosystems and possible responses to perturbations and changing environmental conditions.

2.3 Use of power-law patch-size distributions as indicator

Because power-laws seem to be present in many complex systems, deviations might point to changing conditions or processes. For this purpose, fitting 'truncated' power-laws (see fig 2.9.) or measure the deviation from power-law can be of specific use. In undisturbed ecosystems truncation could point to scale or size dependency of driving processes, because some stress and disturbance mechanisms might act at a specific scale. For example, biophysical constraint to seedlings could be different than for large swards of grass. So, truncation in power-law

distributions of these systems could point to deficient recruitment, or density linked thresholds. So, it is important to know to which pattern an ecosystem converge before inferences about truncations and deviations can be drawn.

When in the literature is referred to 'truncated' power distributions, usually power-laws with an exponential deviation in the tail of the distribution are aimed for (fig.2.5.A). This also is called 'upper-truncation'. So, this means there is a deficiency of patch-sizes above an upper threshold value. This mixed model consists of a power-law term multiplied by an exponential term:

$$f(S) = CS^{-\alpha}e^{-\lambda S} \qquad (2.4)$$

Whereas definitions of all symbols are equal to equation 2.3, but λ is an addition parameter representing the strength of which the distributions deviates exponentially from power-law presence. Usually this parameter is written as the inverse ($S_x=1/\lambda$) and depict the point where the power-law begins to deviate (often referred to as 'truncation point', see e.g. Jordano, et al., 2003; Kéfi, et al., 2007a).

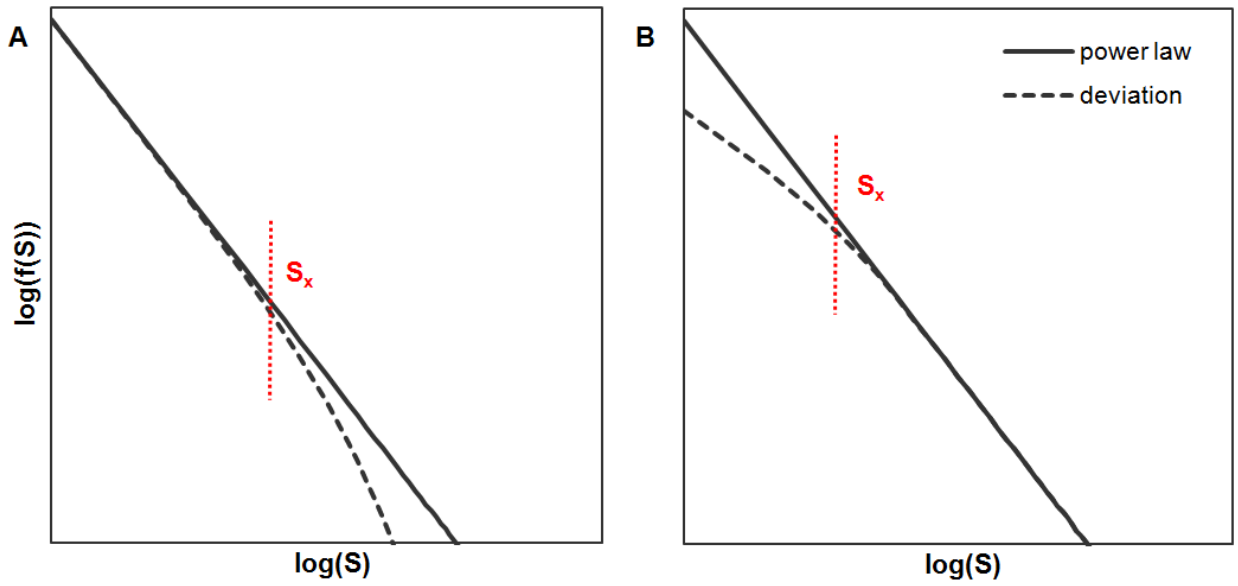

Figure 2.5. Deviations in the upper (A) and lower (B) part of the power law. S_x depicts the 'truncation point' from where the deviation becomes significant.

Opposite of the 'upper-truncated' power-law is the 'lower-truncated' power-law. Here, less small patches are found then would be expected if the pattern follows a pure power-law. This mixed model also consists of two terms, a power-law and exponential one:

$$f(S) = CS^{-\alpha}\left(1 - e^{-\lambda S}\right) \qquad (2.5)$$

Parameters in this model have similar explanation as in equation 2.4. Note, that here S_x denotes the upper limit where deviation from power-law is significant, whereas S_x in the 'upper-truncated' distribution depicts the lower threshold (fig.2.5.B).

To assess disturbance effect on ecosystems Halloy and Barratt (2007) proposed another method to measure distance from the assumed pattern: the normalized distance to log normal measure, ΔL. The measure proposed is a variation on the χ^2-test. This measure is fairly general and can be used for other distributions or patterns as well. Here, we propose to use it to measure the deviation from power-laws. Patch-size distributions with a low ΔL are considered to follow the

power-law good and appear more 'linear' on logarithmical axis. The normalized distance to power law is depicted by:

$$\Delta L = \chi^2 / k = \sum \left[\frac{(y - \hat{y})^2}{\hat{y}} \right] \Big/ k \qquad (2.6)$$

Where, *y* is *f(S)* of the real data, and $\hat{y}$ is the estimated *f(S)* from the best fitted power-law. To normalize and make different distributions comparable the Chi-square value is divided by the number of classes or bins, *k*, used in the analysis. Furthermore, this measure can be used to asses current status and track changes in time.

2.4 Technical issues

2.4.1 Lack of scale and observations

A common critique on power-law methodology in general, which also applies to spatial data, is the lack of observed scales (Avnir, et al., 1998; Halley, et al., 2004). It is obvious that lack of observed scales is problematic if the aim is to show the existence of scale-invariance. Usually the order of magnitude difference observed, *ΔS*, is considered equivalent to the observed data range as the logarithmic difference of the minimum and maximum patch size observed (see fig.1):

$$\Delta S = \log(S_{\max}) - \log(S_{\min}) \qquad (2.7)$$

Generally, a scaling relationship sustained over less than two orders of magnitude is considered to be no strong evidence of indisputable power-law presence (Halley, et al., 2004). In most empirical data-sets, the range of usable scales is small (Avnir, et al., 1998; Halley, et al., 2004), which makes it hard to show scale-invariance. Furthermore, no ecological pattern can be truly scale invariant at every scale of observation. The extent of all real-world objects, like ecosystems, is always restricted just like the smallest possible scale. For instance, the maximum size of spatial patterns in grassland cannot reach beyond the total extent of the area, and similarly the scale of the individual grass plants set the lower scale limit. Consequently, an object or phenomenon can only show power-law scaling over a finite range of scales. Likewise, simulated fractal patterns have a finite extent and a minimum resolution imposed by computational and observational limitations (Halley, et al., 2004).

Problems to lack of scale and observation numbers are not only caused by the quality of the data-set. To a large extent are these problems inherent to the power-law distribution itself. From the probability function (fig.2.1.) it becomes apparent that large events (patch sizes) are relatively rare compared to small patches. Moreover, with increasing scaling exponent (increasing steepness on logarithmic plot) the probability that large patches occur decreases. As a consequence, the number of observations has to increase to fulfill the criterion that the observed range of scales has to be over two orders of magnitude (see fig.2.1.). On top, the observed maximum size is subject to large stochastic variation, limiting reliability of the magnitude difference estimation (*ΔS*). So it would be more robust to use a more conservative estimation derived from the best fitted power-law, like:

$$\Delta S = \log(S_{f(1)}) - \log(S_{f(C)}) \qquad (2.8)$$

Where $S_{f(1)}$ is the patch-size with a frequency of occurrence of one, and $S_{f(c)}$ is the patch-size at a frequency of occurrence of the constant *C*. (see gray arrow in fig.2.1). Using this conservative approach, the minimum number of observations needed to show power-law presence (in data without noise) if the data scales with an exponent of 1.5, is 4,000. This number increases with increasing scaling exponent. If the power-law scales with an exponent of 2.0 or 2.5, the number of observations needed becomes 25,000 and 251,000 respectively (see fig.2.6). Consequently, the number of observations needed to show scale-invariance over sufficient range of scales depends on the ecological phenomenon under investigation. Furthermore, noise can be an additional source of obscuring power law presence which makes it even more difficult to prove that data-sets exhibit power-laws. So data-sets have to be large enough and of good quality to be sufficient.

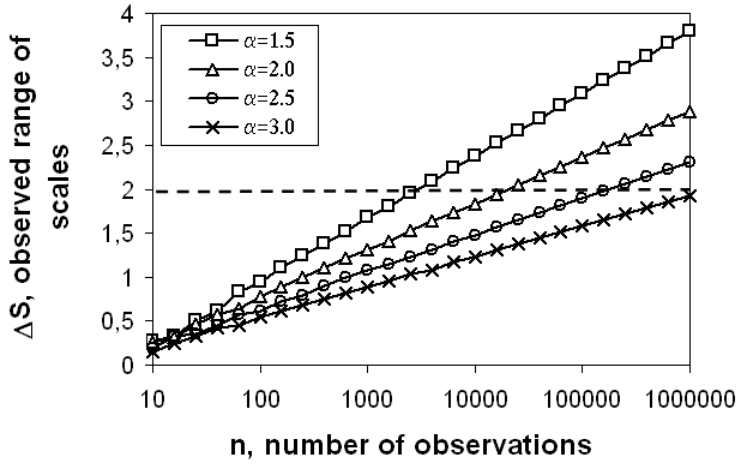

Figure 2.6. The relation between scaling exponent, observation number and perceived orders of magnitude using conservative estimation (eq. 2.8).

To resolve the problems of limited scale and number of observation, it can be necessary to pool data or to amount time or area over which data is record. However, it is not always possible to increase the extent over which patchiness is obtained in case of spatial data. Furthermore, by increasing the extent a larger variability in environmental forcing can be included into the data, this can limit the use of the power-law patchiness. So, in some cases it will not be possible to fulfill all necessary requirements to show spatial patchiness really exhibits power-laws.

2.4.2 Truncation and deviation

Truncation of patch-size data refers to a certain threshold size where below, or above, no data is present, whereas a *deviation* refers to the phenomena where there are less, or more, patches than expected based upon the patch-size distribution. So, although closely related, truncation and deviation of patch-size distributions refer to two distinct phenomena. Furthermore, these phenomena are often difficult to distinguish in empirical data-sets. Recent literature does not use this terminology in a consistent way, which might lead to differences in interpretation and inferences made.

Truncation of patch-size data can be caused by methodological or technical issues. Examples are truncation of spanning cluster due to the limited extent of the area sampled, or patches that have been cut by the boundary of the sampling plot. A detection threshold can also be

responsible for truncation of small patches. For example, small seedlings might not be visible on aerial pictures. These kind of truncations can lead to biased parameter estimations if not accounted for (Zvuloni, et al., 2008). However, truncation also can have an ecological origin. For instance, in regular spatial patterns, patch development is restricted, limiting the maximum size of patches that can develop. The data-set will be truncated above this limit. In this case truncation can be an indicator that is ecologically relevant, e.g., reflecting the carrying capacity.

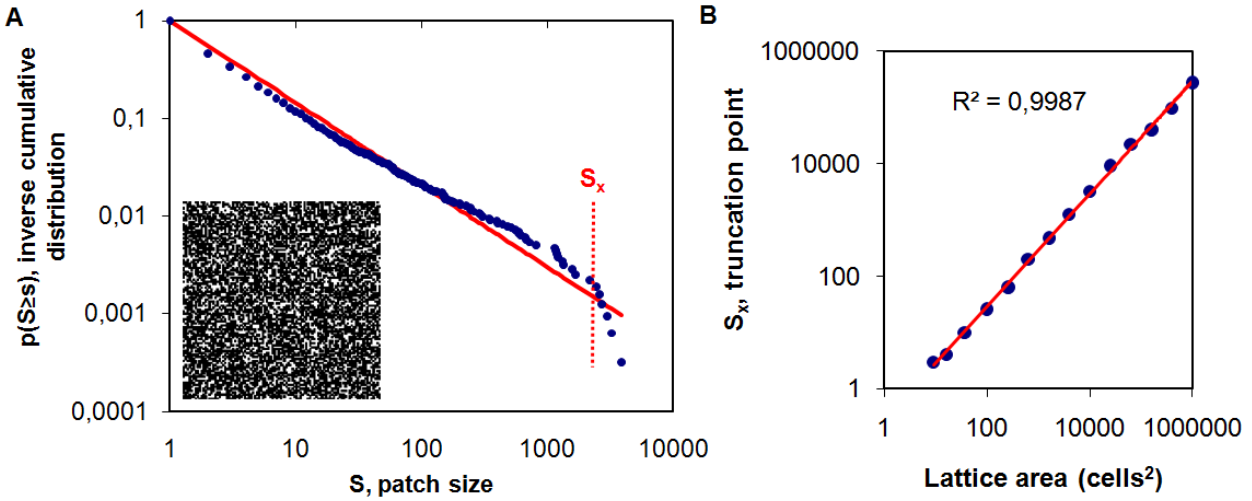

Figure 2.7. (A) Cumulative frequency distribution of random lattice cluster sizes, with (inset) random filled lattice of 100 by 100 cells with critical cover fraction of 0,593 (black is occupied, white is empty). (B) Scale at which power law is cut off (S_x) related to the lattice size derived by Monte Carlo simulations.

It is little realized, but in particular inverse cumulative distributions are sensitive to truncations, resulting in deviations of the patch-size distribution from power-laws (fig.2.7.A). For example, a maximum patch size can be limited by a size of the lattice or photo. Consequently, the truncation point (S_x) estimated on basis of the data will depend on the lattice area used (fig.2.7.B), if no other (ecological) factors are limiting the maximum size. Therefore, truncated power-law distributions almost always outcompetes 'clean' power-laws during model selection.

2.4.3 Parameter estimation and model selection

Most recent papers which discuss power-laws in empirical ecological data focus on parameter estimation and model selection (Clauset, et al., 2007; Edwards, et al., 2007; Sims, et al., 2007; White, et al., 2008). Traditionally, estimating power-law scaling exponents in empirical data was done by linear least square fitting of the power-law to logarithmical transformed data (eq.2.1). This method relies on binning of the data, which introduces considerable bias to the parameter estimates obtained (Sims, et al., 2007; White, et al., 2008). Moreover, binning has important consequences because it reduces the degrees of freedom, thereby reducing statistical power of the method. Furthermore, the choice of the binning scheme determines the shape of the patch-size distribution (fig.2.8; Lin, et al., 2010), and its choice is somewhat arbitrary (Kéfi, et al., 2010 in press-a; Lin, et al., 2010).

Using inverse cumulative distributions resolves the problems encountered when using binning. Because, this method does not reduce the degrees of freedom (except for discrete data where the degrees of freedom are reduced to the number of unique values in the data-set), and

introduces no biases due to choice of binning scheme. Therefore, linear fitting against these survival curves is put forward as good alternative (Sims, et al., 2007). In addition, distributions are displayed without large scatter in the tail (large patch sizes). Nonetheless, recently Maximum Likelihood Estimation (MLE) is identified as a more accurate technique to estimate the scaling parameter if enough observations are available (n>50; Clauset, et al., 2007; White, et al., 2008).

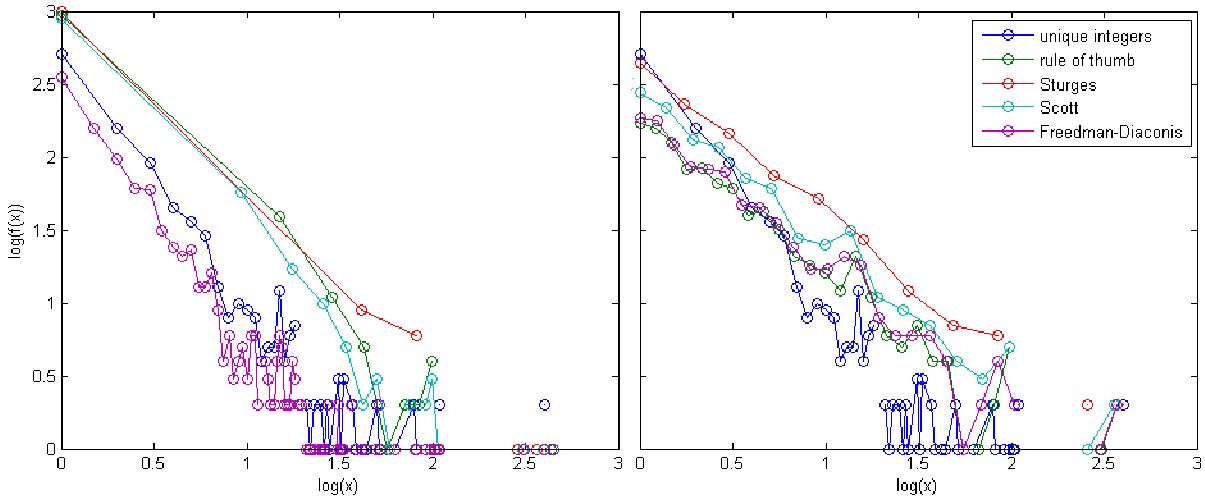

Figure 2.8. Comparison of different binning schemes on distributions power-law distribution (α=1.5, n=1000). Left panels shows normal binning, and right panels show logarithmic binning.

Many of the studies mentioned in this section depart from the assumption that the ecosystem under investigation converges towards a power-law patch-size distribution when the system is undisturbed. It is therefore logical that fitted models are power-laws, or related mixed models, like e.g. truncated power-laws. However, this assumption does not hold for all patchy ecosystems. For example, also more regular patterns could form might be the norm (Rietkerk & van de Koppel, 2008). These underlying mechanism produce patchiness with (log)normal, or fast-decaying exponential distributions. Furthermore, it often difficult to determine between lognormal and power-law distributions (Perline, 2005). Consequently, indentifying the correct distribution to compare the empirical data with is required (Edwards, et al., 2007; Johnson & Omland, 2004).

2.4.4 Acquisition and preparation of spatial data

The technical issues with methodologies described in the previous sections are rather general and apply for almost all power-law fitting problems across scientific disciplines. However, when spatial data is analyzed for the presence of power-laws, a number of additional considerations have to be taken in account. First of all, acquisition and preparation of spatial data can be an important source of variation in patch-sizes obtained, affecting the shape of the distribution. Different methods are used to gather patch-size data in the field. A number of studies report on patch-size distributions obtained by 1-dimensional line-intercepts methods (e.g. Kéfi, et al., 2007a; Maestre & Escudero, 2009), whereas others (e.g. Scanlon, et al., 2007) used 2-dimensional aerial or satellite images for deriving patch-size data. Clearly, 1-dimensional methods are poor representations of the actual 2-dimensional shape of patches (van Belzen, et

al., in prep.). So, when inferences about processes and disturbances have to be drawn upon spatial patterns, 2-dimensional aerial images are preferred (van Belzen, et al., in prep.). However, when using remotely-sensed imagery, classification and smoothing of the spatial data can have significant effects on the final results. Usually, some kind of pre-processing on the images has to be done before presence-absence maps are derived from the imagery (Klemas, 2009). Often, data stretching techniques (e.g. Principle Component Analysis) are employed to highlight features present in the data, followed by applying thresholds, or using (un)supervised classification algorithms, to distinguish between patch presence or absence. Although field surveys can be used to improve classification, assigning pixels to classes can remain somewhat arbitrary. Especially, pixels near patch boundaries can contain mixed spectral information on multiple area classes. So, when contrast and resolution of the used images are low, misclassifications are easily made due to relative high presence of these, so called, 'mixels' (mixed pixels). Particularly when coverage of a area class of interest is low, misclassification will have a marked effect on patch-size distributions, increasing abundance of small patches. The increasing abundance of small patches distorts the actual patch-size distribution, which might result in a false appearance of power law behavior in the lower part of the distribution. If the effect is large, truncated power-laws will be favored above other models in model selection, although the actual underlying spatial pattern exhibits for example an exponential, or (log)normal distribution. Consequently, this can give a false idea about the mechanism that give rise to these patterns.

Smoothing and enhancing techniques can be used to (partly) resolve the problem of misclassification. For instance, sharpening can be used to enhance contrast before classification, and moving average or median filters can be used to remove small patches which are erroneously classified after classification. Another possibility is applying a minimum threshold value on patch sizes that are retained. Although filtering can improve the picture by reducing noise and classification errors, there is a risk of losing relevant data, and smoothing can have an important influence on the patch-size distribution obtained from the data. Figure 2.9 clearly demonstrates the effects of used order and types of filtering on patch-size distributions obtained. In addition, as discussed above, also the nearest neighborhood chosen to define patches can influence patch-size distributions (see fig. 2.9). If it is questionable small patches are artifacts from the used method or caused by relevant ecological processes, it might be better to omit the small patches from the analysis. On the other hand, the risk of leaving out such data is to lose sufficient scale difference. If this is the case, presence of scale-invariance becomes open to discussion, and additional validation of real power-law presence can become necessary. Moreover, interesting ecological phenomena occurring at the small scales might be left unnoticed.

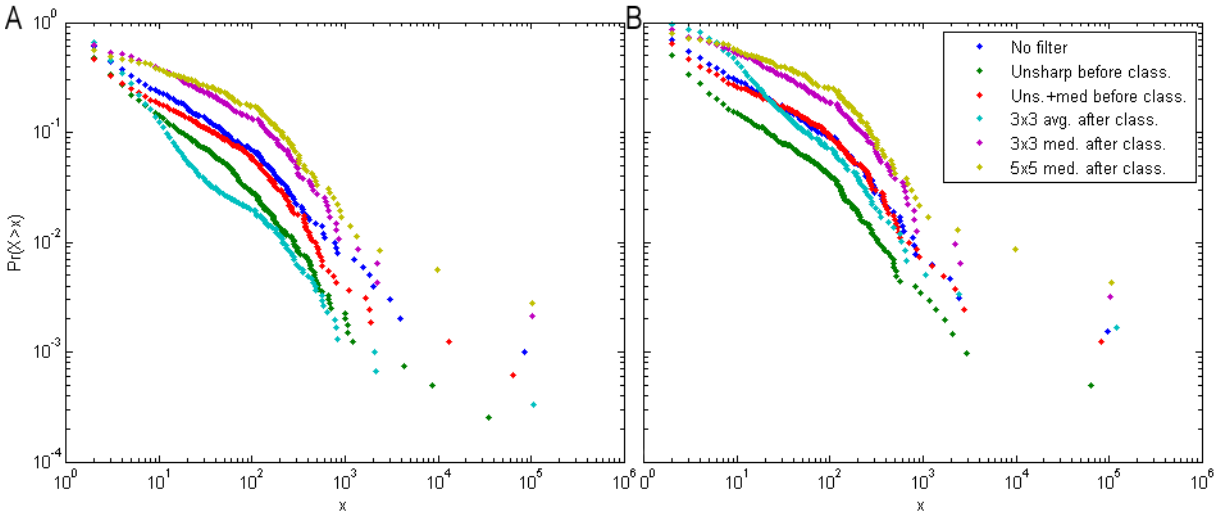

Figure 2.9. Effect of smoothing techniques on patch-size distribution. Inverse cumulative distributions of patch size analysis on aerial picture of coral reef (data from van Belzen, et al., in prep.), using different smoothing techniques before and after classification. In (A) the von Neumann neighbourhood (z=4) is used for the cluster analysis, and in panel (B) the Moore neighbourhood (z=8). Explanation of abbreviations in legend: No filter, unscharp filter applied before classification, unsharp and 3by3 kernel median filter before classification, 3by3 kernel average filter after classification, 3by3 kernel median filter applied after classification. 5by5 kernel median filter applied after classification.

Because power-laws can emerge without necessity of relevant spatially explicit ecological processes near a critical point, it is advocated to test if power-law patchiness is caused by percolation fractals or not. Moreover, comparing spatial patterns with neutral patterns, or null-hypothesis, is considered good practice in spatial statistics (Fortin & Dale, 2005). A neutral-model, lacking the mechanisms which are presumed to generate the pattern, but is capable of generating percolation fractal, can be used as such. This is considered to be a good null-hypothesis and is often referred to as Complete Spatial Randomness (CSR). An extensive randomization procedure (Monte Carlo) can be used to generate a large number of these neutral-model outputs, which can be used to find the mean neutral-pattern and derive a 95% confidence interval which is used to test the empirical pattern for statistical significance. It is assumed that the probability at which the statistical decision of accepting or rejecting the statistical null-hypothesis is made, is proportional to the number of randomizations generated (Fortin & Dale, 2005). In general, 10,000-100,000 randomization of grids of similar size and resolution as the real spatial data should be enough to gain enough confidence to accept or dismiss the CSR null-hypothesis as explanatory model in the spatial analysis (Fortin & Dale, 2005).

Clearly, there are numerous technical and methodological issues affecting the analysis of patch-size distributions, from data gathering in the field to processing of the spatial data. Thus, the spatial methodology used can have significant influence on the obtained results. Understandable, it is propagated to apply some kind of method validation to be sure changes in scaling exponent, truncation or deviation parameters are caused by relevant ecological processes and not by methodological issues. Furthermore, when methodologies are used in a

consistent way throughout the analysis, changes in patch-size distribution shape still can indicate changes in environmental conditions and forcing (van Belzen, et al., in prep.).

2.5 Discussion

The need for new methods to assess ecosystem responses to natural and anthropogenic influences is becoming of increasing importance. Traditional field-based sampling methods are expensive and time consuming, especially at large spatial scale, and such methods are inadequate for today's needs (Ustin, et al., 2004). Air- and space-borne observations are a promising alternative. They provide the only practical means to obtain a synoptic view of Earth's ecosystems, including their spatial distribution, extent, and temporal dynamics (Cohen & Goward, 2004). Nevertheless, appropriate measure to asses ecosystems over multiple scales have to be developed. Therefore, using ecosystems' spatial structure as indicator to asses ecosystems health and predict future changes (Rietkerk, et al., 2004) is a very interesting idea.

An indicator is ideally simple and measurable providing information on the behavior of complex systems (Halloy & Barratt, 2007). As such, power-law patch-size distributions are a good candidate because of their simplicity, describing spatial structures by just their scaling exponent measuring only the relative occurrence of patch sizes. Furthermore, indicators should measure effects of a disturbance forces, like magnitude and frequency. However, universal indicators cannot distinguish between human or natural disturbances without a more detailed study. Recent studies (Kéfi, et al., 2007a; Lin, et al., 2010; Scanlon, et al., 2007) suggests that there is a consistent change in the shape of patch-size distributions with increasing stress. Furthermore, both grazing pressure and decrease in annual rainfall have a similar effect on the distributions shape in those studies (Kéfi, et al., 2007a; Lin, et al., 2010; Scanlon, et al., 2007). Consequently, power-law patch-size distributions seem to be a reasonable indicator. Although disputed by Maestre & Escudero (2009), as mentioned. So, further examination of power-law distributions as leading indicator and early warning signal is justified.

There is lively debate about the use of power-law frequency distributions as indicators of stress and disturbance on ecosystems. Most recent the debate focuses on the findings of power laws in semi-arid ecosystems (Kéfi, et al., 2007a; Scanlon, et al., 2007). Kéfi and co-workers (2007a) showed deviations from power-law patch-size distributions could point to proximity of imminent desertification in arid ecosystems. Recently this claim was disputed by Maestre and Escudero (2009), who tested if other indicators of desertification, like chemical properties of soil samples, correlated with difference in scaling exponent between sites. They come to the conclusion that patch-size distributions cannot be used in such a way. Resolving these conflicting findings is important for the development of power-laws as valuable tool in ecosystem assessments. However, for now the question remains if the spatial structure of an ecosystem is a good indicator of its health. Likewise, it is still unresolved if patch-size distributions are a good tool for assessing this spatial structure and stress and disturbance imposed on the spatially organized ecosystem.

Although it is suggested that all complex systems tend to converge to power-law behavior (Solé, 2007), it remains questionable if these scaling laws can be used without detailed knowledge on the dynamics of the ecosystem under investigation. For example recent studies have shown that regular patterning can be an alternative endpoint of the spatial structure of ecosystems (Rietkerk & van de Koppel, 2008). Therefore, it is essential, when the underlying mechanism has

to be clarified, to get the pattern right. As discussed, an extensive body of literature focuses on the methodology used to analyze patch-size distributions. Using different methods can produce different results, and can influence conclusion inferring from the data. So, it is important to have enough confidence in the used techniques to be sure an apparent power-law distribution is present in the data. Getting the pattern right should help scientists to draw inferences and draw meaningful questions (Edwards, et al., 2007; Sims, et al., 2007). So, to yield reliable results it is obvious highly biased estimation methods should be avoided if possible.

Nonetheless, we also have to ask ourselves how strict we have to be to avoid missing out on existing relationships. Before we invest a great deal of afford to prove presence of real power-law behavior, we also have to ask ourselves how strict we have to be. It depends on the objective of the investigation if it matters if patch-size distributions exhibit real power-law behavior, or not. Moreover, power-law distributions may be seen as exploratory tool, simplifying realism, which helps us to understand certain characteristics of reality, without necessarily having to be strictly true itself. For example, in case the objective is to monitor quantitative changes due to stresses or disturbances, fitting data to power-law distributions might be a powerful tool just to keep track of qualitative changes of the spatial structure. On the other hand, if a mechanistic understanding of the system is needed to get insight into the behavior of the system under changing environmental conditions, than detailed understanding of the mechanisms or processes that give rise to the patch-size distributions is preferred. However, even so power-laws may provide the most capable tool available for describing and predicting spatial patterns at multiple scales.

3. Spatiotemporal analysis of salt-marsh pioneer vegetation

3.1. Introduction

In the previous chapter theoretical concepts, methodologies and technical issues concerning the use of power-laws and patch-size distributions are reviewed in a more general context. The main objective of this chapter is to use this theory and methodologies to specifically address the two main research questions on vegetation patchiness at the salt-marsh pioneer zone.

First, it was investigated if erosion and recovery processes shape the spatial structure of the vegetation at the salt-marsh pioneer zones in such a way that they exhibit power-laws. This is done by:

1) Demonstrating that qualitative changes in time of vegetation patches at the pioneer zone are related to erosion and recovery processes;
2) Analyzing the spatial irregularity of the vegetation patches at the pioneer zone;
3) Testing if the patch-size distribution if the vegetation patches exhibit power-laws.

Second, it was investigated if power-laws can be used as indicators of stress and disturbance exerted on the pioneer zone vegetation. Therefore, it was investigated if the spatial vegetation structure can be related to the local hydrodynamic forces at the pioneer zone, by means of vegetation patch-size distributions.

3.2. Materials & methods

3.2.1. Field sites and hydrodynamic conditions

A restricted geographical area, containing multiple sites to test and compare vegetation patchiness at salt-marsh pioneer zones, is preferable for comparison of pioneer vegetation structures. Sites must have a similar environmental context, thereby excluding confounding factors, like climate, sedimentology, and species composition, which might affect differences in vegetation structure, as much as possible. Hence, six salt-marshes along the Westerschelde (see fig.1.6) are selected, which have a pioneer zone present. These salt-marshes are under influence of a meso to macro tidal regime with a Spring Tidal Range between 4.4 and 4.9 m (van der Wal, et al., 2008). Exposure to waves can be another important hydrodynamic factor along the Westerschelde, because the fetch over which waves can build up energy is large at most locations (Callaghan, et al., 2010; van der Wal, et al., 2008). Since, the site-specific level of exposure to currents and waves are potentially a major determinant in limiting vegetation development at the pioneer zone, sites are used which are clearly distinct in their level of exposure to the different hydrodynamic conditions.

In table 3.1 the six sites are characterized for their hydrodynamic conditions based on the analysis by van der Wal et al. (2008). Indicators for hydrodynamic conditions can roughly be divided into exposure to 1) currents, and 2) waves, like e.g. current velocity, proximity to nearby navigation channel, fetch over which waves can gain energy, and frequency of onshore winds. A more detailed explanation on the used indicators of hydrodynamic conditions (tab.3.1) is given in chapter 3.2.5.

Table 3.1. Estimated hydrodynamic conditions by modelling and GIS analysis of the study sites (van der Wal, et al., 2008).

Site	Modelled inundation duration (%)	Modelled current velocity (m/s)	Modelled current velocity gradient	Frequency of onshore winds (%)	Frequency of onshore winds ≥6Bft (%)	Modelled average fetch at Mean High Water (m)	Modelled average wave height (m)	Modelled average wave height ≥6Bft (m)
Baarland	11,8	0,22	2,54	74,77	6,69	3313	0,13	0,47
Hellegatpolder	46,2	0,19	0,46	7,14	0,64	6441	0,17	0,38
Hoofdplaat	18,1	0,30	2,65	6,03	0,54	9779	0,18	0,19
Paulinapolder	35	0,14	4,05	2,88	0,26	3554	0,13	0,14
Thomaespolder	27,2	0,21	5,3	1,39	0,12	3534	0,13	0,12
Zuidgors	30,2	0,33	10,02	86,83	7,77	3836	0,15	0,48

3.2.2. Mapping of vegetation presence, growth and erosion

Multi-spectral aerial photographs (fig.3.1.a) of the six sites were available from previous research at the NIOO-CEME (van der Wal, et al., 2008) and are provided by Rijkswaterstaat. From each site, photographs of the marshes at different stages in their development over a period of about 25 years were used (tab.3.2). These images were scanned at high resolution, rectified, geo-referenced, and mosaiced in a Geographical Information System (GIS) to yield images with a pixel size of 0.25 by 0.25 m. Presence of salt-marsh vegetation was determined by supervised classification. The near-infrared (NIR), red, and green bands of multi-spectral aerial photographs (False Colour Composites, FCC) were used to classify presence of vegetation, thereby creating binary presence-absence maps (fig.3.1.b; van der Wal, et al., 2008). From these resulting vegetation maps, clusters of less than 4 cells, using the Moore neighborhood (z=4), were removed. This resolves problems caused due to small differences in resolution and possible wrong classifications. For example, benthic or macro algae can easily be classified wrongly as *Spartina anglica* due to chlorophyll, which can give a lower reflectance in the red band. These vegetation maps where used for the analysis of growth and erosion patches, the spatial structure of the pioneer zone, and their patch-size distributions.

Table 3.2. Multi-spectral aerial photographs used in the analysis from which vegetation maps are made.

Site	Years of aerial photographs present
Baarland	’82, ’93, ’98, ‘04
Hellegatpolder	’76, ’82, ’93, ’98, ‘04
Hoofdplaat	’82, ’93, ’98, ‘04
Paulinapolder	’82, ’98, ‘04
Thomaespolder	’82, ’98, ‘04
Zuidgors	’82, ’93, ’98, ‘04

Only vegetation present at the pioneer zones was analyzed, and not the whole salt-marsh area. Therefore, the boundaries of the analysis had to be determined. The pioneer zones were delineated manually, creating binary masks which overlay the vegetation maps. These masks depict pioneer zones presence and absence. Because the pioneer zone should comprise al area that is suitable for pioneering vegetation to settle, a conservative estimate of the extent of pioneer zone is made by looking at the consecutive vegetation maps. The outer seaward boundary on the mud flat is estimated by connecting the patches on one of the vegetation maps where the patches are farthest out toward the sea. The landward boundary of the pioneer zone was set to be the edge of the continuous salt-marsh plateau, in most cases clearly presented by an eroding cliff. In case no higher marsh plateau was present, the toe of the dike was the landward boundary of the pioneer zone.

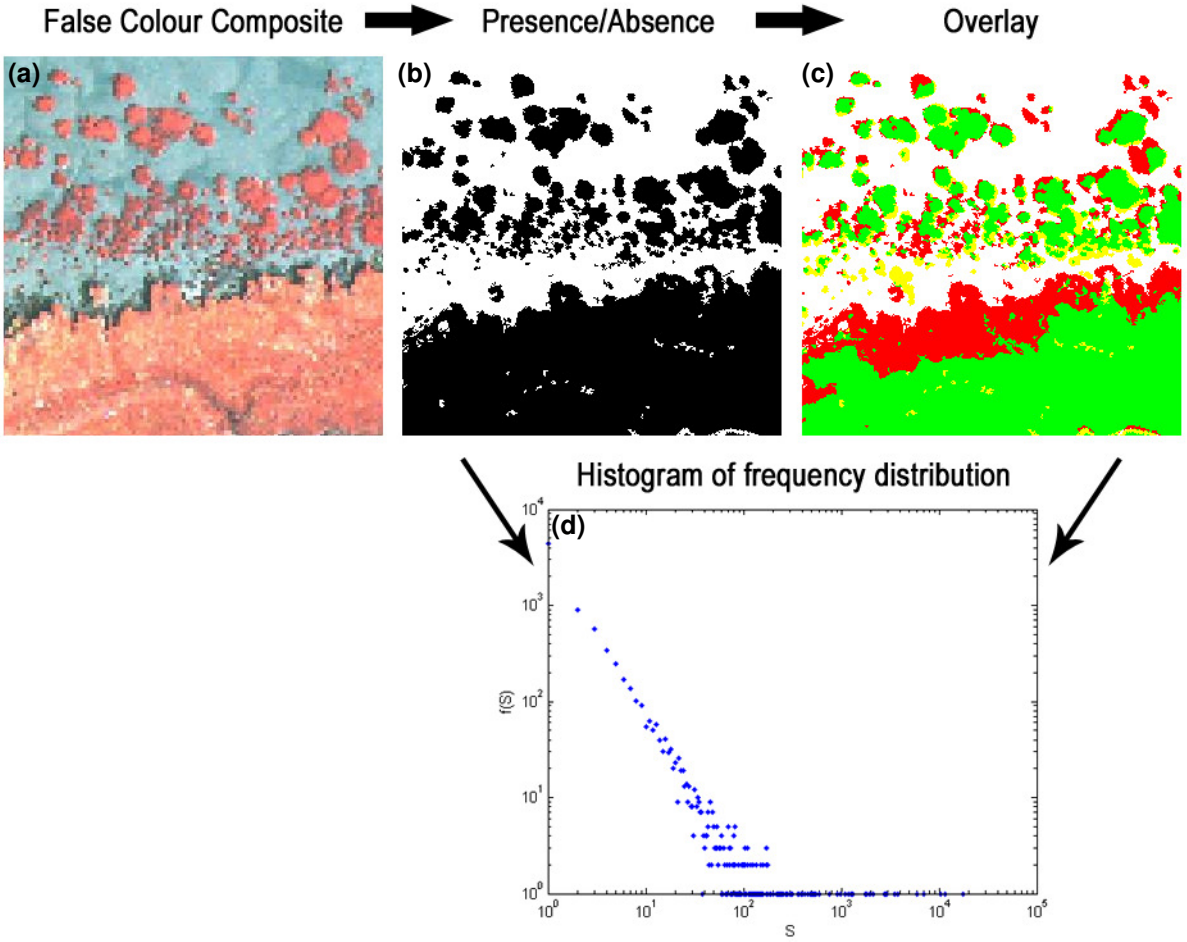

Figure 3.1. Method used to analyze spatial structure of pioneer-zone vegetation. From the (a) false colour composite, vegetation is classified resulting in (b) presence-absence map, which can be analyzed for the (d) patch-size distribution. Furthermore, successive years can be (c) overlaid to map erosion (red) and growth (yellow), and compare to stable vegetation (green). Patch-size distribution of these erosion and growth patches are analyzed as well.

To visualize that salt-marsh pioneer vegetation is shaped by erosion and growth processes consecutive vegetation maps were overlain (see fig.3.1.c). The created vegetation change maps consist of four discrete classes: 1) stable vegetation (green), where no change between two consecutive vegetation maps is present, 2) erosion (red), where there is vegetation in the oldest map but not in the youngest, 3) growth (yellow), where there is vegetation in the youngest vegetation map and not in the oldest map, and 4) no vegetation in both maps (white).

3.2.3. Analysis of spatial structure in pioneer vegetation

Power-laws are usually closely associated with irregularity of spatial patterns (Kéfi, et al., 2010 in press-b; Pascual & Guichard, 2005). Therefore, the regularity of the pioneer zone vegetation was measured to test if it is reasonable to expect power-laws in the patch-size distributions of the pioneer vegetation. To determine spatial regularity a two-dimensional spectral analysis (Barbier, et al., 2006; van de Koppel, et al., 2005b) and Moran's I spatial autocorrelation (Fortin & Dale, 2005; van de Koppel, et al., 2005b) was determined for the pioneer zone vegetation. Because calculations are computational demanding for memory and processing time, three subsections of vegetation maps, randomly selected, are used in these analyses. Subsections of 250 by 250 pixels were taken from: Hellegatpolder 1982, Paulinapolder 1993, and Hellegatpolder 1993.

Spectral analysis provides a measure of regularity by looking at how many times a simple cosine repeats itself in the spatial pattern (Fortin & Dale, 2005). When this analysis is done for multiple direction within the picture this is called two-dimensional spectral analysis. For the three subsections a periodogram and spatial radial spectrum was obtained. The periodogram gives the frequency of wave numbers found in all direction. The radial spectrum, on the other hand, gives the dominant wave number, irrespective of direction. These two measures give information on the periodicity, and, thus, if vegetation is regularly spaced. If there is a clear spatial regularity, than clear wave numbers dominate the pattern. This will be shown by the radial spectrum.

Spatial autocorrelation analysis will support spectral analysis if there is clear regularity. This statistical technique calculates the correlation between two points at some distance from each other (Fortin & Dale, 2005). If the pattern is regular, autocorrelation will show a wave-like curve, with significantly negative and positive correlation values, at increasing spatial distance. Absence or weak negative autocorrelation is in evidence of irregularity of the patchiness.

3.2.4. Analysis of patch-size distributions in pioneer vegetation

Vegetation patches present in the pioneer zone were defined by cluster analysis which labels occupied adjacent cells with the same number. The cluster analysis uses the Moore neighbourhood, or 8 nearest neighbours (z=8), similar to the neighbourhood used during the vegetation mapping (Ch.3.2.2). The patch-size was calculated by summation of all cells with the same label. This way a vector of patch-sizes was constructed. From these data, patch-size distributions are constructed and subjected to the methodology of power-law analysis explained in the previous chapter (Ch.2). The scaling exponent is estimated by the maximum likelihood method (MLE; Clauset, et al., 2007), the Hill estimator, which is the most accurate method available (White, et al., 2008). To visualize the patch-size distributions the inverse cumulative distribution are used, because they give a better qualitative indication when the distribution is deviating from power-law (Ch.2.2.1).

To get insight into the possible deviation from the power-law distribution, different models are fitted against the inverse cumulative distribution. Next to power-law distributions (PL), the data was fitted against an exponential (EXP), an upper-truncated power-law (UTPL), and a lower-truncated power-law distribution (LTPL). The best fitted distribution was selected based on minimizing Akaikes Information Criterion (AIC), which is a measure for the goodness of fit (Johnson & Omland, 2004). AIC gives a penalty to models that have more parameters. Thus, the AIC procedure, for selecting the best fitting model, prefers more simple models (e.g. power-law, with one parameter) above complex models (e.g. truncated power-laws, with two parameters).

To measure the deviation from power-law the normalized distance to power-law, ΔL, was measured (eq.2.6 in Ch.2.3). Small values compared to large values of ΔL mean that the patch-size distribution approximates the power-law better, or is more 'linear' at a plot on logarithmical axis. Furthermore, this measure is used to compare patch-size distributions of erosion and growth to compare their relative contribution to the development of the vegetation patches at the pioneer zone.

Patch-size data of the same sites, but at different moments during their development (tab.3.2), where pooled to get hold of a larger number of patch-sizes per site. This was necessary because in most locations the number of patches was too few to fit models with statistical significance. However, due to pooling of the data, some patches are included more than once, thereby creating a partly auto-correlated data set. However, the results on the additional individual patch development analysis (appendix A) shows that large changes occur mostly among small patch-sizes. So, due to erosion and growth most patches have changed between two consecutive vegetation maps. Small patches have an overriding effect on the shape of patch-size distributions because they make up over 80% of the data. Therefore, there is significant difference in patch-size data between consecutive aerial photographs, and the effect on the patch-size distributions is expected to be trivial. Furthermore, the patch-size distribution of erosion and growth patches (appendix B) show similar distributions. Consequently, these additional tests give confidence that pooling the data has no notable effects on the obtained results.

3.2.5. Relating vegetation patchiness to hydrodynamic climate

To investigate if power-laws can be used as indicator of the stress and disturbance exerted on the pioneer zone vegetation, the correlation between the scaling exponent of the fitted power-laws and the hydrodynamic conditions was calculated. Data on estimated hydrodynamic conditions was used from a previous study by van der Wal et al. (2008; see table 3.1). Hydrodynamic factors considered that represent exposure to currents, are: modelled current velocity, and the modelled current velocity gradient. The current velocity gradient indicate proximity to the navigation channel and is calculated as the ratio between the current velocity 250 m in front of the most seaward edge of *Spartina*, and the current velocity at this *Spartina* edge. Exposure to waves is represented by five indicators, where it is assumed that waves are mainly wind-induced. These five indicators are: the frequency of onshore winds, the frequency of onshore at winds of ≥6 Bft., the average fetch calculated for Mean High Water (MHW), average wave height, and average wave height at winds of ≥6 Bft. Moreover, the modelled inundation duration is taken into account as hydrodynamic conditions. The estimated fraction of the time that the pioneer vegetation is flooded, is a measure of stress which effects growth.

In support of the correlative analysis, an additional multivariate analysis was done. In appendix C this additional analysis by Principal Component Analysis (PCA) was used to get more insight in the correlation structure between the different hydrodynamic conditions, power-law scaling exponent, and the vegetation cover fraction at the pioneer zone.

3.3. Results

3.3.1. Pioneer vegetation changes in time

The vegetation change maps in figure 3.2 demonstrate clearly that erosion and growth processes occur at the same time. The changes occurring in the pioneer vegetation are, furthermore, spatially correlated. This means that, for example, erosion is not distributed randomly but is confined to areas where already erosion is happening. Likewise, growth occurs mainly adjacent to areas with grown or stable vegetation (yellow and green respectively in figure 3.2). So, these qualitative changes in vegetation strongly suggest that erosion and growth are the main processes structuring the pioneer zone, and that those processes are spatially correlated.

Although erosion and growth occurs at the same time, there are clear differences during different stages of pioneer zone development, as figure 3.2 shows. The 28 year long analysis of sequential aerial photographs from Hellegatpolder is exemplary for this temporal variability (fig.3.2.a-d). Vegetation changes show that, in time, vegetation loss decreases and the vegetation expands at the pioneer zone. However, the relative importance of erosion or growth for development of the pioneer vegetation differs per period. For example, in the period 1998 to 2004 some marked erosion occurs in the north-east of the subsection, where in the period before, 1993-1998, erosion is less pronounced, but scattered across patch boundaries in the whole area. So, there is temporal and spatial variability in the development of pioneer vegetation within sites.

→ *Figure 3.2. Vegetation change maps of salt-marshes pioneer zones. Only subsections at equal scales (120 by 80 m) of most active parts of the pioneer zone are shown for comparison. The different colours depict four classes: stable vegetation (green), erosion (red), growth (yellow), and no vegetation (white). The first four subsection (a-d) show changes of pioneer vegetation at Hellegatpolder over the period from 1976 to 2004. Next four subsections show pioneer vegetation change over 5-6 year period for four other locations with various temporal trends: (e) Zuidgors with large lateral erosion of salt-marsh plateau and little development of pioneer vegetation; (e) Paulinapolder shows erosion and growth of pioneer vegetation at similar rates; (g) Hoofdplaat shows growth of pioneer vegetation is the dominant process; and at (h) Baarland growth is also the dominant process, but also experiences some erosion.*

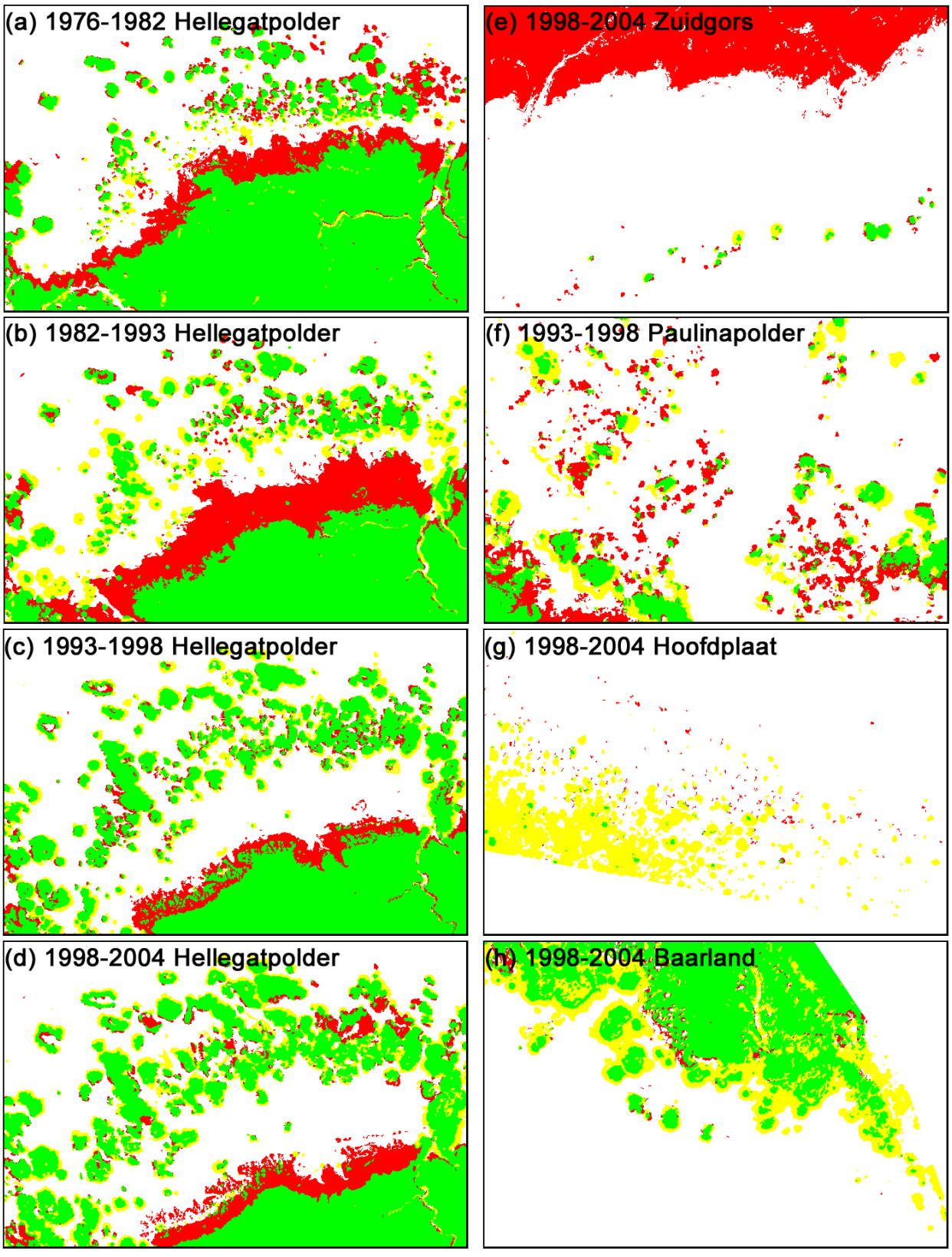
(a) 1976-1982 Hellegatpolder
(b) 1982-1993 Hellegatpolder
(c) 1993-1998 Hellegatpolder
(d) 1998-2004 Hellegatpolder
(e) 1998-2004 Zuidgors
(f) 1993-1998 Paulinapolder
(g) 1998-2004 Hoofdplaat
(h) 1998-2004 Baarland

Development of the pioneer vegetation at different sites also shows clear differences, as shown in figure 3.2.e-h. Zuidgors, the site that experiences high exposure to currents and waves, has a markedly different vegetation structure and development at its pioneer zone compared to the sheltered site of Paulinapolder. Zuidgors has, in spite of a very wide pioneer zone (2.6 km, not shown in fig.3.2), only a few patches that hardly grow and experience little erosion. In contrast, at Paulinapolder (a pioneer zone of 1.6 km wide, shown in fig.3.2) many patches are present that grow and erode quickly. Moreover, Hoofdplaat and Baarland gain much more vegetation than is lost by erosion. Consequently, these differences in the spatial structure and development of the pioneer vegetation suggest that differences are caused by different local hydrodynamic conditions at each site.

Temporal and spatial variability within and between sites can be caused by changes in hydrodynamic conditions. Therefore an additional analysis was done to get some extra insight into the fate and development of individual patches (appendix A). This analysis reveals that small patches are more dynamic in their behaviour. They come and go more easily than large patches, and this can vary greatly in time, as can be seen in figure 3.3, which shows that the balance between recruitment and loss of patches for different periods in time. Therefore, it seems likely that small patches are more vulnerable for disturbances. So, if we can separate small from large patches in the analysis this might give important information on local disturbances halting the development of vegetation at the pioneer zone.

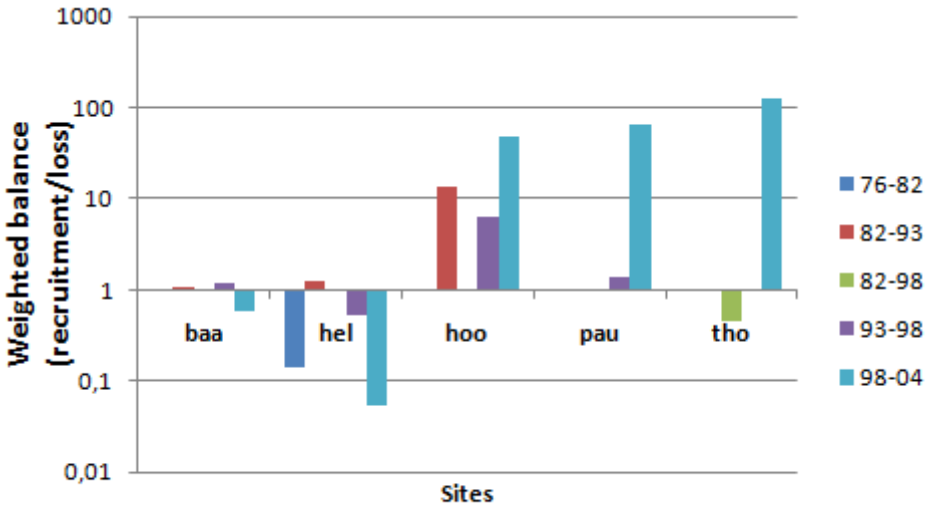

Figure 3.3.Weighted balance of recruited and lost patches per time period. Procedure for calculating the balance between recruitment and loss of patches can be found in appendix A.

3.3.2. Spatial structure of pioneer vegetation

The structure of vegetation at the pioneer zone is clearly irregular as two-dimensional spectral analysis and auto-correlation show (fig.3.4). There are no clear structures present in the periodograms of the three subsections. Furthermore, there are no dominant waves present in the spatial structure shown by the radial spectrum plots. So, both measures of the spectral

composition indicate the absence of clear regularity in the spatial structure of the pioneer zone vegetation of Hellegatpolder and Paulinapolder. Moreover, analysis of spatial auto-correlation supports the findings by the spectral analysis. There is only some weak and insignificant negative auto-correlation at a distance of 2 to 3 meters in all locations, which is not in favour of regularity. Consequently, because the spatial structure is not regular power-laws can be expected in the patch-size distributions of the pioneer vegetation.

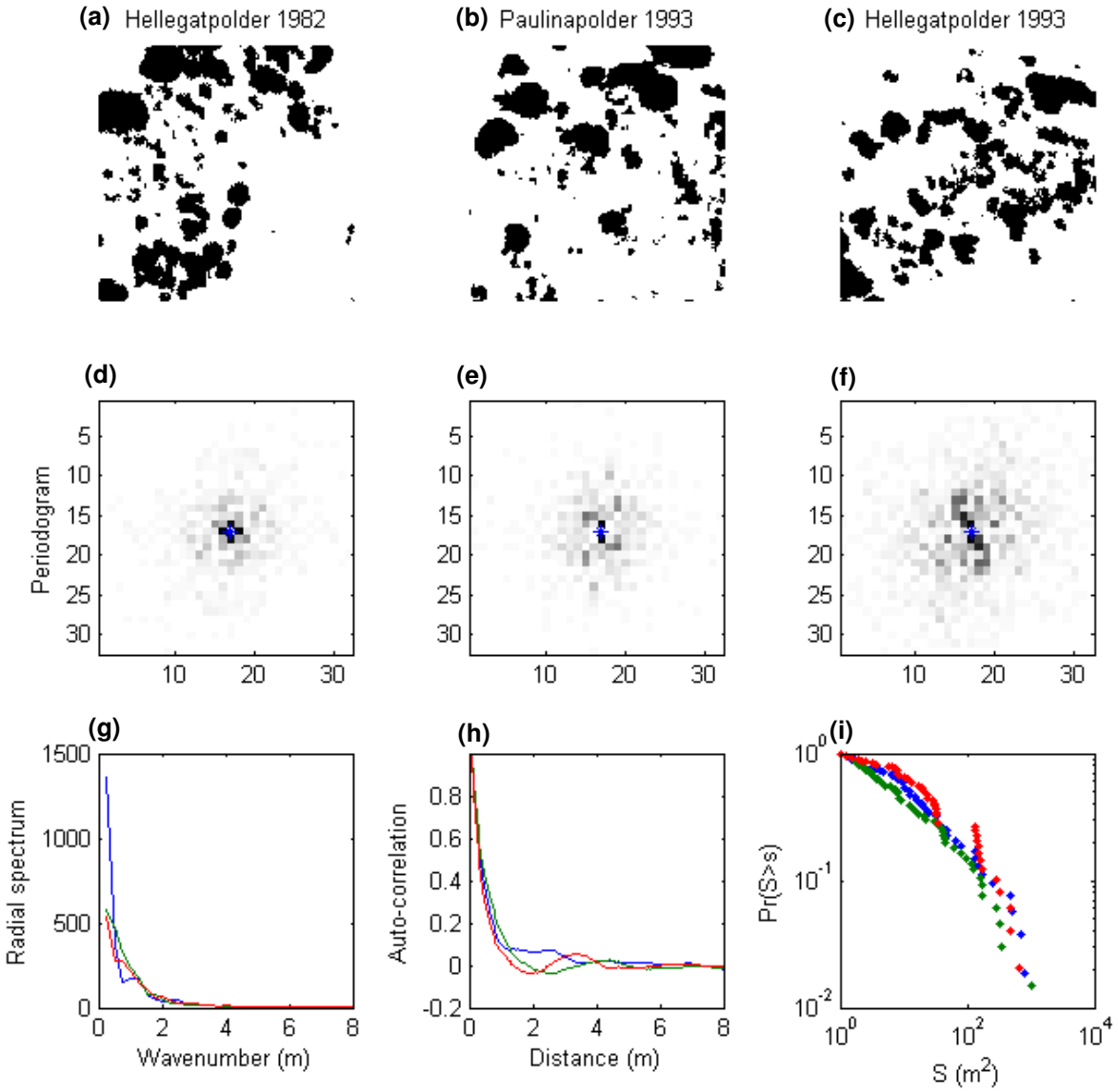

Figure 3.4 Spatial structure analysis of pioneer zone vegetation. Top figures (a-c) show three square grids (250 by 250 cells) of pioneer-zone vegetation at different locations. Middle figures (d-f) show periodograms derived from the spectral analysis on the top figures (a-c). Bottom figures show, from left to right, (g) radial spectrum, (h) auto-correlation (Moran's I), and (i) power-law patch-size distributions of top figures (Hellegatpolder 1982 is blue, Paulinapolder 1993 is green, and Hellegatpolder 1993 is red).

3.3.3. Patch-size distributions in pioneer vegetation

The vegetation patch-size distributions found at pioneer zones of the six different locations all approximate power-laws (fig.3.5). The coefficient of determination R^2 is high (>0.9) for all location, and the patch-size distributions span over more than two orders of magnitude, which supports the power-law claim (Ch.2.4.1). Furthermore, the presence of power-law distributions in the erosion and growth patches (see appendix B) strengthens confidence in the idea that erosion and growth processes structure pioneer vegetation. Consequently, it is likely that differences in the relative importance of erosion and growth processes will result in differences in the patch-size distribution.

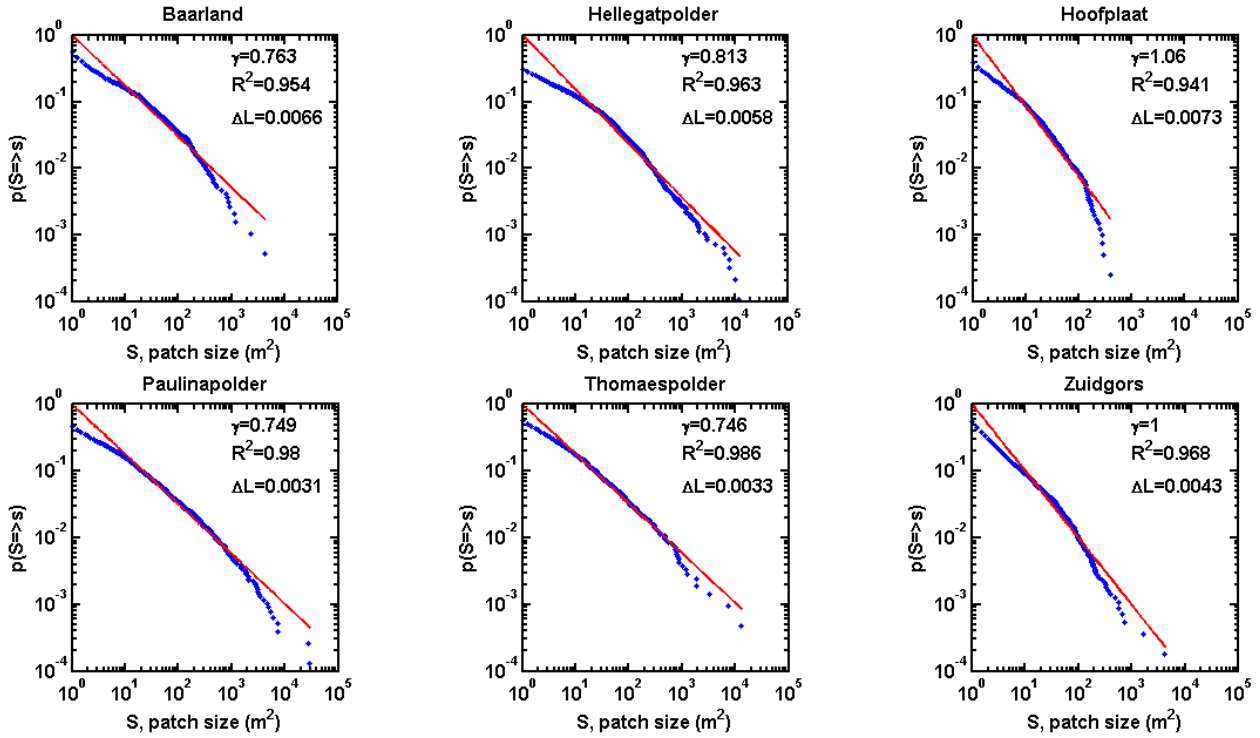

Figure 3.5. Patch-size distributions at pioneer zones of six salt-marshes. The inverse cumulative distributions all approximate the power-law, were the red line is best fitting power-law to the distribution.

Table 3.3. Estimated scaling exponents and deviations of power-laws.

site	α	ΔL	α erosion	ΔL erosion	α regrowth	ΔL regrowth	cover
Baarland	1.59	0.0066	1.88	0.0004	1.57	0.0100	4-7%
Hellegatpolder	1.47	0.0058	1.59	0.0026	1.75	0.0076	11-21%
Hoofdplaat	1.68	0.0073	2.04	0.0062	1.72	0.0064	1-6%
Paulinapolder	1.52	0.0031	1.66	0.0053	1.52	0.0057	12-16%
Thomaespolder	1.54	0.0033	1.67	0.0051	1.53	0.0052	7-10%
Zuidgors	1.80	0.0043	1.80	0.0033	1.61	0.0079	1-5%

Table 3.4. Estimated scaling exponents and deviations of power-laws.

site	C	γ	λ	R^2	Best fit
Baarland	3797	0.675	0.00016	0.978	UTPL
Hellegatpolder	21445	0.749	0.00004	0.976	UTPL
Hoofdplaat	4949	0.701	0.00212	0.996	UTPL
Paulinapolder	18245	0.714	0.00002	0.988	UTPL
Thomaespolder	5226	0.720	0.00002	0.990	UTPL
Zuidgors	19284	0.968	0.00008	0.972	UTPL

Despite the fact that the patch-size distributions exhibit power-law distributions, they all have clear deviations. However, the amount of deviation is variable as the normalized distance from power-law (ΔL) shows (fig.3.4 & tab.3.3). Furthermore, as table 3.3 (and patch-size distributions in appendix B) shows, patch-size distributions from growth patches deviate more clearly than patch-size distributions from erosion patches. It seems that in most sites growth is the dominant process shaping the patch-size distribution, because deviations from power-law resemble those of growth better. So, it is likely that processes responsible for settlement and growth of vegetation are more variable, and dependent on local conditions, than erosion processes.

The previous observation that the patch-size distributions are not perfect power-law distributions, but just approximations is supported by the distributions that fit the data best. In all locations the inverse cumulative distribution is best fit by the upper-truncated power-law distribution (table 3.4). However, in most locations the value of the truncation point λ is not relevant, because the value is near the maximum patch-size found on the location (Ch.2.4.2). Only Baarland and Hoofdplaat show to have a high truncation point that can be ascribed to differences in local conditions, and not to effects due to the size pioneer zone area. Both locations also show the largest vegetation development (e.g. fig.3.2.g-h), which might be explained by their low inundation time (tab.3.1). The patch-size distribution at the pioneer zone of Hoofdplaat is even stronger truncated than Baarland, in accordance with the strong development of Hoofdplaat in all aerial photographs. So, it seems that patch-size distributions of locations where growth is less stressed become strongly truncated compared to locations where growth is less pronounced.

3.3.4. power-laws related to hydrodynamic conditions

Correlation analysis reveals that the spatial structure can be related to the local hydrodynamic conditions. There is a strong Spearman correlation between current velocity and the scaling exponents (fig.3.6) found in the patch-size distributions at the pioneer zones (r_s=0.943, p=0.017). The same strong, but negative, correlation is found for the vegetation cover of the pioneer zones (r_s=-0.943, p=0.017). The additional PCA (see appendix C) further supports the correlation analysis. From the PCA it becomes clear that the scaling exponent, vegetation density and current velocity are strongly correlated (fig.B.3). Consequently, it will be possible to infer local current velocities from the power-laws scaling exponent found in the vegetation patch-size distribution.

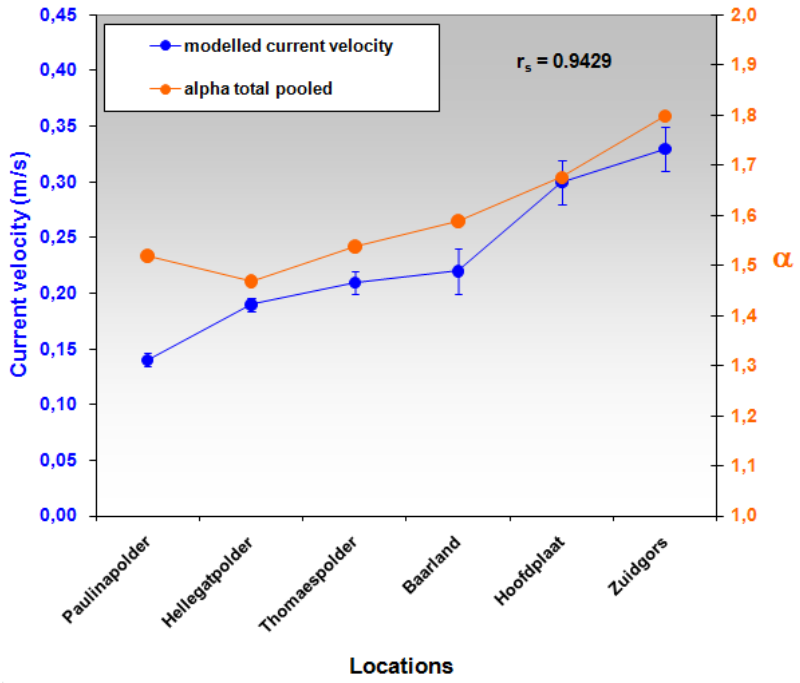

Figure 3.6. Relation between current velocity, and scaling exponent. Sites are ordered from low to high of current velocities, were Paulinapolder experience least current velocity and Zuidgors the most depicted by the blue line. The orange line shows the power-law scaling exponents at the six different pioneer zones.

Although the correlative analysis on the pooled patch-size data shows that there is a clear relation with the level of hydrodynamic exposure, the separate patch-size distribution per vegetation map shows there is considerable variability from photograph to photograph. Figure 3.7. compares patch-size distributions for the vegetation maps of 1998 and 2004. For most sites, except Thomaespolder and Zuidgors, there is a clear difference in the number of small patches between the consecutive aerial photographs. This variability in small patches is also found by the individual patch development analysis (appendix A), which also showed that most dynamics occur in the small patches. If the vegetation structure indeed reflect the local hydrodynamic conditions at the mud-flat, than this suggests that there is a clear change in hydrodynamic conditions at the pioneer zones where these changes in patch-size distribution occur. However, there was no year specific data available of exposure to currents and waves to test if changes in vegetation structure coincide with changes in local hydrodynamic conditions.

3.4. Discussion

It was confirmed that erosion and recovery processes most likely shape the spatial structure of the vegetation at the salt-marsh pioneer zones. The vegetation change maps clearly show that erosion and growth at the pioneer zone is spatially correlated. Furthermore, the pioneer vegetation is irregularly structured and exhibits power-law patch-size distributions, which further supports the applicability of disturbance-recovery dynamics. Consequently, the question if power-laws can be used as indicator of the stress and disturbance of the pioneer zone vegetation became relevant for answering. The correlative analysis reveals that there is a strong relation between exposure to currents and the power-law scaling exponent of vegetation patch-

size distributions. So, this suggests that power-law distributions can be used as indicator of local hydrodynamics conditions at the salt-marsh pioneer zone.

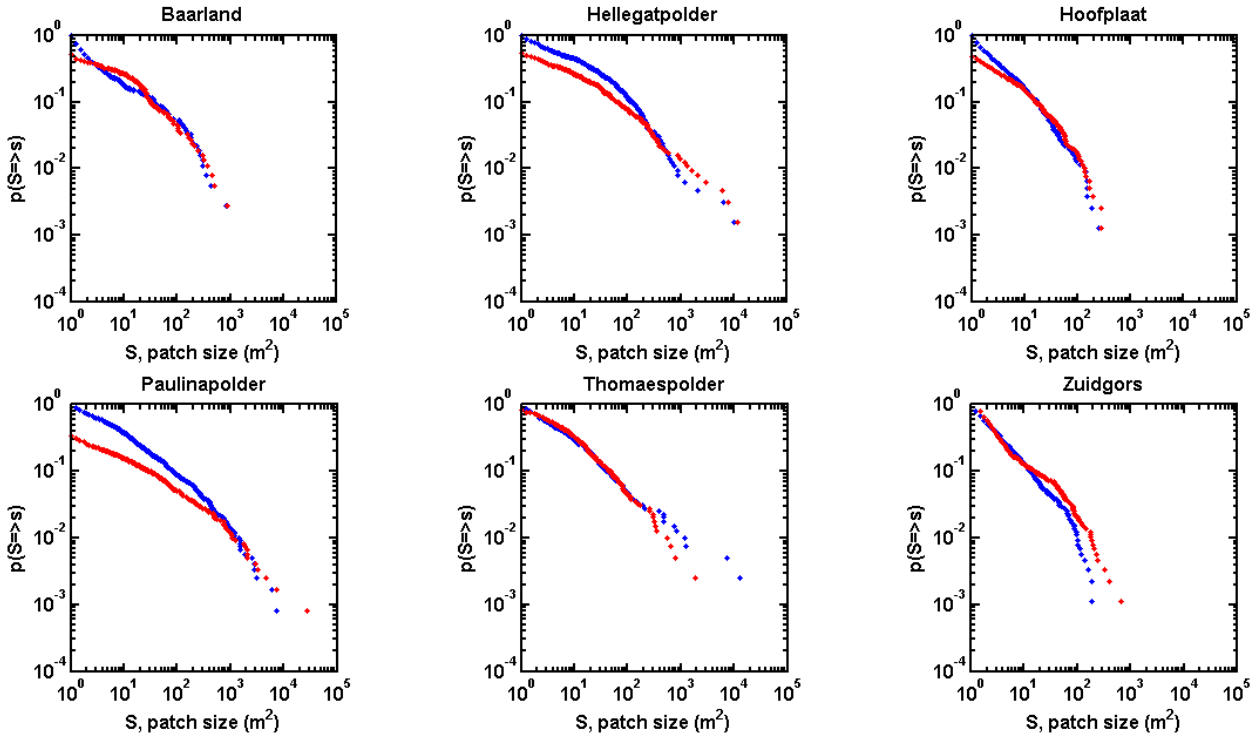

Figure 3.7. Patch-size distributions at pioneer zones of six salt-marshes separated for the years 1998 (blue) and 2004 (red) data.

Acquisition and preparation of spatial data can be an important source in variation in patch-sizes obtained, as discussed in the previous chapter (Ch.2.4.4). Small errors in mosaicing and georeferencing of the aerial pictures can lead to small displacements, which can result in areas that appear to have eroded or grown on vegetation change maps, but have not. Differences in classification of consecutive aerial photographs can be another sources of patch size variation. Due to weather conditions, inclination of the sun, and seasonal differences in the development of vegetation, the contrast between vegetated and unvegetetad area on the aerial photographs is altered, which will affect the accuracy of the classification. These classification errors also will give a false appearance of erosion or growth on vegetation change maps. However, due to such errors exponential distributions can be found in the patch-size distributions of erosion and growth patches (results not shown). The fact that the patch-size distributions of erosion and growth patches of the six pioneer zones exhibit power-law distributions suggests that errors in mosaicing and georeferencing are small.

Although the pioneer zones contain too few patches to show statistically sound that power-law distributions exhibit the vegetation structure of unpooled data, it can be shown that there are consistent qualitative changes in the patch-size data from aerial photograph to photograph. Furthermore, to reduce variations in patch-size distribution caused by technical issues (Ch.2.4) all data acquisition and preparation methods have been conducted in a consistent manner, automated with scripts where possible. Moreover, results are extensively validated by checking if similar qualitative results were obtained when changing details of these procedures (data not shown). For example, changing the neighbourhood type used in the cluster analysis, from

Moore to von Neumann, gives different patch-size distributions and, consequently, different scaling exponents. But, these scaling exponents still show the trend that sites with high hydrodynamic exposure have higher scaling exponents. So, patch-size distributions change in an consistent way suggesting that results are robust, provided that all analysis have been done with the same procedures.

4. Modeling disturbance and recovery at the pioneer zone

4.1. Introduction

The main objective of this chapter is to test the hypothesis that disturbance-recovery processes can explain the spatiotemporal patterns found in salt-marsh pioneer zones, as was described in the previous chapter. Therefore, a spatial explicit model was constructed, incorporating specific spatial processes presumed to govern the patch dynamics at the pioneer zone. It is investigated if this model can produce similar qualitative trends as were found in the empirical data. So, the model should produce:

1) Patch-size distributions exhibiting power-laws
2) Increasing power-law's scaling exponent with increasing hydrodynamic disturbance

Additionally, the behaviour of the model was studied over a wider range of parameters setting, thereby simulating different hydrodynamic conditions. This analysis gave supplementary information on behaviour of vegetation at the pioneer zone that can be expected under different levels of hydrodynamic conditions.

4.2. Model description

Because of the typical stochastic nature of disturbances, the use of continuous state (grid based) models, which model dynamics by partial differential equations (PDE) is not appropriate. Since these models do not allow incorporating of random disturbance events, another type of model is more appropriate. Cellular automata (CA) models do have the ability to integrating disturbance and recovery as stochastic processes (Guichard, et al., 2003; Pascual & Guichard, 2005). These models have been used to simulate spatial-explicit processes, like forest fires (Bak, 1997; Malamud, et al., 1998), disturbance of mussel beds on rocky shores (Guichard, et al., 2003), and spread of contagious diseases (Pascual, et al., 2002a). Potentially, this kind of models can be used to study erosion and growth processes determining the spatial structure of salt marsh pioneer zones.

The salt-marsh pioneer zone is modelled spatial explicit by a cellular automaton following the model of Guichard et al., (2003) used for modelling disturbance and recovery of mussels beds on rocky shores. Cellular automata have an analogy with a chessboard (Balzter, et al., 1998), were the lattice is the playing board with a number of discrete sites. Each site can be only in a limited set of discrete states, like the limited set of chess pieces allowed to play with. Stochastic transition rules, from one to another state, are the rules of the game, and govern the dynamics of the model. Disturbance can be modelled explicitly by introducing a disturbance state. In addition, disturbance and recovery can be modelled as a function of the configuration of neighbouring sites.

In case of the pioneer zone, an even sized lattice of 250 by 250 discrete cells represents the habitat. Each cell (or site) represents an area of approximate 0.25 by 0.25 m (so, area modelled is 62.5 by 62.5 m), equivalent to the ground sample distance (GSD) used in the aerial photographs. The model is stochastic at the cell level, so transitions between cell states occur with a probability per unit of time. Each cell can be in one of three possible states, σ. The unoccupied state, denoted by {0}, represents bare mud-flat. The occupied state, denoted by {+}, depict a cell covered with pioneer zone vegetation. The disturbed cell state, denoted {-}, correspond to a situation where disturbance of the vegetation is at hand, the disturbed edge.

The fundamental processes that are presumed to patch dynamics at the pioneer zone are erosion and growth. Erosion occurs mainly by disturbance of patch edges (cells change from {+} to {-}), called edge erosion. Growth by colonization of the bare mud-flat mainly occurs by vegetative growth (cells change from {0} to {+}), by means of rhizomal spread. This recovery process is hereafter referred to as positive feedback. See a conceptual outline of model in figure 4.1.

In this model disturbance and recovery are spatial feedback processes and depend on the local configuration, the state of the nearest neighbouring cells. The neighbourhood of a cell σ is defined as the eight nearest neighbours (z = 8), or Moore neighbourhood (Ch.2.2.2; Balzter, et al., 1998). The fraction of {σ}-cells in the neighbourhood of a {σ'} is expressed as $q_{\sigma|\sigma'}$. Finally, to keep track of the global development in the lattice the fraction of each cell state in the lattice is recorded as ρ_σ.

4.2.1. Edge erosion

Erosion is considered a self-propelling process ones initiated, spreading through adjacent vegetation like an infection or fire. Patch edges are more exposed for hydrodynamic conditions, like currents and waves, and therefore more vulnerable. At patch edges rhizomes of *S. anglica* can get dislodged resulting in disturbed edges (see fig.1.4.A&B). Once such disturbance is initialized it is likely to spread to occupied neighbouring sites. As a result, disturbance of the more susceptible unstable edges can trigger self-propelling erosion. So, transition from vegetated to disturbed edge state is modelled by:

$$P_{(+\rightarrow -)} = \varepsilon\eta_1 + \beta\eta_0 \qquad (4.1)$$

This means, the probability P of a cell to change from the vegetated state {+} to the disturbed edge state {-} depends on presence of and adjacent disturbed edge (the first term $\varepsilon\eta_1$) or the presence of adjacent mud-flat (the second term $\beta\eta_0$). If not one of the adjacent cells is disturbed, or $q_{-|+} = 0$, than $\eta_1 = 0$. However, if there is at least one adjacent cell disturbed, or $q_{-|+} > 0$, than $\eta_1 = 1$. So, in the first term an occupied cells becomes disturbed with probability ε if at least one of its neighbours is disturbed. The ε parameter in the transition rule represents disturbance by the local hydrodynamic conditions of pioneer vegetation due to exposure to currents and waves, and is a value between 0 for benign and 1 for extremely harsh conditions. The second term describes initiation of edge erosion. Parameter β is the initial disturbance probability and also depended on the neighbourhood configuration because it is assumed edges are more likely to become disturbed, in comparison to vegetation in the middle of a patch. So $\eta_0 = 0$, if $q_{0|+} = 0$ and $\eta_0 = 1$, if $q_{0|+} > 0$. This parameter can be seen as a mechanical failure probability due to exposure to currents and waves. So, this value is set, dependent on the

simulation, typically a factor 100-1000 lower than the ε term. Although this value is very low, without this last term edge erosion will not be set in motion and is essential for the dynamics of the system.

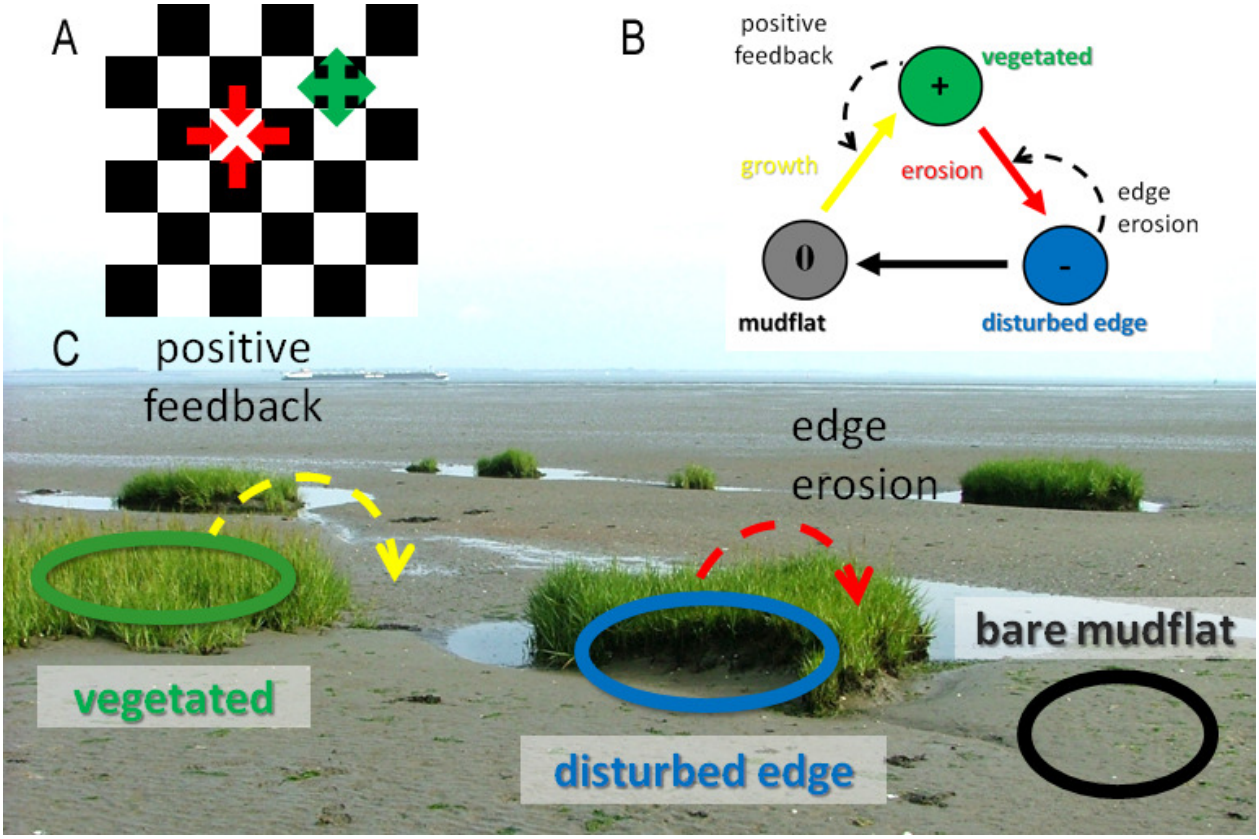

Figure 4.1. Conceptual outline of the cellular automata model describing the main processes presumed to explain patch dynamics at the pioneer zone. (A) The cellular automata is a square grid (the chessboard) in which cells can be influenced by neighbouring cells (red arrows) or exerts influence on its neighbours (green arrows). (B) Each cell can be in one of three states (mud-flat, vegetated, or disturbed edge) and transitions from one to the other state depends on the current state of the grid cells and configuration of the adjacent cells. (C) Due to a local positive feedback bare mud-flat can be turned into vegetation, if vegetation is present in an adjacent cell. Edge erosion is counteracting colonization in a similar way. Once a patch edge is disturbed, adjacent vegetation become more vulnerable causing a self-propelling erosion cascade turning vegetation back into mud-flat.

4.2.2. Growth

Because *Spartina anglica* mainly grows as patch-forming clones through lateral spread of rhizomes (Hemminga, et al., 1998), spatial facilitation of growth by neighbouring vegetation is assumed to result in a positive feedback. Colonization by germination of seeds is a rear event, but does occur. Therefore the rate of colonization of an unoccupied cell is depending on the fraction of surrounding vegetation and chance of seed germination and is represented by:

$$P_{(0\rightarrow+)} = g + fq_{+|0} \qquad (4.2)$$

So, the probability of a cell to change from a bare mud-flat {0} to a vegetated state {+} depends on the germination probability (the first term *g*) and the local presence of vegetation and strength of positive feedback (second term $fq_{+|0}$). Because the germination rate, *g*, is kept at a very low value (similar as *ϐ*), colonization of the mud-flat by growth is mainly facilitated by the positive feedback process. The strength of this positive feedback by neighbouring vegetation is represented by *f*, and determines the growth rate of the vegetation. This parameter is a value between 0 and 1, where assigning low values represent high stress, e.g. high duration of inundation, salinity or soil redox. Higher values for the positive feedback parameter represent little stress on the vegetation, and growth rates are high. Possible facilitative effects on germination is not included in this model. Moreover, the likely facilitative effect of neighbouring vegetation on preventing mortality is not included to keep the model transparent and easier for interpretation. In a more complex and predictive model these facilitation effects could be considered.

4.2.3. Mortality

An additional erosion processes included in the model (not shown in fig.4.1.B) is mortality, which turns occupied sites back into unoccupied sites. Mortality can be ascribed due to aging of the vegetation or by other random lethal disturbances, e.g. deposition of wrack or algal mats on top of the patch. As noted before, it is assumed that there is no facilitative effects of surrounding vegetation on preventing mortality by alleviate effects of stressors.

$$P_{(+\rightarrow0)} = m \qquad (4.3)$$

In this equation *m* is the mortality rate of the vegetated cells. During the simulations this value is kept at similar values as the germination probability and the initial erosion probability. By increasing this parameter, the influence of random, instead of spatially correlated, disturbances on the patch dynamics is increased.

4.2.4. Stabilization

After a site gets disturbed and edge erosion took place the site will be bare mud flat again. So, to keep the model dynamics traceable, it is assumed that cells will always return to the unoccupied state once they have been disturbed:

$$P_{(-\rightarrow0)} = 1 \qquad (4.4)$$

4.3. Model analysis

The conceptual model was analysed qualitatively by simulating vegetation dynamics at the pioneer zone as described in the previous section (Ch.4.2) at different parameter setting (see table 4.1). The objective of this exercise is to explore if the behaviour of the spatial model shows similar trends in model output as is found in the empirical data. Therefore, patch-size distributions generated by the model at different parameter settings are compared. Because this is just an qualitative model exploration, no attempts have been made to calibrate parameters with field data or estimations derived from the aerial photographs.

To keep results easy to interpret, only two model parameters are changed. The positive feedback *f* and the disturbance probability *ε* were varied over a full gradient, from no effect (0) to full influence (1). These two parameters represented the ability to grow (or the level of stress on the vegetation), and the level of disturbance by erosion, respectively. The parameters are increased with steps of 0.025, resulting in a total of 1681 combinations of parameters settings. For each of these settings the model ran for 10,000 time steps. However, recording of the patch-size distributions started after 8,000 time steps to allow the modelled system to reach an equilibrium state first. Then, patch-size data was recorder every 100 time steps resulting in 20 samples. In this way, autocorrelation between samples was minimized. Next, these samples where pooled for the analysis of the patch-size distribution. Furthermore, the cover fractions of the three states, bare mud-flat, vegetated, and disturbed edge, were recorded at every time step of the model run to track systems development in time.

Table 4.1. Parameters values used in the cellular automata model.

Parameter	Value	Description
ε	Between 0 and 1	Disturbance probability, due to hydrodynamic exposure. The change that a disturbed edge spreads to adjacent vegetation
β	0.0002	Initial disturbance probability. The change that a patch edge become an disturbed edge .
g	0.000001	Germination probability. The change that vegetation germinates on the mud-flat, without the influence of the positive feedback process.
f	Between 0 and 1	Growth probability by local positive feedback. Mud-flat is more likely to become vegetated if vegetation is present in an adjacent cell.
m	0.000001	Mortality probability. Change that vegetation dies at random.

4.4. Model results

4.4.1. Trends in patch-size distributions

The simulated vegetation structure (see figure 4.2.a-c) is in reasonable agreement with the vegetation structure found in real salt-marsh pioneer zones (see for example figure 3.2). Moreover, patch-size distributions of the simulated pioneer zone vegetation approximate power-law distributions (fig.4.2.e). Consequently, the model is able to capture an important property of the vegetation structure found in real salt-marsh pioneer zones.

There seems to be a good correlation between the disturbance probability and the power-law scaling exponents found in the simulated patterns, as figure 4.3 demonstrates. Like in the empirical data, here, the Hill estimator is used to estimate the scaling exponent in the simulated patterns. The model results seem to support the idea that a higher disturbance probability prevents patches of becoming large, which result in an increase of the scaling exponent. Figure 4.2.e shows that an increased disturbance probability truncates the patch-size distribution at the upper-part, thereby, increasing the scaling exponent. However, decreasing the positive feedback of plant growth can also increase the scaling exponent because less large patches will develop, as revealed by figure 4.2.e. Consequently, increasing stresses at the pioneer zone by inducing more erosion, or reduced growth can result in a higher scaling exponent in the patch-size distribution.

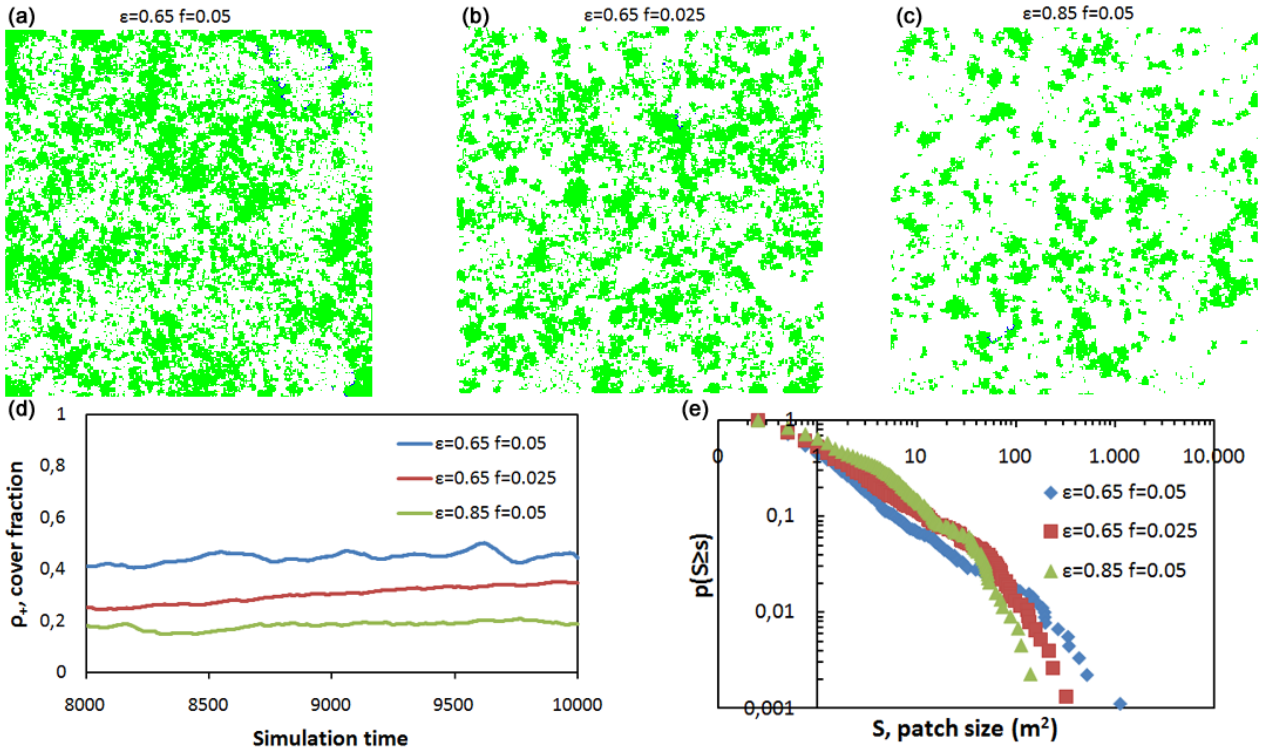

Figure 4.2. Results of model simulations. Three snapshots (a-c) of the spatial model output at different parameter setting. Here, white cells are unvegetated bare mud-flat, green cells are vegetated, and blue cells depict disturbed edges. (d) Shows vegetation cover in last 2000 time steps of model run for the parameter settings in the snapshots (a-c). (e) Shows patch-size distributions for the simulated vegetation in the snapshots (a-c).

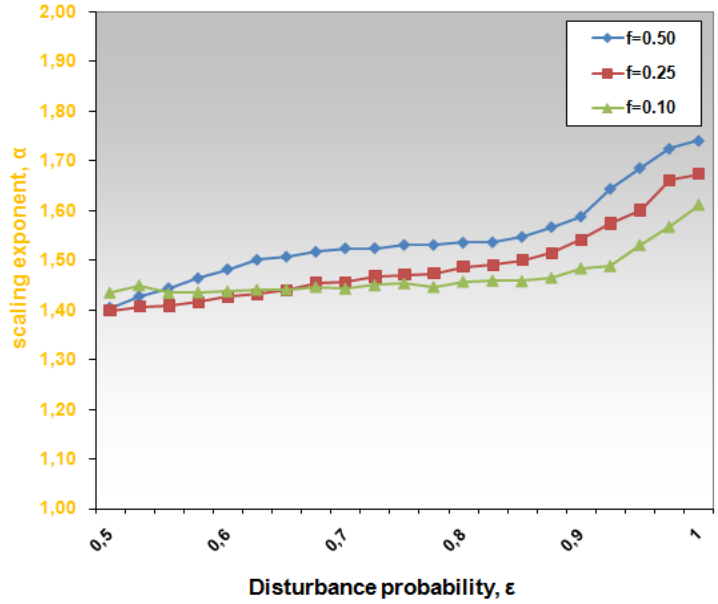

Figure 4.3. Scaling exponent related to level of disturbance at different facilitation strengths in non-global feedback model.

4.4.2. Behaviour of disturbance-recovery model

The model reveals that the response of the pioneer zone vegetation to increasing hydrodynamic conditions is non-linear. Figure 4.4. shows the average cover fraction, or vegetation density, at a given combination of parameter settings. Thus, the average cover fraction differs for every combination of disturbance probability and positive feedback strength. From these results it is clear that the balance between disturbance and recovery determines the average vegetation density the system develops to. If the positive feedback of the vegetation is strong enough, the pioneer zone vegetation response to disturbance by edge erosion is characterized by a threshold. Above this threshold the pioneer zone vegetation breaks open from fully covered mud-flat into a patchy structured vegetation (in figure 4.4. a clear threshold is present for f = 0.05 and 0.1 for $\varepsilon > 0.4$). Below the thresholds, edge disturbance will cause some small gaps, but the pioneer zone vegetation can recover fast enough to keep a high vegetation coverage.

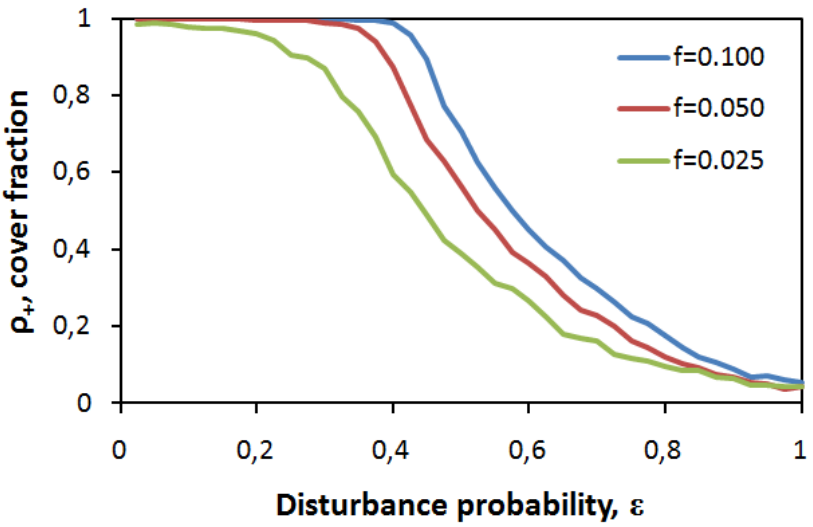

Figure 4.4. Behaviour of disturbance-recovery model at different strengths of positive feedback. The average cover fraction over the last 2000 time steps at different levels of disturbance probability represent the salt-marsh pioneer zone state.

If the level of disturbance reduces the cover fraction below approximately 0.53 (data not shown), the patch-size distributions in the simulated spatial patterns exhibit power-law distributions. So, the range of parameter settings, both disturbance probability ε, and positive feedback f, over which power-law distributions can be found in the model results is wide. Therefore, the disturbance-recovery model qualifies as a robust critical system (Ch.2.2.3).

4.5. Discussion

The vegetation structure and patch-size distributions simulated by the model seem a reasonable representation of the vegetation structure and patch-size distributions found in real salt-marsh pioneer zones. The simulated vegetation structure resembles the structure found in on the aerial photographs, and the patch-size distributions in the simulated spatial patterns exhibit power-law distributions. Moreover, the qualitative trends in results from the disturbance-recovery model are in agreement with the trends found in the six salt-marshes along the

Westerschelde: power-laws scaling exponents increase with an increasing disturbance probability, which is analogous to the increasing exposure to hydrodynamic conditions.

Although the model results are in agreement with the empirical data, during model analysis some simplifying assumptions have been made to keep result tractable. Most important, in the model analysis the parameters are constant in time and space during the model run. However, in a real setting it is likely that hydrodynamic conditions vary over time and space. For instance, it is most likely that the mud-flat, which pioneer vegetation tries to colonize, is characterized by a disturbance gradient. Cross-shore an elevation gradient can be found, with higher elevation near land and decreasing elevations toward the navigation channel. Due to this gradient currents near land will be weaker than toward the channel, and also waves will be attenuated more over shallow water than in deeper parts of the mud-flat when flooded. As a consequence, the patch-size distributions found in the aerial pictures will have developed under non-stationary conditions. The fact that there are great differences between the different locations, however, suggests that the hydrodynamic conditions are distinct enough to lead to obviously different vegetation structures at the pioneer zones.

No attempts have been made to calibrate the model. Therefore, the model results must be interpreted in a qualitative, rather than a quantitative, way. However, the objective of the conceptual modelling approach was not to come-up with specific predictions on future development of salt-marshes, but rather to get more insight into to generic pioneer zone vegetation responses to different levels of hydrodynamic exposure. The model results show that the local behaviour of the pioneer zone vegetation depends on the relative balance between disturbance and recovery processes, and that this response is non-linear. This means that the pioneer vegetation can become suddenly patchy when a threshold is surpassed. In this way the spatial structure can be an important indicator of changing hydrodynamic conditions. So, when an sudden shift from closed cover to patchy occurs, or the scaling exponent increases, this might be an important indication of changing local conditions.

5. Discussion and conclusions

5.1. Discussion

Understanding of the processes that govern salt-marsh vegetation establishment is of crucial importance to the management of coastal zones in many estuaries. The analysis presented in this thesis suggests that disturbance and recovery of vegetation patches by erosion and growth are the governing processes determining the spatial configuration of vegetation at the salt marsh-mud flat interface along the Scheldt-estuary. Analyses of multi-spectral aerial photographs revealed an irregularly spaced patchy pioneer vegetation that exhibits power-law distributions. It was demonstrated by means of a generic spatial explicit model that the vegetation structure, that was observed in the pioneer zones, can be explained by the interplay of disturbance and recovery processes. This results in spatial self-organization of vegetation, which exhibits power-law patch-size distributions, when the opposing processes are relatively balanced.

Results from both model and data analysis suggests that vegetation patchiness can be used as indicator of salt-marsh dynamics to asses current status and future development of the pioneer vegetation. Interplay between disturbance and recovery processes results in non-linear threshold responses to hydrodynamic conditions, as shown by the model results (fig.4.4). When the probability of disturbance increases, e.g. due to increasing hydrodynamic forcing, the salt-marsh will shift from fully covered, to patchy vegetation, to a bare mud flat (comparable to the sequence in fig.2.4). Hence, the appearance of patchiness at the interface between salt-marsh and mud-flat provides an indication that the ecosystem is nearing its limits. Therefore, patch-size distributions can give important information on proximity of a shift to a bare mud-flat state when hydrodynamic conditions are worsening.

The spatial analysis of the multi-spectral aerial photographs reveals that there is a strong link between the spatial structure and the rate of development of the pioneer zone. First, there is a strong correlation between scaling exponent and hydrodynamic forcing, like current velocity (fig.3.6). The scaling exponent increases with increasing currents. So, less large patches are observed at stronger currents, suggesting that it is more difficult for large patches to develop under strong hydrodynamic conditions. Second, differences in the obtained path-size distributions mainly reflect differences in growth between sites. In contrast, patch-size distributions of erosion patches are alike between sites, closely resemble each other in scaling exponent and do not deviate much from a power-law distributions (these distributions are very much ‘linear’ see small ΔL in tab.3.3, fig.B.1, and tab.B.1). Unlike erosion, distributions in growth patches differed considerably between sites (the distributions on growth are not nicely ‘linear’, larger ΔL in tab.3.3, fig.B.2, and tab.B.2), suggesting that these patch-size distributions reflect variations in growth between sites and in time. Therefore, patch-size distributions of growth patches are likely to be most useful as indicator monitoring the recovery of pioneer vegetation. Moreover, these results imply that the potential for growth, instead of disturbance by erosion processes, is most important for the establishment and development of salt-marsh pioneer

vegetation. Consequently, further studies should aim to identify key factors limiting growth of pioneer vegetation on mud flats, like seedling establishment and patch development.

Power-law patch-size distributions in ecosystems can emerge in multiple ways. Therefore, it is crucial to identify underlying mechanisms before inferences on the salt-marsh dynamics by interpreting patch-size distributions can be made (Pascual & Guichard, 2005). Power-laws can emerge in randomly patchy systems with no apparent driving mechanisms at a particular cover level, as is predicted by the concept of classical criticality (Ch.2.2.3). However, the vegetation cover in the pioneer zones in this study are all well below this value. Hence, the concept of classical criticality is no explanation for the observed patterns. Moreover, the concept of self-organized criticality (Ch.2.2.3), where autogenic mechanisms drive the system toward the critical point, is no reasonable explanation either, as we cannot envision such an autogenic mechanism in our salt-marsh system. Also, power-laws in those kinds of systems only develop if rates over which recovery and disturbance occur are clearly separated. This kind of dynamics is not found in the salt-marsh pioneer zone vegetation in this study. Pioneer vegetation is characterized by disturbance and recovery processes occurring at the same time, at similar rates (see fig.3.2. red and yellow patches are distributed equally between successive years). Accordingly, the spatiotemporal dynamics at salt-marsh pioneer zones can best be regarded as a robust critical system.

I have proposed a disturbance-recovery model that is capable of explaining the spatiotemporal patterns found at the pioneer zone. Disturbance of *Spartina anglica* tussocks involves self-propelling erosions, starting from disturbed tussock edges. Recovery results mainly from the lateral spread of *S. anglica* by means of rhizomes. These two spatially correlated processes can generate power-law patch-size distributions over a wide variety of parameters settings, revealing robust power-law characteristics over a broad range of hydrodynamic conditions. The scaling exponent that characterizes the vegetation patterns, as predicted by the model, also decreases with increasing vegetation density in the range of vegetation densities found in the aerial photographs. This implies that the vegetation dynamics at the pioneer zone can in general be described by the proposed disturbance-recovery processes, as described by the model. So, the model captures the transient dynamics of the pioneer vegetation, and trends in model output are in agreement with observations on the sequential aerial photographs.

Recently another type of robust critical dynamics is described, which is not classified well by the disturbance-recovery concept as put forward in this thesis. Scanlon (2007) and Kéfi (2007a) and their co-workers showed that power-laws also can emerge in resource limited systems. They studied arid ecosystems, where water limits vegetation growth, can generate a patchy landscape. In these systems the interaction between random grazing and local facilitation by the vegetation result in power-law patch-size distributions. The main disturbing agent their study was grazing, which was assumed to distribute themselves randomly over the area. Spread of vegetation occurs mostly close to existing vegetation, and is therefore a spatially correlated process. Their system differs from the salt-marsh pioneer zone in that disturbance is not random but occurs in the form of eroding edges. Thus, in salt-marshes, both erosion and growth are spatially correlated. Although disturbance processes are clearly different in both ecosystems, our combined studies, however, underline the importance of the spatial spread of vegetation in the ability to cope with harsh environments.

Effects of capital dredging events in the Scheldt-estuary

A prime political and social concern in the Netherlands is the effect of dredging on the Westerschelde estuary, and is often subject of political debate. Maintenance dredging, to keep the navigation channel accessible, is performed on a regular basis. However, in last half century the navigation channel has been broadened and deepened three times by capital dredging events, to allow larger ships to reach the harbours of Antwerpen. These major dredging activities took place between 1970-1975, 1997-1998, and the last in 2010. Because of this deepening, the tidal amplitude has increased by about one meter near Antwerpen (from 4.3 in 1900 to 5.2 m in 1990; Meire, et al., 2005). Consequently, currents became stronger at the scale of the whole estuary.

Most likely, effects of dredging on the pioneer zone vegetation will be noticeable in the years directly after the capital dredging activities took place, because than hydrodynamics and the concentration of suspended solid in the water column will be influenced most. Due to changes in the morphology of the estuaries channels the tidal volume entering the estuary increases clearly, as evidenced by the marked increase in tidal amplitude measured after capital dredging events (Meire, et al., 2005). Although there will be some local variation, in some cases resulting in a decrease of the currents instead, deepening and widening of the navigation channel will affect the whole estuary. Therefore, I expect to find clear changes in the patch-size distributions of the pioneer zone vegetation after a capital dredging event took place.

The available data set of multi-spectral aerial photographs, used in this thesis, allows to seek for influences of the second capital dredging event of 1997-1998 (tab.3.2) only. From most sites, aerial photographs are available since 1982. Hence, no earlier reference can be made, except for Hellegatpolder were a photograph of 1976 is available. Nevertheless, data is available from all sites during and after the second major dredging event, which allows us to investigate if effects of dredging are noticeable in the aerial pictures of 2004.

There seems to be a marked effect of the second capital dredging in the patch-size distributions for most locations. Comparing patch-size distributions of 1998 and 2004 data (fig.3.7) gives the impression that dredging has affected patch-size composition. Notably, in most cases, but not all, the small scale patches of 2004 lay well below the number found in 1998. This deficiency of small scale patches truncates the patch-size distribution in the lower patch-size scales. Only for Thomaespolder and Zuidgors there is no clear difference in the smaller patches. Most likely differences in patch-size data between 1998 and 2004 can be ascribed to (1) methodological problems while obtaining patch-size data, or (2) capital dredging.

The loss of small scale patches could be caused by methods for data acquisition and processing (chapter 2.3.2). Problems with classification can explain differences between sites and subsequent years. Although, the resolution and scale of the aerial photography is equal within one photo series (year), algae can be wrongly classified as vegetation, or in some photographs contrast between salt-marsh and mud-flat is not clear resulting in misclassification. However, these effects would differ per site, so this cannot explain estuary wide trends. Another explanation could be differences in the water level at the time of photographing, resulting in submergence of small patches. But, this is only occurring in some locations of the 1993 data. So, this does not have relevance for the comparison between 1998 and 2004 data. Another possibility affecting these results is differences in resolution between aerial photographs series. However, as noted above, the trend is not consistent for all locations. Some locations show no, like Zuidgors, or little deviation between years. Consequently, it is likely errors from

misclassification and differences in resolution can be ruled out as possible explanation. This leaves us by the possibility of ecological relevant explanations for the differences in patch-size data between years.

To get more insight into the vegetation dynamics between 1998 and 2004 the development of individual patches was tracked. Comparison of the balance (fig.3.3) between recruited and lost patches for five sites in different periods, indicates that in most sites the balance is positive, recruiting more patches then are lost. This view is supported by the trend in increasing vegetation cover, present in most sites, revealed by the patch development analysis (appendix C). Hence, it seems the differences in patch-size distributions are not the result of growth deficiency, but due to lack of establishment of new patches. In most locations a distinct shifts in the balance between the '98-'04 and previous period can be noted. The balance between recruitment and losses shifts from values close to one, to value one to two orders of magnitude in difference. Moreover, in case of Hellegatpolder a similar shift is noticeable for the earlier '76-'82 period, coinciding the first deepening event. Only Hoofdplaat breaks this trend. This might be because around 1981 a breakwater was constructed and the mud flat elevation has increased considerable of this location, which most likely invoked the rapid vegetation development observed, and explains why the balance between recruitment and loss is high for all periods analyzed. So, although still speculative, because the evidence is still very anecdotal, it seems there is a noticeable effect of the major dredging activities in the estuary on the patch-size composition of the six pioneer zones. However, these results are not straightforward. The net gain in some sites and net loss in other locations might also be caused by other processes, like sediment transport and channel migration not related to the capital dredging events, but to natural temporal variability in the estuary. This temporal variability was not considered further in this study. So, to draw firm conclusions of the effects on capital dredging needs more thorough analysis. The future availability of aerial pictures after the last (2010) capital dredging might give the opportunity to test hypothesis posed here.

Outlook

Although patterns found in the field are well explained by the model, and the mechanisms modelled all seem reasonable descriptions of processes at the pioneer zone, the mechanisms still remain somewhat speculative. Using aerial photographs and conducting small-scale manipulative experiments at vegetation patches should be possible to validate and test the model assumptions, building confidence on the generality of this model to explain salt-marsh pioneer vegetation dynamics. For instance, parameter estimation and validation could start by calibrating model parameters to analysing sequential aerial photographs (like e.g. Satake, et al., 2004). Furthermore, combined field measurements on erosion rates and *in situ* manipulative experiments to measure propagation of disturbed edges or lateral expansion, the model could be validated and improved. The use of models to infer emergence of landscape-scale patterns from the individual patch behaviour is the only possible way to study such large scale dynamics, because it is not feasible to conduct experiments at this spatial and temporal scale. Gaining more insight into the main processes that control and limit establishment and growth of patches will allow us to develop better understanding how to interpret patch-size distributions and its deviations. Therefore, further development of power-law patch-size distributions as indicator of salt-marsh status and future expansion might give decision-makers tools to mitigate effect of man-made stressors, disturbances and climate change.

5.2. Conclusions

The aim of this thesis was to address the two main research questions:

Research Question 1:

> ***Do disturbance and recovery processes at the pioneer zone of tidal salt-marshes determine spatial structure of salt-marsh pioneer vegetation in such a way that patch-size distributions exhibit power-laws?***

From the results presented in this thesis it can be concluded that erosion and recovery processes at the pioneer zone of tidal salt marshes determine to a large extent the spatial structure of salt-marsh pioneer vegetation. Moreover, in a broad range of hydrodynamic conditions the patch-size frequency distributions approximate power-laws.

Because the question to the first research question is positive, the second research question becomes relevant:

Research Question 2:

> ***Can these vegetation patch-size distributions be used as indicators of vegetation dynamics to assess current status and future development of salt-marsh ecosystems at the interface with the tidal flats?***

The use of these power-law patch-size distributions as indicator of ecomorphological dynamics seems promising. Deviations from the power-law pattern could be used to assess influence of hydrodynamic disturbance on recovery processes, and can, therefore, indicate potential for future development in a synoptic way. In addition, the shape of the patch-size distribution could, in combination with vegetation density and number of patches, be used to assess progress of transient toward full-cover endpoint. However, further research is necessary to interpret deviations from power-laws in terms of vegetation recruitment and growth limitations.

Glossary

Definitions as used by Jones et al (1997), Pascual and Guichard (2005), and Rietkerk and van de Koppel (2008).

Cell: a discrete site at a lattice (see lattice based models).

Cellular automaton: lattice based model with discrete sites and states (see lattice based models).

Connectedness: two sites are connected if they belong to the same patch (or cluster). In lattice models, a patch can be defined by starting at a given site and adding all the sites among its neighbors that are occupied by the same species or state (e.g. trees, grass or mussels). The neighborhood itself is defined by the local rules of interaction. One measure of connectedness is the size of the largest patch relative to the total size of the system.

Criticality: in statistical mechanics, the state of a system is said to be critical if poised at a phase transition. Many phase transitions have a critical point associated with them, which separate one or more phases. As a system approaches a critical point, large-scale structures appear despite the fact that the system is driven only by local interactions. At criticality, these patterns are typically characterized by scale invariance.

Ecosystem engineer: organisms that directly or indirectly control the availability of resources to other organisms by causing physical state changes in biotic or abiotic materials. Physical ecosystem engineering by organisms is the physical modification, maintenance, or creation of habitats. The ecological effect of engineering on other species occurs because the physical state changes directly or indirectly control resources used by these species.

Fractal: usually refers to a geometric shape that is self-similar. Such as shape is constructed from parts that are more or less alike at every scale of observation, and, therefore, have a irregular or rough structure. Thru fractals have infinite detail, but most fractals in nature have a limit to the range of scale over which fractal behavior is found. Fractals can be generated by iterative processes and do not only occur in geometric shape, but also other data like time series.

Irregular patterns: spatially patterns without characteristic cluster size. These patterns are not evenly spaced (e.g. power law clustering).

Lattice (or grid) based models: a dynamical system in which space is a network of discrete sites. The values of a site can be continues (real value e.g. biomass, or water level) or discrete (integer values, states e.g. presence/absence vegetation cover). In a reaction-diffusion models values are continues and processes and diffusion between cells are modeled by differential equations. In case of discrete states and discrete time model is referred to as synchronic cellular automata. When time is treated as continuous, these models are also known as interacting particle systems or asynchronous cellular automata.

Localized disturbance-recovery processes: disturbance occurs primarily close to a site already disturbed (e.g. by waves or wind) and recovery takes place primarily close to a site that is occupied by organisms (e.g. by local seed dispersal or colonization).

Long-distance negative feedback: ecological interactions resulting in a net negative feedback between organisms and their environment at a particular distance from the organisms.

Long-range competition: the process where organisms, by depleting resources, constrain the establishment and survival of other organisms over a long range.

Oscillating consumer-resource interactions: cyclic dynamics in a predator population and its prey, caused by strong feeding interactions between the two.

Phase transition: an abrupt change in the state of the system as some external parameter is varied. A common example is the gas liquid phase transition undergone by water in relation to temperature.

Power laws: a function y=f(x) is a power law where the dependent variable y varies as a power of the independent variable x (i.e. $y=Cx^{-\alpha}$, where C is a normalization constant and α is a scaling exponent). This relationship exhibits the property of scale invariance, implying that the relation is the same at a range of scales. Power laws are linear functions when the logarithm of both dependent and independent variables are taken.

Regular patterns: spatially periodic patterns with a characteristic cluster size or limited scale of sizes (e.g. the spotted coats of leopards).

Resilience: the amount of disturbance a system can absorb and still remain within the same state or domain of attraction.

Resistance: the amount of environmental change an ecosystem can withstand and still remain in the same state.

Scale-dependent feedback: the strength and sign of a feedback between organisms and their environment varies with distance.

Scale invariance: a distribution characterized by a power law is said to be scale invariant (e.g. the frequency distribution of patch sizes in critical systems). It follows that scale-invariant distributions are independent from the resolution, or scale, at which the system is observed.

Short-distance positive feedback: ecological interactions resulting in a net positive feedback between organisms and the environment near the organisms.

Short-range facilitation: the process where organisms, by creating favorable conditions over a short range, help establishment and survival of other organisms close-by.

Spatial self-organization: the process where large-scale ordered spatial patterns emerge from disordered initial conditions through local interactions.

State shift: in an ecosystem, a sudden and drastic change in the state of the system in space or time. The state can be defined as the presence, the abundance or the distribution of one or many species and/or resources.

Spiral waves: spirals that rotate over time around either meandering or stationary cores.

References

Adam, P. (2002). Saltmarshes in a time of change. *Environmental Conservation, 29*, 39-61.

Allen, J. R. L. (2000). Morphodynamics of Holocene salt marshes: a review sketch from the Atlantic and Southern North Sea coasts of Europe. *Quaternary Science Reviews, 19*, 1155-1231.

Avnir, D., Biham, O., Lidar, D., & Malcai, O. (1998). Is the geometry of nature fractal? *Science, 279*, 39-40.

Baeyens, W., van Eck, B., Lambert, C., Wollast, R., & Goeyens, L. (1998). General description of the Scheldt estuary. *Hydrobiologia, 366*, 1-14.

Bak, P. (1997). How Nature Works: The science of self-organized criticality. Oxford: Oxford University Press.

Balzter, H., Braun, P. W., & Köhler, W. (1998). Cellular automata models for vegetation dynamics. *Ecological Modelling, 107*, 113-125.

Barbier, N., Couteron, P., LeJoly, J., DeBlauwe, V., & LeJeune, O. (2006). Self-organized vegetation patterning as a fingerprint of climate and human impact on semi-arid ecosystems. *Journal of Ecology, 94*, 537-547.

Boorman, L. A. (1999). Salt marshes - present functioning and future change. *Mangroves and Salt Marshes, 3*, 227-241.

Bouma, T. J., van Duren, L. A., Temmerman, S., Claverie, T., Blanco-Garcia, A., Ysebaert, T., & Herman, P. M. J. (2007). Spatial flow and sedimentation patterns within patches of epibenthic structures: Combining field, flume and modelling experiments. *Continental Shelf Research, 27*, 1020-1045.

Callaghan, D. P., Bouma, T. J., Klaassen, P., van der Wal, D., Stive, M. J. F., & Herman, P. M. J. (2010). Hydrodynamic forcing on salt marsh development: distinguishing the relative importance of waves vs. tidal flow. *Estuarine Coastal and Shelf Science, 89*, 73-88.

Camazine, S., Deneubourg, J. L., Franks, N. R., Sneyd, J., Theraulaz, G., & Bonabeau, E. (2001). Self-Organization in Biological Systems. Princeton: Princeton University Press.

Clauset, A., Shalizi, C. R., & Newman, M. E. J. (2007). Power-law distributions in empirical data.

Clutton-Brock, T. H., Albon, S. D., & Harvey, P. H. (1980). Antlers, body size and breeding group size in the Cervidae. *Nature, 285*, 565-567.

Cohen, W. B., & Goward, S. N. (2004). Landsat's role in ecological applications of remote sensing. *BioScience, 54*, 535-545.

Day, J. W., Scarton, F., Rismondo, A., & Aret, D. (1998). Rapid Deterioration of a Salt Marsh in Venice Lagoon, Italy. *Journal of Coastal Research, 14*, 583-590.

Dionne, J.-C. (1985). Tidal marsh erosion by Geese, St. Lawrence estuary, Québec. *Géographie physique et Quaternaire, 39*, 99-105.

Edwards, A. M., Phillips, R. A., Watkins, N. W., Freeman, P., Murphy, E. J., Afanasyev, V., Buldyrev, S. V., da Luz, M. G. E., Raposo, E. P., Stanley, H. E., & Viswanathan, G. M. (2007). Revisiting Levy flight search patterns of wandering albatrosses, bumblebees and deer. *Nature, 449*, 1044-1048.

Enquist, B. J., Brown, J. H., & West, G. B. (1998). Allometric scaling of plant energetics and population density. *Nature, 395*, 163-165.

Enquist, B. J., & Niklas, K. J. (2001). Invariant scaling relations across tree-dominated communities. *Nature, 410*, 655-741.

Eppinga, M. B., Rietkerk, M., Wassen, M. J., & de Ruiter, P. C. (2009). Linking habitat modification to catastrophic shifts and vegetation patterns in bogs. *Plant Ecology, 200*, 53-68.

Fagan, W. F., Fortin, M.-J., & Soykan, C. (2003). Integrating edge detection and dynamic modeling in quantitative analysis of ecological boundaries. *BioScience, 53*, 730-738.

Fortin, M.-J., & Dale, M. (2005). Spatial Analysis: A Guide for Ecologists. Cambridge: Cambridge University Press.

Garlaschelli, D., Caldarelli, G., & Pietronero, L. (2003). Universal scaling relations in food webs. *Nature, 423*, 165-168.

Guichard, F., Halpin, P. M., Allison, G. W., Lubchenco, J., & Menge, B. A. (2003). Mussel Disturbance Dynamics: Signatures of Oceanographic Forcing from Local Interactions. *The American Naturalist, 161*, 889-904.

Halley, J. M., Hartley, S., Kallimanis, A. S., Kunin, W. E., Lennon, J. J., & Sgardelis, S. P. (2004). Uses and abuses of fractal methodology in ecology. *Ecology Letters, 7*, 254-271.

Halloy, S. R. P., & Barratt, B. I. P. (2007). Patterns of abundance and morphology as indicators of ecosystem status: A meta-analysis. *Ecological Complexity, 4*, 128-147.

Harte, J., Kinzig, A., & Green, J. (1999). Self-Similarity in the Distribution and Abundance of Species. *Science, 284*, 334-336.

Hassell, M. P., Comins, H. N., & May, R. M. (1991). Spatial structure and chaos in insect population dynamics. *Nature, 353*, 255-258.

Hemminga, M. A., van Soelen, J., & Maas, Y. E. M. (1998). Biomass production in pioneer *Spartina anglica* patches: evidence for the importance of seston particle deposition. *Esturarine, Coastal and Shelf Science, 47*, 797-805.

Hughes, R. G., & Paramor, O. A. L. (2004). On the loss of saltmarshes in south-east England: methods for their restoration. *Journal of Applied Ecology, 41*, 440-448.

Jacobusse, C., & Hemminga, M. A. (Eds.). (2001). *Zeldzaam Zeeuws: Bijzondere planten en dieren in Zeeland*. Heinkenszand: Stichting Het Zeeuwse Landschap.

Johnson, J. B., & Omland, K. S. (2004). Model selection in ecology and evolution. *Trends in Ecology and Evolution, 19*, 101-108.

Jones, C. G., Lawton, J. H., & Schachak, M. (1997). Positive and negative effects of organisms as physical ecosystem engineers. *Ecology, 78*, 1946-1957.

Jordano, P., Bascompte, J., & Olesen, J. M. (2003). Invariant properties in coevolutionary networks of plant-animal interactions. *Ecology Letters, 6*, 69-81.

Kéfi, S., Rietkerk, M., Alados, C. L., Pueyo, Y., Papanastasis, V., ElAich, A., & de Ruiter, P. C. (2007a). Spatial vegetation patterns and imminent desertification in Mediterranean arid ecosystems. *Nature, 449*, 213-218.

Kéfi, S., Rietkerk, M., van Baalen, M., & Loreau, M. (2007b). Local facilitation, bistability and transitions in arid ecosystems. *Theoretical Population Biology, 71*, 367-379.

Kéfi, S., Alados, C. L., Chaves, R. C. G., Pueyo, Y., & Rietkerk, M. (2010 in press-a). Is the patch size distribution of vegetation a suitable indicator of desertification? Comment. *Ecology*.

Kéfi, S., Rietkerk, M., Roy, M., Alain, F., de Ruiter, P. C., & Pascual, M. (2010 in press-b). Robust scaling in ecosystems and the meltdown of patch size distributions before extinction. *Ecological Letters*.

Kirwan, M., & Temmerman, S. (2009). Coastal marsh response to historical and future sea-level acceleration. *Quaternary Science Reviews, 28*, 1801-1808.

Klausmeier, C. A. (1999). Regular and Irregular Patterns in Semiarid Vegetation. *Science, 284*, 1826-1828.

Klemas, V. V. (2009). Remote sensing of coastal resources and environment. *Environmental Research, Engineering and Management, 2*, 11-18.

Li, B.-L. (2000). Fractal geometry applications in description and analysis of patch patterns and patch dynamics. *Ecological Modelling, 132*, 33-50.

Lin, Y., Han, G., Zhao, M., & Chang, S. X. (2010). Spatial vegetation patterns as early sign of desertification: a case study of a desert steppe in Inner Mongolia, China. *Landscape Ecology*.

MacArthur, R. H., & Wilson, E. O. (1967). The theory of island biogeography. Princton: Princton University Press.

Maestre, F. T., & Escudero, A. (2009). Is the patch size distribution of vegetation a suitable indicator of desertification processes? *Ecology, 90*, 1729-1735.

Malamud, B. D., Morein, G., & Turcotte, D. L. (1998). Forest fires: an example of self-organized critical behavior. *Science, 281*, 1840-1842.

Meire, P., Ysebaert, T., van Damme, S., van den Bergh, E., Maris, T., & Struyf, E. (2005). The Scheldt estuary: a description of a changing ecosystem. *Hydrobiologia, 540*, 1-11.

Millennium.Ecosystem.Assessment. (2005a). Ecosystems and Human Well-being: Synthesis. Washington, DC: Island Press.

Millennium.Ecosystem.Assessment. (2005b). Ecosystems and Human Well-being: Current State and Trends, Volume 1. Washington, DC: World Resource Institute.

Millennium.Ecosystem.Assessment. (2005c). Ecosystems and Human Well-being: Wetlands and Water Synthesis. Washington, DC: World Resource Institute.

Newman, M. E. J. (2006). Power laws, Pareto distributions and Zipf's law. *Contamporary Physics, 46*, 323-351.

Okuyama, T. (2008). Do mutualistic networks follow power distributions? *Ecological Complexity, 5*, 59-65.

Olofson, P., Spellman, M., Grijalva, E., Kerr, D., Hogle, I., & Ericson, S. (2009). San Francisco Estuary Invasive Spartina Project. from http://www.spartina.org

OzCoasts. (2010). Australien Online Coastal Information. from http://www.ozcoasts.org.au/

Pascual, M., Roy, M., & Franc, A. (2002a). Simple temporal models for ecological systems with complex spatial patterns. *Ecology Letters, 5*, 412-419.

Pascual, M., Roy, M., Guichard, F., & Flierl, G. (2002b). Cluster size distributions: signatures of self-organization in spatial ecologies. *Philosophical Transactions of the Royal Society B: Biological Sciences, 357*, 657-666.

Pascual, M., & Guichard, F. (2005). Criticality and disturbance in spatial ecological systems. *Trends in Ecology and Evolution., 20*, 88-95.

Perline, R. (2005). Strong, Weak and False Inverse Power Laws. *Statistical Science, 20*, 68-88.

Rietkerk, M., Dekker, S. C., de Ruiter, P. C., & van de Koppel, J. (2004). Self-Organized Patchiness and Catastrophic Shifts in Ecosystems. *Science, 305*, 1926-1929.

Rietkerk, M., & van de Koppel, J. (2008). Regular pattern formation in real ecosystems. *Trends in Ecology and Evolution, 23*, 169-175.

Rohani, P., Lewis, T. J., Grünbaum, D., & Ruxton, G. D. (1997). Spatial self-organization in ecology: pretty patterns or robust reality? *Trends in Ecology and Evolution, 12*, 70-74.

RWS. Rijkswaterstaat.

Satake, A., Iwasa, Y., Hakoyama, H., & Hubbell, S. P. (2004). Estimating local interaction from spatiotemporal forest data, and Monte Carlo bias correction. *Journal of Theoretical Biology, 226*, 225-235.

Scanlon, T. M., Caylor, K. K., Levin, S. A., & Rodriguez-Iturbe, I. (2007). Positive feedbacks promote power-law clustering of Kalahari vegetation. *Nature, 449*, 209-213.

Scheffer, M., Carpenter, S., Foley, J. A., Folke, C., & Walker, B. (2001). Catastrophic shifts in ecosystems. *Nature, 413*, 591-596.

Scheffer, M., Bascompte, J., Brock, W. A., Brovkin, V., Carpenter, S. R., Dakos, V., Held, H., van Nes, E. H., Rietkerk, M., & Sugihara, G. (2009). Early-warning signals for critical transitions. *Nature, 461*, 53-59.

Scheffer, M. (2009). Critical transitions in nature and society. New Jersey: Princeton University Press.

SIC. (2009). Schelde informatie centrum. from http://www.scheldenet.nl

Sims, D. W., Righton, D., & Pitchford, J. W. (2007). Minimizing errors in identifying Lévy flight behaviour of organisms. *Journal of Animal Ecology, 76*, 222-229.

Sims, D. W., Southall, E. J., Humphries, N. E., Hays, G. C., Bradshaw, C. J. A., Pitchford, J. W., James, A., Ahmed, M. Z., Brierley, A. S., Hindell, M. A., Morritt, D., Musyl, M. K., Righton, D., Shepard, E. L. C., Wearmouth, V. J., Wilson, R. P., Witt, M. J., & Metcalfe, J. D. (2008). Scaling laws of marine predator search behaviour. *Nature, 451*, 1098-1102.

Solé, R. V., Manrubia, S. C., Benton, M. J., Kauffman, S. A., & Bak, P. (1999). Criticality and scaling in evolutionary ecology. *Trends in Ecology and Evolution., 14*, 156-160.

Solé, R. V., & Bascompte, J. (2006). Self-Organization in Complex Ecosystems. Princeton: Princeton University Press.

Solé, R. V. (2007). Scaling laws in the drier. *Nature, 449*, 151-153.

Temmerman, S., Govers, G., Wartel, S., & Meire, P. (2004). Modelling estuarine variations in tidal marsh sedimentation: response to changing sea level suspended sediment concentrations. *Marine Geology, 212*, 1-19.

Temmerman, S., Bouma, T. J., van de Koppel, J., van der Wal, R., de Vries, M. B., & Herman, P. M. J. (2007). Vegetation causes channel erosion in a tidel landscape. *Geology, 35*, 631-634.

Thompson, J. N., Reichman, O. J., Morin, P. J., Polis, G. A., Power, M. E., Sterner, R. W., Couch, C. A., Gough, L., Holt, R., Hooper, D. U., Keesing, F., Lovell, C. R., Milne, B. T., Molles, M. C., Roberts, D. W., & Strauss, S. Y. (2001). Frontiers of Ecology. *BioScience, 51*, 15-24.

Ustin, S. L., Roberts, D. A., Gamon, J. A., Asner, G. P., & Green, R. O. (2004). Using imaging spectroscopy to study ecosystem processes and properties. *BioScience, 54*, 523-534.

van Belzen, J., Eppinga, M. B., Kéfi, S., van der Wal, D., Rietkerk, M., & van de Koppel, J. (in prep.). Comparing patch-size distributions derived from 1-dimensional line-intercepts and 2-dimensional aerial pictures.

van de Koppel, J., van der Wal, R., Bakker, J. P., & Herman, P. M. J. (2005a). Self-Organization and Vegetation Collapse in Salt Marsh Ecosystems. *The American Naturalist, 165*, E1-12.

van de Koppel, J., Rietkerk, M., Dankers, N., & Herman, P. M. J. (2005b). Scale-Dependent Feedback and Regular Spatial Patterns in Young Mussel Beds. *The American Naturalist, 165*, E66-77.

van der Wal, D., & Pye, K. (2004). Patterns, rates and possible causes of saltmarsh erosion in the Greater Thames area (UK). *Geomorphology, 61*, 373-391.

van der Wal, D., Wielemaker-van den Dool, A., & Herman, P. M. J. (2008). Spatial patterns, rates and mechanisms of saltmarsh cycles (Westerschelde, The Netherlands). *Estuarine, Coastal and Shelf Science, 76*, 357-368.

van Hulzen, J. B., van Soelen, J., & Bouma, T. J. (2007). Morphological variation and habitat modification are strongly correlated for autogenic ecosystem engineer *Spartina anglica* (Common cordgrass). *Estuaries and Coasts, 30*, 3-11.

van Wesenbeeck, B. K., van de Koppel, J., Herman, P. M. J., & Bouma, T. J. (2008). Does scale-dependent feedback explain spatial complexity in salt-marsh ecosystems? *Oikos, 117*, 152-159.

Vandermeer, J., Perfecto, I., & Philpott, S. M. (2008). Cluster of ant colonies and robust criticality in a tropical agroecosystem. *Nature, 451*, 457-459.

Weerman, E. J., van de Koppel, J. v., Eppinga, M. B., Montserrat, F., Liu, Q.-X., & Herman, P. M. J. (2010). Spatial self-organization on intertidal mudflats through biophysical stress divergence. *The American Naturalist, 176*, E15-E32.

White, E. P., Enquist, B. J., & Green, J. L. (2008). On estimating the exponent of power-law frequency distributions. *Ecology, 89*, 905-912.

Wolters, M., Bakker, J. P., Bertness, M. D., Jefferies, R. L., & Möller, I. (2005). Saltmarsh erosion and restoration in south-east England: squeezing the evidence requires realignment. *Journal of Applied Ecology, 42*, 844-851.

Zvuloni, A., Artzy-Randrup, Y., Stone, L., van Woesik, R., & Loya, Y. (2008). Ecological size-frequency distributions: how to prevent and correct biases in spatial sampling. *Limnology and Oceanography: Methods, 6*, 144-152.

Appendices

A. Individual patch development analysis

Introduction

To get more insight into the development of patches and the processes involved, at the individual patch level, shaping the frequency distributions, an algorithm was developed to track the behavior of the individual patches between two subsequent aerial photographs. The algorithm records the changes of the individual patches of successive presence-absence maps, and allows comparing the behavior of different size classes. Unfortunately, no such analysis could be done for Zuidgors due to computational limitations. The size of the data set (lattice) of Zuidgors was to large resulting in memory shortage for the algorithm.

Method

There are a number of possibilities how patches develop between t_0 and t_1 (fig.A.1), these development classes are:

1. New patch: by establishment of seedlings or clone fragments a new patch can grow.
2. Loss of patch: by erosion the patch disappears completely
3. Stable: no growth or erosion
4. Growth: a patch expands because of vegetative growth
5. Erosion: a patch contracts because of erosion
6. Growth & erosion: a mixture of the two subsequent processes, a patch grows and erodes at the same time
7. Merge: two (or more) patches merge to one bigger patch
8. Split: a patch splits in two (or more) smaller patches because of erosion
9. Complicated: Like growth and erosion can occur at the same time, merging and splicing of patches can occur simultaneously as well. If too much is going on, the algorithm cannot track it, and classifies it as 'complicated'.

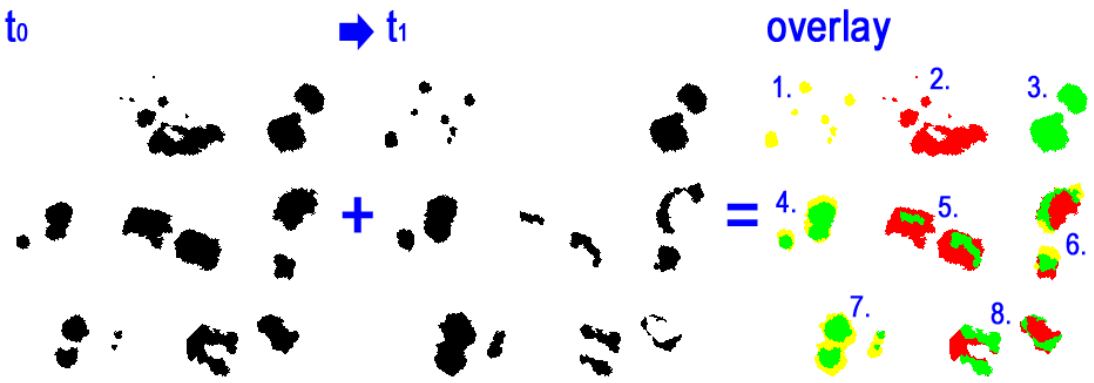

Figure A.1. Different possibilities in patch development, if vegetation presence of two subsequent times, t_0 and t_1, is compared differences can be represented by the coloured overlay map. Here, green is stable vegetation (present at t_0 and t_1) yellow is new grown vegetation (only present in t_1), red is eroded vegetation (only present in t_0). An explanation of the numbers is found in the text.

Each patch is assigned one of the above development possibilities by tracking patches on two consecutive vegetation maps. Next, a logarithmic binning scheme (Sturges formula, where the number of bins is $k=ceiling(log_2 n+1)$) is used to classify the labeled patches in size classes (bins). Finally, the abundance of each development possibility is displayed as a stacked bar graph. Additionally, the effect of the patch development for each bin is depicted, which results in 20 routes:

1. Stable: as in development class 3, nothing happened with these patches.
2. New: as in development class 1.
3. Lost: as in development class 2.
4. Growth 1: Patches have grown but did not outgrown bin size, and stay in bin.
5. Growth 2: Patches have outgrown a lower bin, and becomes part of this bin.
6. Growth 3: Patches have outgrown bin, and are lost to higher bins.
7. Erosion 1: Patches have eroded but did not go below bin size, and stay in bin.
8. Erosion 2: Patches have eroded below bin size, and are lost to lower bins.
9. Erosion 3: Patches have eroded below higher bin sizes, and becomes part of this bin.
10. Gro.ero 1: Patches have grown and eroded, but net effect did not go outside bin size, so these patches stay in bin.
11. Gro.ero 2: Patches have grown and eroded, and net effect did outgrow

lower bin size, so these patches become part of this bin.

12. Gro.ero 3: Patches have grown and eroded, and net effect did go below bin size, these patches are lost to lower bins.
13. Gro.ero 4: Patches have grown and eroded, and net effect did go below higher bin sizes, so these patches become part of this bin.
14. Gro.ero 5: Patches have grown and eroded, and net effect did outgrow bin size, so these patches become part of higher bins.
15. Merge 1: Loss of patches by merging
16. Merge 2: Gain of patches by merging
17. Split 1: Loss of patches by splitting
18. Split 2: Gain of patches by splitting
19. Compl. 1: Loss of complicated patches
20. Compl. 2: Gain of complicated patches

Because of the complicated nature of development of the last 6 (15-20) development routes, only loss and gain of all patches is given. If a patch merges or splits it becomes new, so only net results of these development routes are recorded.

Results

A

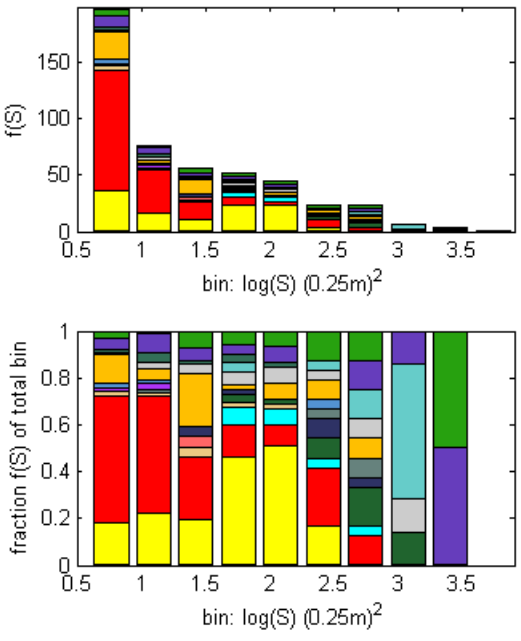

B

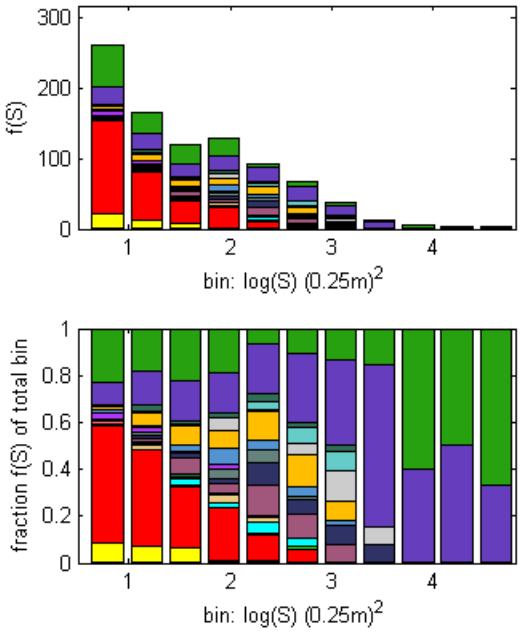

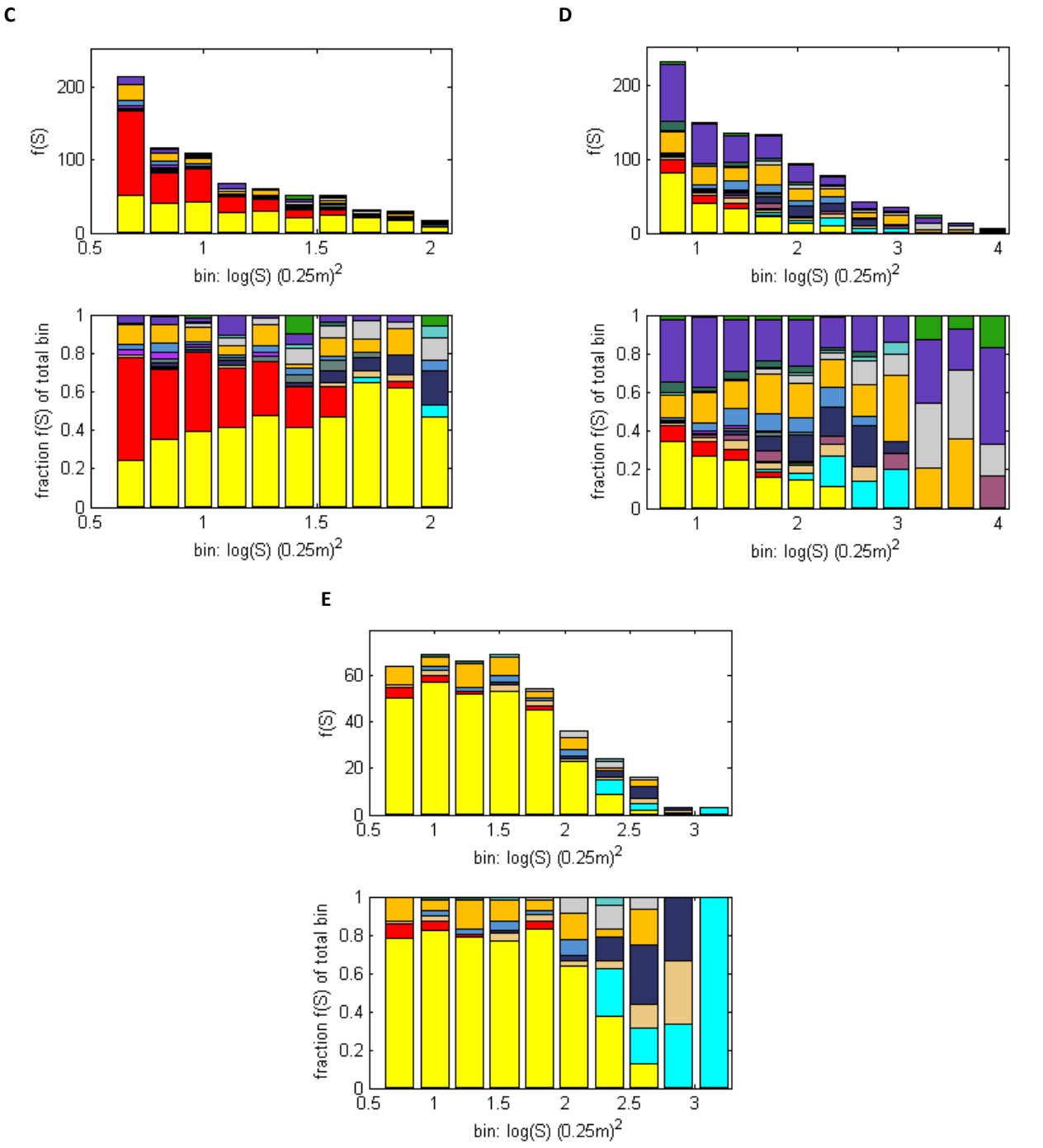

Figure A.2. Results of the patch development analysis of five locations (A-E) depicted by three plots: (1) The top panels show stacked bar graph of patches' development routes, were (2) bottom panel shows same data as in middle panel, but as fraction of total bin frequency. Locations are: (A) Baarland, (B) Hellegatpolder, (C) Hoofdplaat, (D) Paulinapolder, and (E) Thomaespolder.

The results of the patch development analysis is show in figure A.2.A-E. Unfortunately, due to computational limitations on memory, Zuidgors was not analyzed because of the large size of the lattice. All locations show a distinct patch development composition.

From the analysis on individual patch development it becomes clear that loss (red bars) and recruitment (or establishment, yellow bars) of patches up to about 500 lattice cells (~30m^2) is fairly common. So, most vegetation change occurs in the small patches. Because of these results the loss and recruitment of patches was analyzed more closely.

The net effect of disturbance and recovery processes is reflected by the patch-size distribution. Because loss and recruitment of patches seems to influence the patch-size distribution significantly, it can be argued that signatures of hydrodynamic conditions can be found in the loss and recruitment of patches at the pioneer zone.

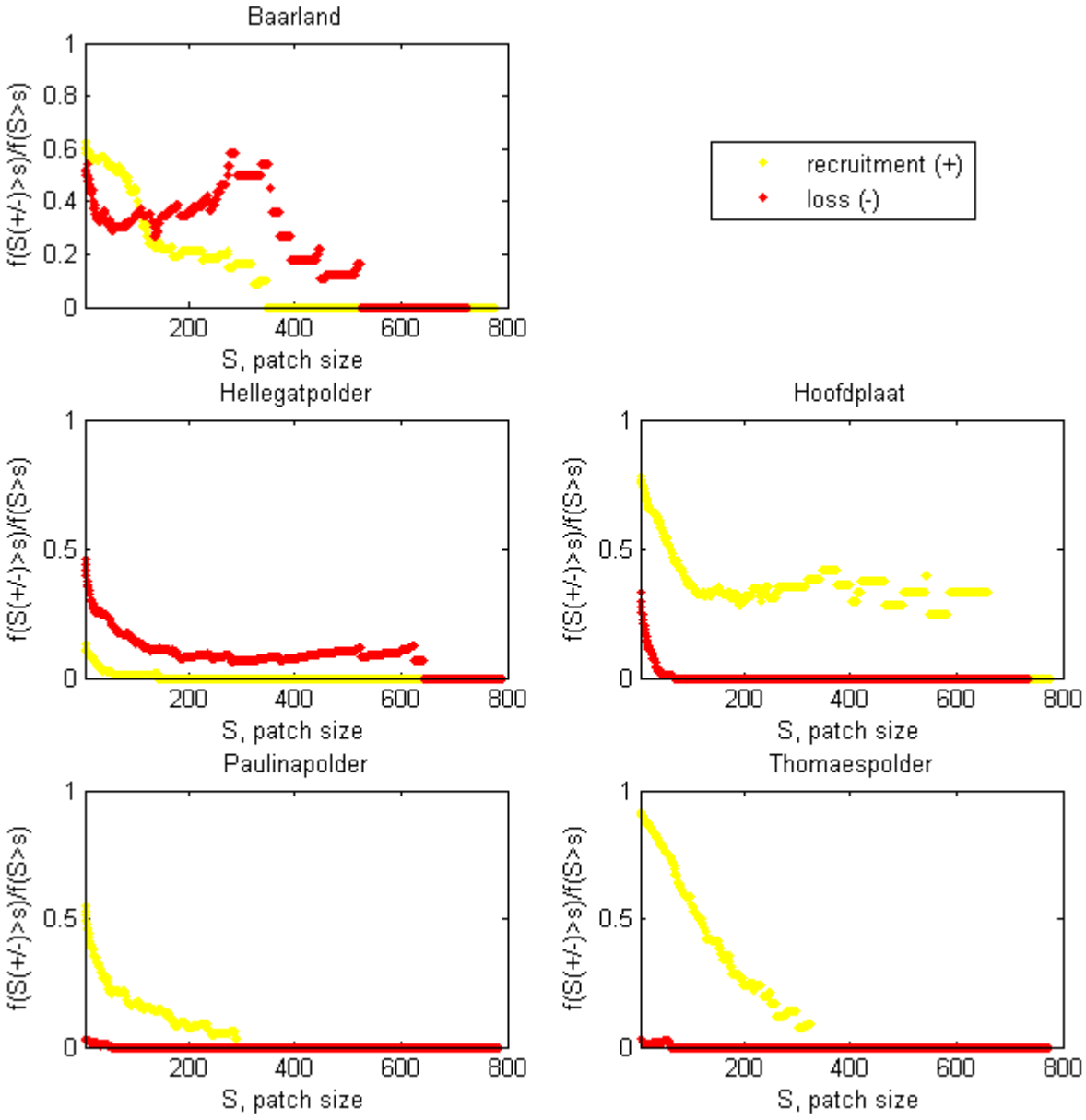

Figure A.3. Results of the patch development analysis specific for loss and recruitment of patches (development classes 1 and 2) of five locations.

To characterize each site, the inverse cumulative fraction of recruited and lost patches was plotted (fig.A.3), like:

$$\psi = \frac{f(S_{+/-} \geq s)}{f(S \geq s)} \qquad (A.1)$$

were {+} or {-} depict the patches labeled new or lost respectively. These statistics give a signature on the relative importance of loss (red) and recruitment (yellow) as function of the patch size. Furthermore, the area below the curves gave an indication on the relative importance of loss and recruitment of patches of each site. This method gives extra weight to larger patches, which is arguable a better method in comparison to only counting the total number of lost or recruited patches at each site, because it is more difficult to gain or lose larger patches in comparison to small patches. So, in addition, these values were added to an PCA of the 1998-2004 comparison (fig.A.4).

The first three principle components in this PCA explain 86.34% of the variance in the dataset, were PC1 explains 34.17%, and PC2 and PCA3 explain 27.72% and 24.45 of the variance respectively.

Abbreviation:	**Description:**
frac	cover fraction
recr	recruited patches
loss	lost patches
bala	balance (ratio) between recruitment and loss
inun	inundation duration
cvel	current velocity
cvgr	current velocity gradient
frow	frequency of onshore winds
frw6	frequency of onshore winds ≥6 Bft
afet	average fetch
awav	average wave height
wav6	average wave height at ≥6 Bft

The PCA reveals an interesting correlation structure of the hydrodynamic forcing factors in relation to the relative importance of loss and recruitment of patches. Loss of patches seem strongly correlated to the frequency of onshore winds, the frequency of onshore winds over 6 Beaufort, and average wave height by winds over 6 Beaufort. Recruitment, on the other hand, seems to correlate well with the inverse of inundation duration and cover fraction. These results seems to support the idea that exposure to currents and waves is mainly linked to erosion. Initiation of erosion (the disturbed patch edges) seems to be caused by exposure to waves, further eroded due to the currents. On the other hand, growth is linked more closely to physiological stressors, in this case the duration of inundation of the vegetation.

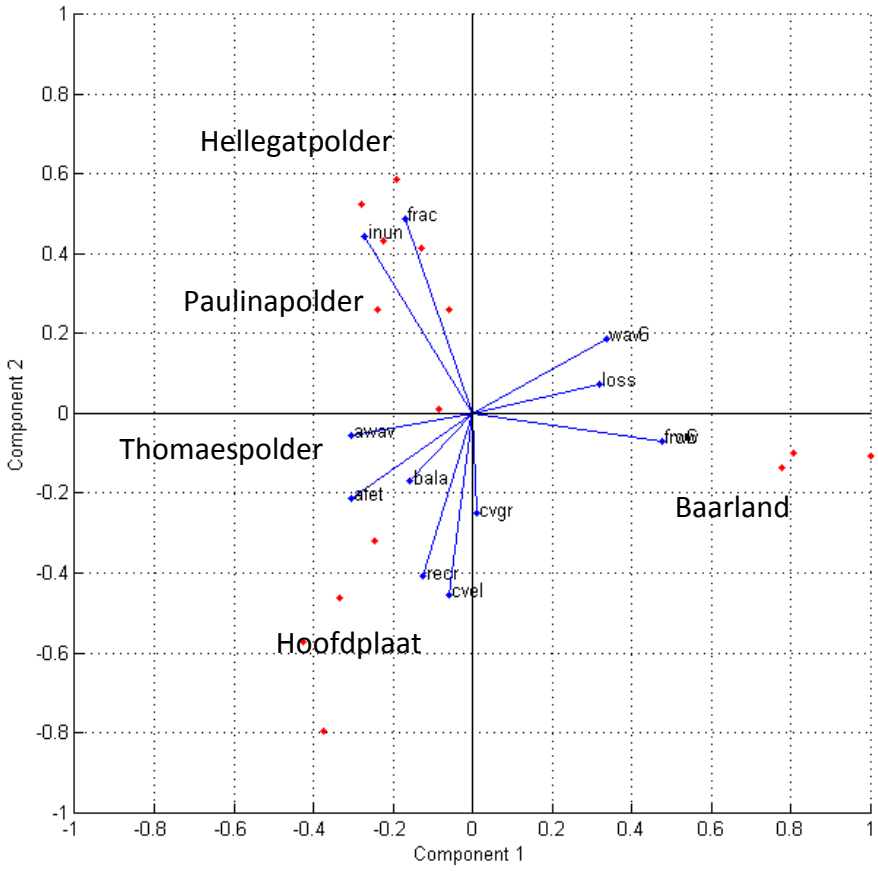
Hellegatpolder
Paulinapolder
Thomaespolder
Baarland
Hoofdplaat
frac
inun
wav6
loss
awav
bala
afet
cvgr
recr
cvel
Component 1
Component 2

A

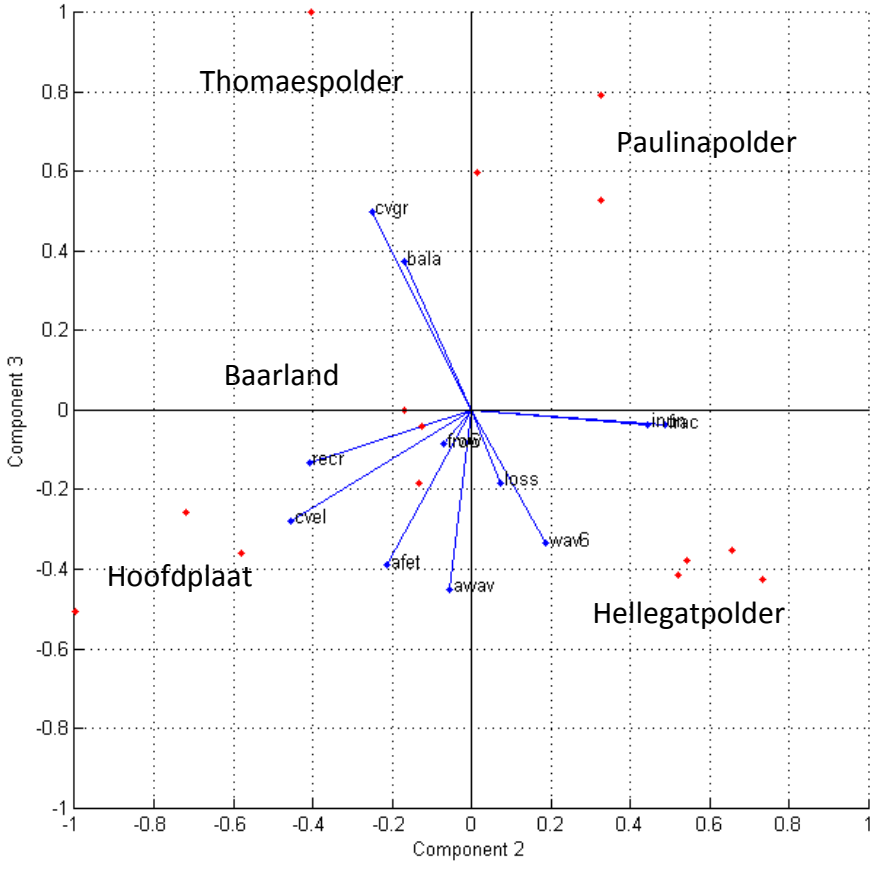
Thomaespolder
Paulinapolder
Baarland
Hoofdplaat
Hellegatpolder
cvgr
bala
recr
cvel
loss
wav6
afet
awav
Component 3
Component 2

B

← *Figure C.4. Biplot of PCA on hydrodynamic forcing, scaling exponents, vegetation cover, normalized distance to power-law, and relative importance of loss and recruitment of patches at the pioneer zone. (A) shows first two principle component, and (B) displays principle component 2 and 3. For clarification: 'inun' and 'frac' lay very close , and 'frow' and 'frw6' lay on top of each other in both biplots.*

B. Patch-size distributions of erosion and growth

Introduction

As figure 3.1. shows, not only patch-size distributions of the vegetation itself can be analyzed, but also the differences between subsequent vegetation maps. In this appendix the results of this additional analysis is presented. So, only erosion (red) and growth (yellow) patches from the vegetation change maps (overlays) are used to construct patch-size distributions.

Results

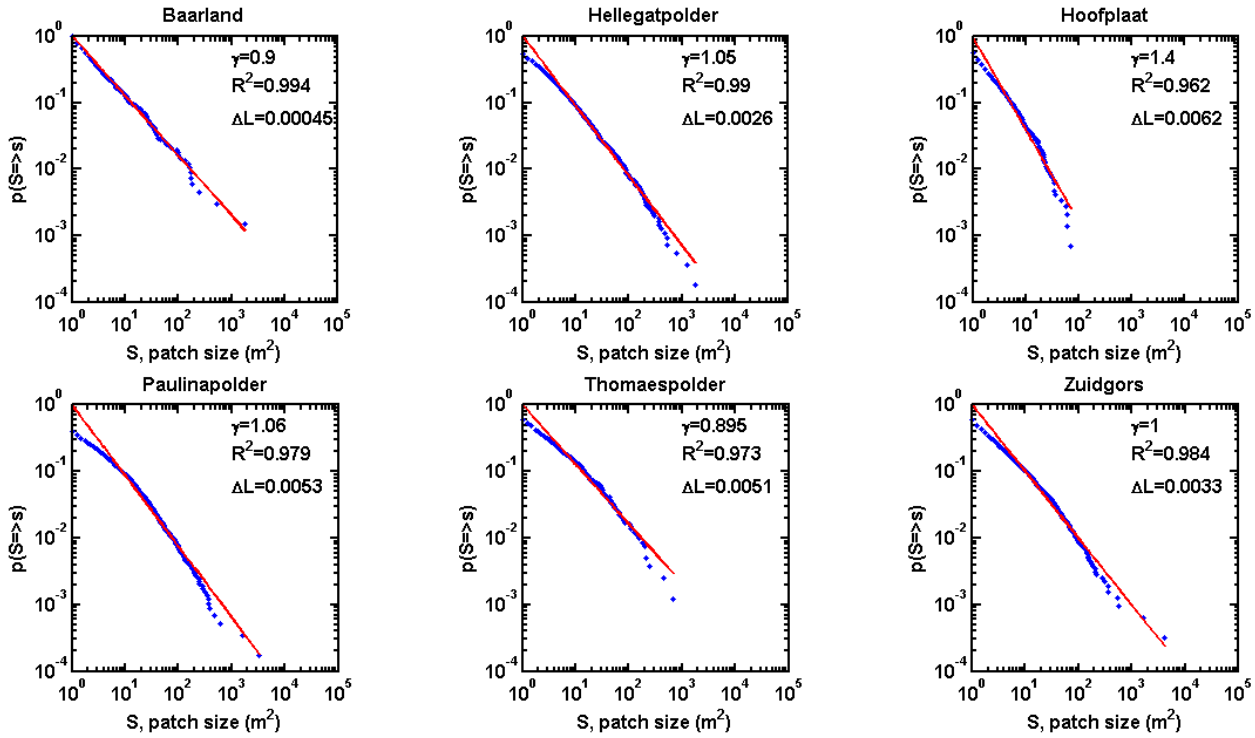

Figure B.1. Patch-size distributions of erosion patches at pioneer zones of size salt-marshes. The inverse cumulative distributions all approximate the power-law, were the red line depicts the best fitting power-law to the distribution.

Table B.1. Power-law pparameters estimated by least square method on inverse cumulative distributions (fig.B.1).

site	C	γ	λ	R^2
Baarland	2329	0,900	-	0,994
Hellegatpolder	17843	0,983	0,00020	0,996
Hoofdplaat	3240	0,953	0,00845	0,995
Paulinapolder	23071	1,041	0,00006	0,981
Thomaespolder	1860	0,774	0,00065	0,991
Zuidgors	12872	1,005	-	0,984

The analysis of erosion and growth patch-size distributions (fig.B.1&2 and tab.B.1&2 respectively) reveals that the presence of power-law distributions in the vegetation at the pioneer zone is valid. Because, if the dynamic processes (disturbance and recovery) are responsible for the pioneer zone vegetation to exhibit power-laws distributions, loss and gain of vegetation should follow power-law distributions as well. Thus, PL+/-PL=PL. As a consequence, if growth or erosion does not results in a power-law distribution, the resulting patch-size distribution will also not be a power-law distribution. Potentially, these patch-size distributions of differences between patches in time, can be used to gain more insight into the relative importance of growth and erosion processes at the salt-marsh sites. Figure B.1&2 and additional estimated parameter values in table A.1&2 show these distribution for erosion and growth respectively. Clearly, the patch-size distributions of erosion more closely follow the power-law distribution, than the distributions for growth.

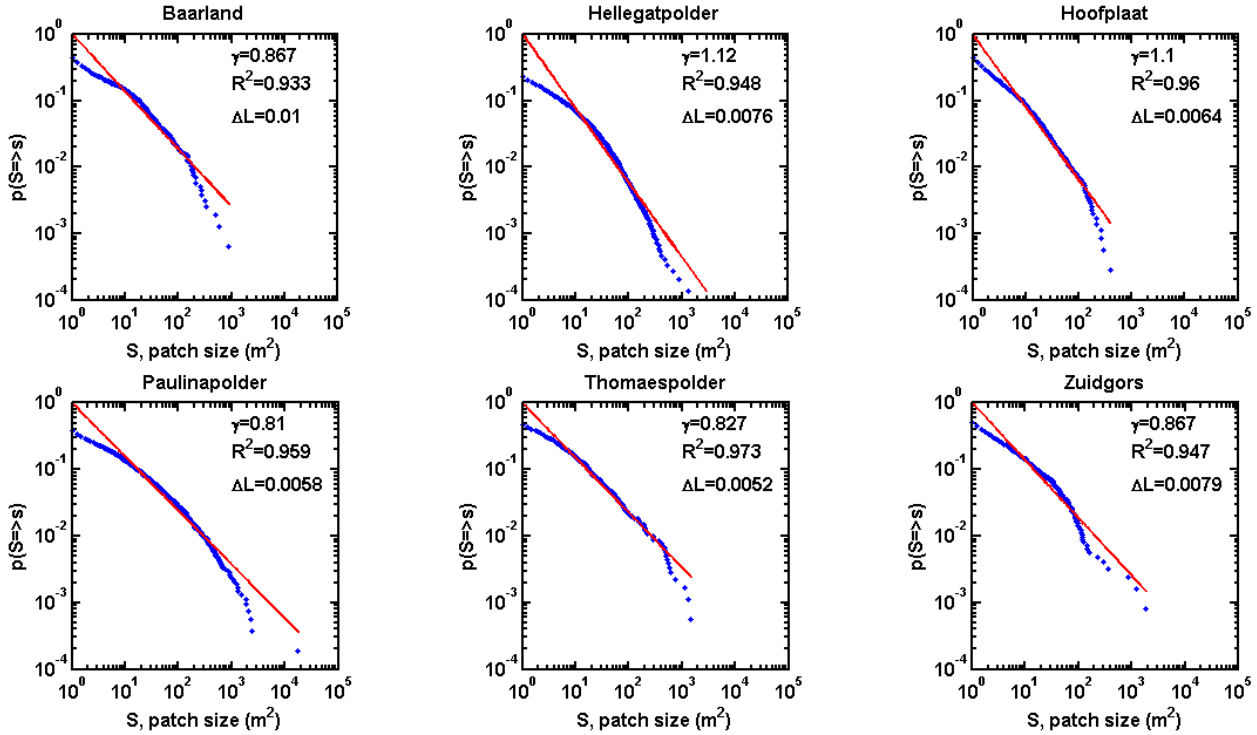

Figure B.2. Patch-size distributions of erosion patches at pioneer zones of size salt-marshes. The inverse cumulative distributions all approximate the power-law, were the red line depicts the best fitting power-law to the distribution.

Table B.2. Power-law pparameters estimated by least square method on inverse cumulative distributions (fig.B.2).

site	C	γ	λ	R^2
Baarland	2424	0,655	0,00092	0,984
Hellegatpolder	48323	1,031	0,00025	0,960
Hoofdplaat	6100	0,814	0,00174	0,996
Paulinapolder	14343	0,782	0,00003	0,964
Thomaespolder	3450	0,705	0,00031	0,993
Zuidgors	3298	0,810	0,00017	0,954

C. Principal Component Analysis of hydrodynamic conditions and vegetation structure

Introduction

Additional to the correlation analysis, a PCA on data of hydrodynamic conditions and the estimated scaling exponent and cover fraction of the six salt-marsh sites was performed. The values on hydrodynamic conditions used in the PCA can be found in table 3.1, and the estimated scaling exponents and cover fraction in table 3.3.

Results

The first three principle components in this PCA (fig.C.1) explain 89.4% of the variance in the dataset, were PC1 explains 47.3%, and PC2 and PC3 explain 25.5% and 16.6% of the variance respectively.

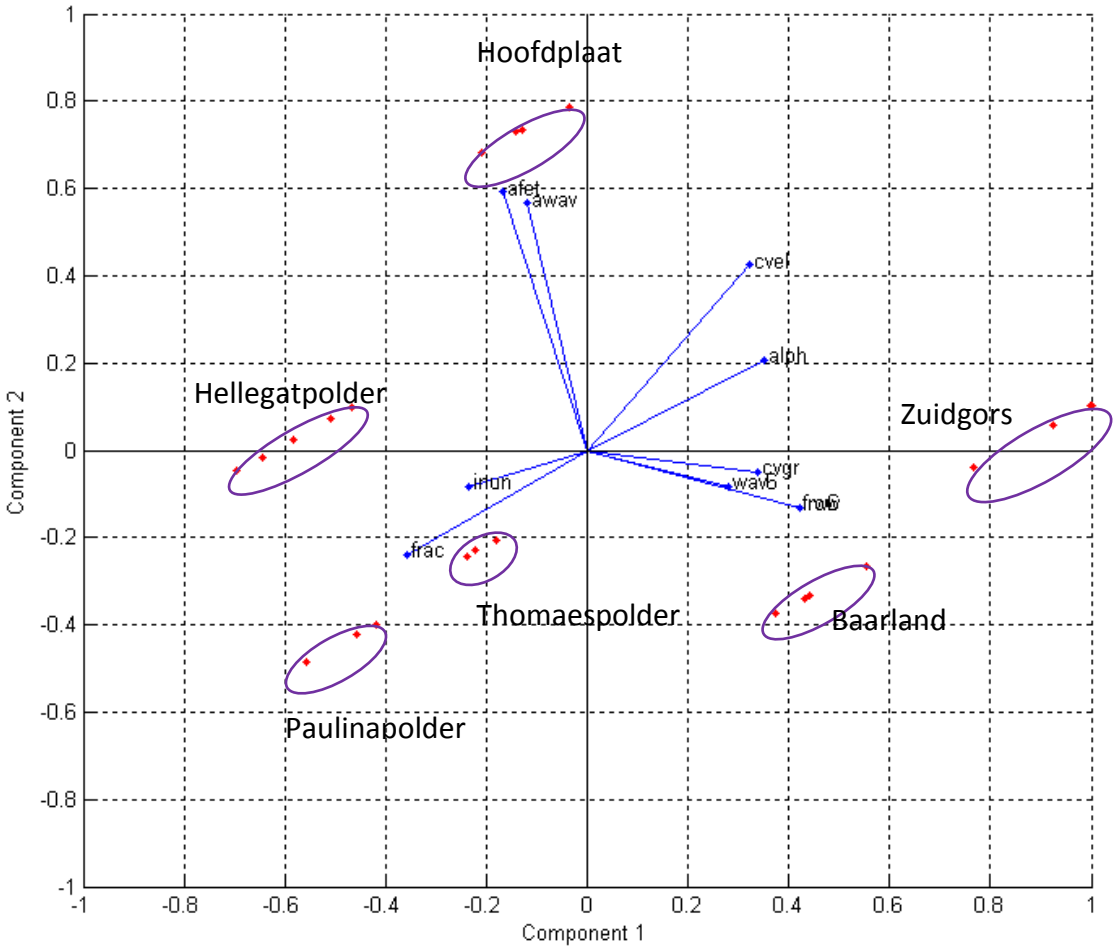

Figure C.1. Biplot of PCA on hydrodynamic forcing, scaling exponents and pioneer zone vegetation cover.

Abbreviation:	Description:
frac	cover fraction
alph	scaling exponent, alpha
inun	inundation duration
cvel	current velocity
cvgr	current velocity gradient
frow	frequency of onshore winds
frw6	frequency of onshore winds ≥6 Bft
afet	average fetch
awav	average wave height
wav6	average wave height at ≥6 Bft

The PCA shows (fig.C.1) a similar correlation structure as expected from the correlation analysis (Ch.3.3.4). Here, the modeled current velocity (cvel) and the scaling exponent (alph) point almost in the same direction with a vector of comparable length, which explains there strong correlation. In opposite direction cover fraction (frac) shows a strong negative correlation with current velocity and the scaling exponent. These three parameters are significantly correlated to the first Principle Component (PC1 on x-axis) of the PCA (see table C.1). Furthermore, the average wave height from 6 Beaufort and stronger (wav6) is strongly correlated with PC1, together with current velocity gradient (cvgr), and frequency of onshore winds (frow & frw6). This support the idea recently posed by Challaghan, et al. (2010) that extreme wave conditions are more important than average conditions. Average fetch (afet) and average wave height (awav) are strongly correlated with the second Principle Component (PC2 on y-axis), thereby not explaining differences in vegetation structure per site. Consequently, the initiation of edge erosion is only possible by disturbance of patch edges due to strong waves. Increases of the of storm frequency, or other sources for strong wave action, can potentially induce more erosion of the pioneer zone vegetation due to the initiation of edge erosion.

Table C.1. Correlation coefficients and p values between hydrodynamic variables evaluated, parameters derived from analysis (scaling exponent and vegetation cover fraction), and the principle components.

Variable	PCA component							
	1		2		3		4	
	r	p	r	p	r	p	r	p
Cover fraction	0,792	0,000	-0,368	0,084	0,390	0,065	-0,083	0,707
Scaling exponent, α	-0,774	0,000	0,321	0,136	-0,067	0,761	-0,289	0,182
Inundation duration	0,521	0,011	-0,128	0,559	0,548	0,007	-0,629	0,001
Current velocity	-0,715	0,000	0,656	0,001	-0,001	0,998	-0,117	0,595
Current velocity gradient	-0,746	0,000	-0,076	0,731	-0,228	0,296	-0,584	0,003
Frequency of onshore winds	-0,930	0,000	-0,202	0,356	0,264	0,223	0,142	0,520
Frequency of onshore winds ≥6 Bft	-0,929	0,000	-0,202	0,356	0,265	0,222	0,141	0,520
Average fetch	0,367	0,085	0,912	0,000	0,071	0,747	0,146	0,505
Average wave height	0,264	0,223	0,872	0,000	0,407	0,054	-0,041	0,852
Average wave height at ≥6 Bft	-0,617	0,002	-0,127	0,563	0,744	0,000	0,210	0,337


NIOO